

BRIGHAM YOUNG UNIVERSITY

GEOLOGY

S T U D I E S

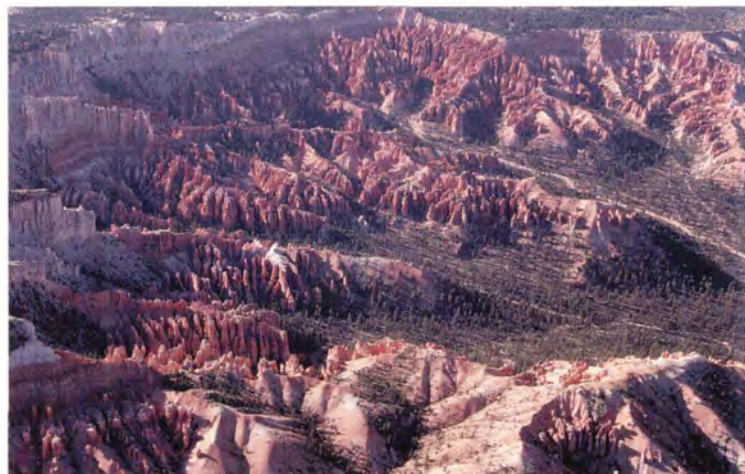
GEOLOGICAL SOCIETY OF AMERICA



FIELD TRIP GUIDE BOOK



1997 ANNUAL MEETING • SALT LAKE CITY, UTAH



EDITED BY PAUL KARL LINK AND BART J. KOWALLIS

V O L U M E 4 2 • 1 9 9 7

PART *1* ONE

PROTEROZOIC TO RECENT STRATIGRAPHY, TECTONICS, AND VOLCANOLOGY, UTAH, NEVADA, SOUTHERN IDAHO AND CENTRAL MEXICO

Edited by
Paul Karl Link and Bart J. Kowallis

BRIGHAM YOUNG UNIVERSITY GEOLOGY STUDIES

Volume 42, Part I, 1997

CONTENTS

Neoproterozoic Sedimentation and Tectonics in West-Central Utah	Nicholas Christie-Blick	1
Proterozoic Tidal, Glacial, and Fluvial Sedimentation in Big Cottonwood Canyon, Utah	Todd A. Ehlers, Marjorie A. Chan, and Paul Karl Link	31
Sequence Stratigraphy and Paleocology of the Middle Cambrian Spence Shale in Northern Utah and Southern Idaho	W. David Liddell, Scott H. Wright, and Carlton E. Brett	59
Late Ordovician Mass Extinction: Sedimentologic, Cyclostratigraphic, and Biostratigraphic Records from Platform and Basin Successions, Central Nevada	Stan C. Finney, John D. Cooper, and William B. N. Berry	79
Carbonate Sequences and Fossil Communities from the Upper Ordovician-Lower Silurian of the Eastern Great Basin	Mark T. Harris and Peter M. Sheehan	105
Late Devonian Alamo Impact Event, Global Kellwasser Events, and Major Eustatic Events, Eastern Great Basin, Nevada and Utah	Charles A. Sandberg, Jared R. Morrow and John E. Warme	129
Overview of Mississippian Depositional and Paleotectonic History of the Antler Foreland, Eastern Nevada and Western Utah	N. J. Silberling, K. M. Nichols, J. H. Trexler, Jr., P. W. Jewell and R. A. Crosbie	161
Triassic-Jurassic Tectonism and Magmatism in the Mesozoic Continental Arc of Nevada: Classic Relations and New Developments	S. J. Wyld, and J. E. Wright	197
Grand Tour of the Ruby-East Humboldt Metamorphic Core Complex, Northeastern Nevada: Part 1 — Introduction & Road Log	Arthur W. Snoke, Keith A. Howard, Allen J. McGrew, Bradford R. Burton, Calvin G. Barnes, Mark T. Peters, and James E. Wright	225
Part 2: Petrogenesis and thermal evolution of deep continental crust: the record from the East Humboldt Range, Nevada	Allen J. McGrew and Mark T. Peters	270

Part 3: Geology and petrology of Cretaceous and Tertiary granitic rocks, Lamoille Canyon, Ruby Mountains, Nevada	Sang-yun Lee and Calvin G. Barnes	276
Part 4: Geology and geochemistry of the Harrison Pass pluton, central Ruby Mountains, Nevada	Bradford R. Burton, Calvin G. Barnes, Trina Burling and James E. Wright	283
Hinterland to Foreland Transect through the Sevier Orogen, Northeast Nevada to North Central Utah: Structural Style, Metamorphism, and Kinematic History of a Large Contractional Orogenic Wedge	Phyllis Camilleri, W. Adolph Yonkee, Jim Coogan, Peter DeCelles, Allen McGrew, Michael Wells	297
Part 2: The Architecture of the Sevier Hinterland: A Crustal Transect through the Pequop Mountains, Wood Hills, and East Humboldt Range, Nevada	Phyllis Camilleri and Allen McGrew	310
Part 3: Large-Magnitude Crustal Thickening and Repeated Extensional Exhumation in the Raft River, Grouse Creek and Albion Mountains	Michael L. Wells, Thomas D. Hoisch, Lori M. Hanson, Evan D. Wolff, and James R. Struthers	325
Part 4: Kinematics and Mechanics of the Willard Thrust Sheet, Central Part of the Sevier Orogenic Wedge, North-central Utah	W. A. Yonkee	341
Part 5: Kinematics and Synorogenic Sedimentation of the Eastern Frontal Part of the Sevier Orogenic Wedge, Northern Utah	W. A. Yonkee, P. G. DeCelles and J. Coogan	355
Bimodal Basalt-Rhyolite Magmatism in the Central and Western Snake River Plain, Idaho and Oregon	Mike McCurry, Bill Bonnicksen, Craig White, Martha M. Godchaux, and Scott S. Hughes	381
Bimodal, Magmatism, Basaltic Volcanic Styles, Tectonics, and Geomorphic Processes of the Eastern Snake River Plain, Idaho	Scott S. Hughes, Richard P. Smith, William R. Hackett, Michael McCurry, Steve R. Anderson, and Gregory C. Ferdock	423
High, Old, Pluvial Lakes of Western Nevada	Marith Reheis, and Roger Morrison	459
Late Pleistocene-Holocene Cataclysmic Eruptions at Nevado de Toluca and Jocotitlan Volcanoes, Central Mexico	J. L. Macias, P. A. Garcia, J. L. Arce, C. Siebe, J. M. Espíndola, J. C. Komorowski, and K. Scott	493

A Publication of the
Department of Geology
Brigham Young University
Provo, Utah 84602

Editor

Bart J. Kowallis

Brigham Young University Geology Studies is published by the Department of Geology. This publication consists of graduate student and faculty research within the department as well as papers submitted by outside contributors. Each article submitted is externally reviewed by at least two qualified persons.

Cover photos taken by Paul Karl Link.

Top: Upheaval Dome, southeastern Utah.

Middle: Lake Bonneville shorelines west of Brigham City, Utah.

Bottom: Bryce Canyon National Park, Utah.

ISSN 0068-1016
9-97 700 23348/24218

Preface

Guidebooks have been part of the exploration of the American West since Oregon Trail days. Geologic guidebooks with maps and photographs are an especially graphic tool for school teachers, University classes, and visiting geologists to become familiar with the territory, the geologic issues and the available references.

It was in this spirit that we set out to compile this two-volume set of field trip descriptions for the Annual Meeting of the Geological Society of America in Salt Lake City in October 1997. We were seeking to produce a quality product, with fully peer-reviewed papers, and user-friendly field trip logs. We found we were bucking a tide in our profession which de-emphasizes guidebooks and paper products. If this tide continues we wish to be on record as producing "The Last Best Geologic Guidebook."

We thank all the authors who met our strict deadlines and contributed this outstanding set of papers. We hope this work will stand for years to come as a lasting introduction to the complex geology of the Colorado Plateau, Basin and Range, Wasatch Front, and Snake River Plain in the vicinity of Salt Lake City. Index maps to the field trips contained in each volume are on the back covers.

Part 1 "Proterozoic to Recent Stratigraphy, Tectonics and Volcanology: Utah, Nevada, Southern Idaho and Central Mexico" contains a number of papers of exceptional interest for their geologic synthesis. Part 2 "Mesozoic to Recent Geology of Utah" concentrates on the Colorado Plateau and the Wasatch Front.

Paul Link read all the papers and coordinated the review process. Bart Kowallis copy edited the manuscripts and coordinated the publication via Brigham Young University Geology Studies. We would like to thank all the reviewers, who were generally prompt and helpful in meeting our tight schedule. These included: Lee Allison, Genevieve Atwood, Gary Axen, Jim Beget, Myron Best, David Bice, Phyllis Camilleri, Marjorie Chan, Nick Christie-Blick, Gary Christenson, Dan Chure, Mary Droser, Ernie Duebendorfer, Tony Ekdale, Todd Ehlers, Ben Everitt, Geoff Freethy, Hugh Hurlow, Jim Garrison, Denny Geist, Jeff Geslin, Ron Greeley, Gus Gustason, Bill Hackett, Kimm Harty, Grant Heiken, Lehi Hintze, Peter Huntoon, Peter Isaacson, Jeff Keaton, Keith Ketner, Guy King, Mel Kuntz, Tim Lawton, Spencer Lucas, Lon McCarley, Meghan Miller, Gautam Mitra, Kathy Nichols, Robert Q. Oaks, Susan Olig, Jack Oviatt, Bill Perry, Andy Pulham, Dick Robison, Rube Ross, Rich Schweickert, Peter Sheehan, Norm Silberling, Dick Smith, Barry Solomon, K.O. Stanley, Kevin Stewart, Wanda Taylor, Glenn Thackray and Adolph Yonkee. In addition, we wish to thank all the dedicated workers at Brigham Young University Print Services and in the Department of Geology who contributed many long hours of work to these volumes.

Paul Karl Link and Bart J. Kowallis, Editors

Hinterland to foreland transect through the Sevier Orogen, Northeast Nevada to North central Utah: structural style, metamorphism, and kinematic history of a large contractional orogenic wedge

PHYLLIS CAMILLERI

Department of Geology and Geography, Austin Peay State University, Clarksville, Tennessee

ADOLPH YONKEE

Department of Geosciences, Weber State University, Ogden, Utah

JIM COOGAN

PETER DECELLES

Department of Geosciences, University of Arizona, Tucson, Arizona

ALLEN MCGREW

Department of Geology, University of Dayton, Dayton, Ohio

MICHAEL WELLS

Department of Geoscience, University of Nevada, Las Vegas, Nevada

INTRODUCTION

The purpose of this field trip is to examine the structural style, metamorphism, and kinematic history of the Sevier orogenic wedge along a hinterland to foreland transect (Fig. 1). The Sevier orogen (Armstrong, 1968a) is a retroarc fold and thrust belt that developed from Middle Jurassic to early Tertiary, and forms part of the much larger Cordilleran fold-thrust belt flanking the western margin of North America. The Sevier orogen exhibits many classic components of continental contractional belts such as a variably metamorphosed and polydeformed hinterland, foreland thrust system, and adjacent foreland basin, but mid-Tertiary to Recent extension has fragmented the orogen. Because of this fragmentation the orogen is unique in that footwalls of younger normal faults provide middle to upper crustal cross sections across various parts of the orogenic wedge. On this field trip we will view these unique cross sectional tracts from exposed structurally deep, partially melted levels of the hinterland to near surface levels of the Sevier foreland where we will observe the record of synorogenic foreland basin deposits. From these crustal cross sections, we will piece together the tectonic, metamorphic, and depositional architecture of the orogen.

This field trip is divided into three successive parts covering the western, central, and eastern regions of the Sevier orogenic wedge. Each area is discussed separately in detail in the accompanying mini papers by: Camilleri and McGrew (day 1) and Wells et al. (day 2) for the western region; Yonkee (day 2) for the central region; and Yonkee et al. (day 3) for the eastern region. For simplicity we have combined references for all mini papers and have numbered figures sequentially. In this overview paper we summarize data from the mini papers, integrating new structural and geochronologic data from the hinterland and foreland, to set up the large-scale geologic framework for the trip, and to develop a general model for the development and subsequent collapse of the Sevier orogenic wedge.

GEOLOGIC FRAMEWORK

The field trip covers a ~300 km west-to-east transect from the Sevier hinterland in northeastern Nevada to the foreland in north-central Utah (Fig. 2). This area lies east of accreted Paleozoic to early Mesozoic terranes that flank the western margin of North America and partly within the younger Basin and Range extensional province (Fig. 1). We divide the Sevier orogenic wedge into three principal

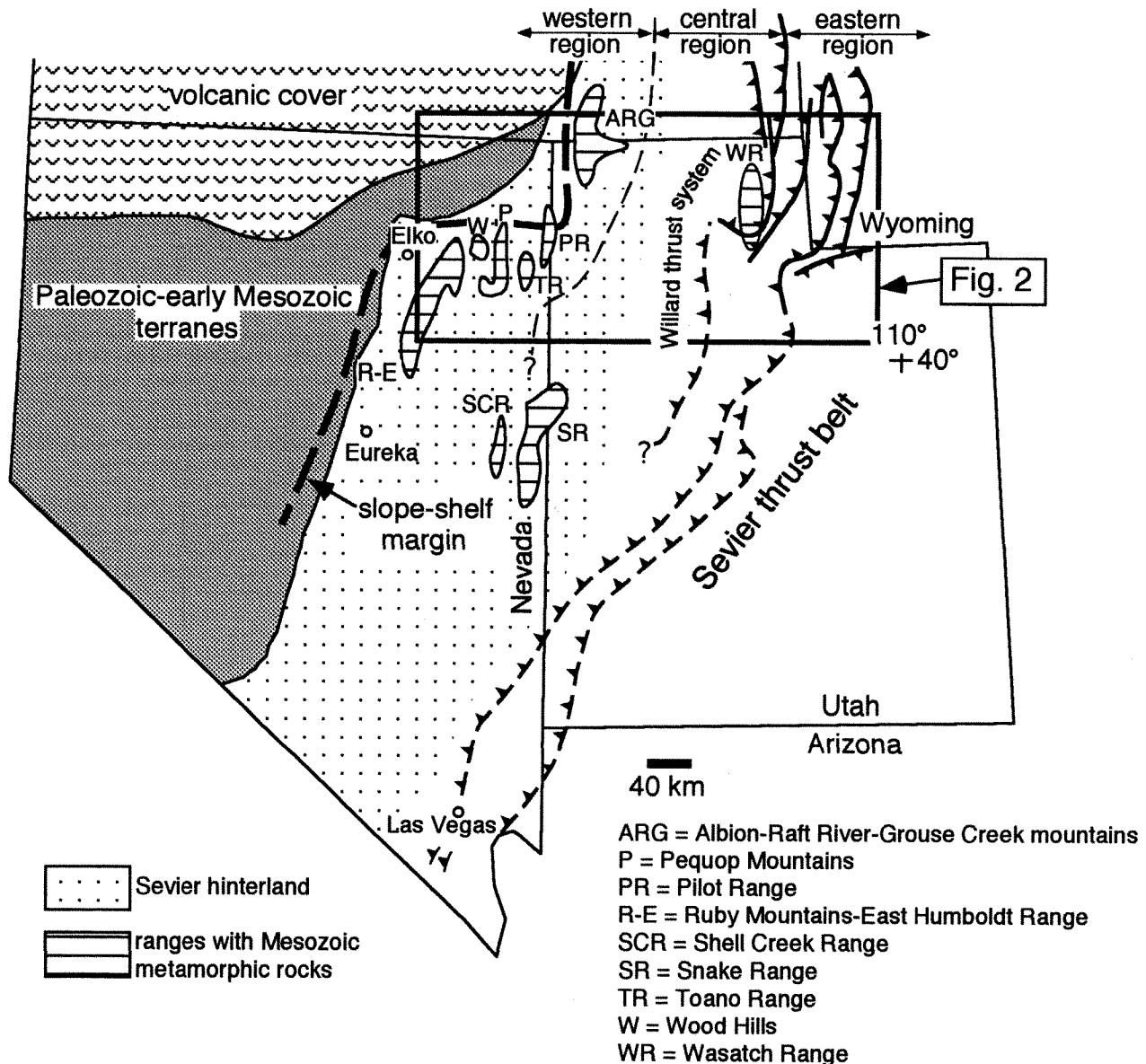


Figure 1. Simplified map showing locations of the Sevier orogen, mid-Paleozoic and younger accreted terranes, and the boundaries between the western, central, and eastern regions. Position of the slope-shelf margin is modified after Miller et al. (1991). The Cordilleran hinge line (not shown) lies approximately along the trace of the Willard thrust.

parts: (1) a western region consisting of the variably metamorphosed, polydeformed hinterland part of the wedge; (2) a central region consisting mostly of the areally extensive Willard thrust sheet; and (3) an eastern region consisting of the unmetamorphosed, imbricated frontal part of the Sevier orogenic wedge and associated foreland basin (Fig. 2). The boundary between the eastern and central regions lies along the leading edge of the Willard thrust system, and the boundary between the central and west-

ern regions lies just east of a belt of northeast trending metamorphic terranes (Figs. 1 and 2).

The Sevier orogen developed within a westward thickening sedimentary wedge of Neoproterozoic, Paleozoic, and Lower Mesozoic platform, shelf, and slope strata deposited on Archean and Proterozoic basement. The Paleozoic slope-shelf margin lies within the western region and generally trends northward, but it makes a sharp east-west bend in northwestern Utah and northeastern Nevada (Miller et al.,

1991) (Fig. 1). Miller et al. (1991) infer that the bend in the shelf margin is a primary feature influenced by west-trending tectonic boundaries within Precambrian basement. In addition to slope and shelf strata, the western region also contains synorogenic detritus shed from the late Paleozoic Antler orogenic belt. The central region contains a shelf sequence that is transitional with the shelf sequence in the western region. The eastern region contains relatively thin Paleozoic to lower Mesozoic platform strata deposited on stable basement, as well as overlying late Mesozoic Sevier foreland basin deposits. The platform-shelf margin or "Cordilleran hinge line" has an overall northerly trend and lies along the leading edge of the Willard thrust system (Fig. 1).

Regionally, the Sevier orogenic wedge is characterized by east- to southeast-verging folds and thrust faults, and by belts of localized tectonic thickening and regional metamorphism. The eastern region contains a Late Cretaceous to early Tertiary, overall eastward younging sequence of top-to-the-east, thin-skinned thrusts, including the Crawford, Medicine Butte, Absaroka, and Hogsback thrusts (Armstrong and Oriel, 1965; Armstrong, 1968; Royse et al., 1975; Dixon, 1982; Lamerson, 1982; Wiltschko and Dorr, 1983; Allmendinger, 1992; Heller et al., 1986; Royse, 1993; Fig. 2), which we refer to as the eastern thrust system. These thrusts imbricate the platform and foreland basin deposits, and share a basal decollement in Cambrian shale (Coogan and Royse, 1990). The basal decollement of the eastern thrust system ramped down into basement rocks to the west, and slip along the Ogden thrust system imbricated and folded basement into a complex anticlinorium, referred to as the Wasatch anticlinorium (Schirmer, 1988; Yonkee, 1992; DeCelles, 1994), which flanks the western edge of the eastern thrust system and lies along the shelf-platform margin (Fig. 2). The central region overall has limited structural relief and much of the shelf sequence is concealed by sediment filling Cenozoic extensional basins (Fig. 2). The prominent feature within the central region is the Willard thrust sheet that was transported more than 50 km east to southeast during the Early to early Late Cretaceous. Western parts of this thick sheet were also deformed by the Late Jurassic Manning Canyon decollement (Allmendinger et al., 1984; Fig. 2). The structural geometry of the western region is less well constrained than that of the other regions because of discontinuous exposures and overprinting by Cenozoic normal faults and shear zones. The western region contains an extensive belt of metasedimentary rocks and Precambrian basement that underwent Mesozoic polyphase deformation and Barrovian regional metamorphism (Fig. 2), with partial melting at deep levels. Significantly, the metamorphic rocks record tectonic burial of up to 30 km and represent a localized area of large-magnitude crustal thickening, which paral-

els the ancient shelf-slope margin. Thrust faults responsible for tectonic burial in this region largely were excised by Late Cretaceous (?) and Tertiary normal faults and shear zones, and although there is ample evidence to infer thrust faulting, few thrust traces are exposed in this region (Fig. 2).

Precambrian and Paleozoic structural and depositional features appear to have partly controlled the overall structural geometry and kinematics of the Sevier orogenic wedge. Within the eastern region, shortening was roughly east-west, normal to the platform-shelf margin, and localized basement deformation and crustal thickening were concentrated near this margin (Yonkee, 1992). In the western region, shortening directions are locally southeast-northwest, roughly normal to the bend in the slope-shelf margin, and localized basement deformation and crustal thickening were concentrated near the slope-shelf margin. Whereas inferred ancient tectonic boundaries in Archean-Proterozoic basement probably influenced Neoproterozoic to Early Mesozoic depositional patterns within the sedimentary wedge, they also probably focussed contraction/thickening and locally rotated shortening directions during the Sevier orogeny (e.g., Bryant and Nichols, 1988; Bradley and Bruhn, 1988; Miller et al., 1991; Yonkee, 1992; Camilleri et al., 1992).

TECTONIC AND METAMORPHIC CHARACTERISTICS OF THE SEVIER OROGENIC WEDGE

In this section we summarize the characteristics of the Sevier orogenic wedge in specific areas to be visited during the field trip. Collectively, these areas represent a regional transect from the western hinterland to eastern foreland. Data from these areas will later be integrated into a general interpretation of the spatial and temporal evolution of the orogenic wedge.

Western Region

Metamorphic terranes within the western region of the Sevier orogenic wedge record both Late Jurassic and Cretaceous deformation and metamorphism. Jurassic deformation produced minor thrusting, folding, and locally extension (Allmendinger and Jordan, 1984; Miller and Allmendinger, 1991; Glick, 1987; Hudec, 1992; Miller and Hoisch, 1992, 1995). Late Jurassic contractional deformation is well preserved in the Pilot and Toano-Goshute ranges, and deformation overlapped in time with emplacement of Late Jurassic granitoids and development of metamorphic aureoles (Fig. 2). Vast tracts of the western region also underwent Cretaceous, low- to high-grade Barrovian metamorphism associated with large-magnitude crustal thickening (Fig. 2). On this trip we will focus on two areas that record Cretaceous metamorphism: the East Humboldt

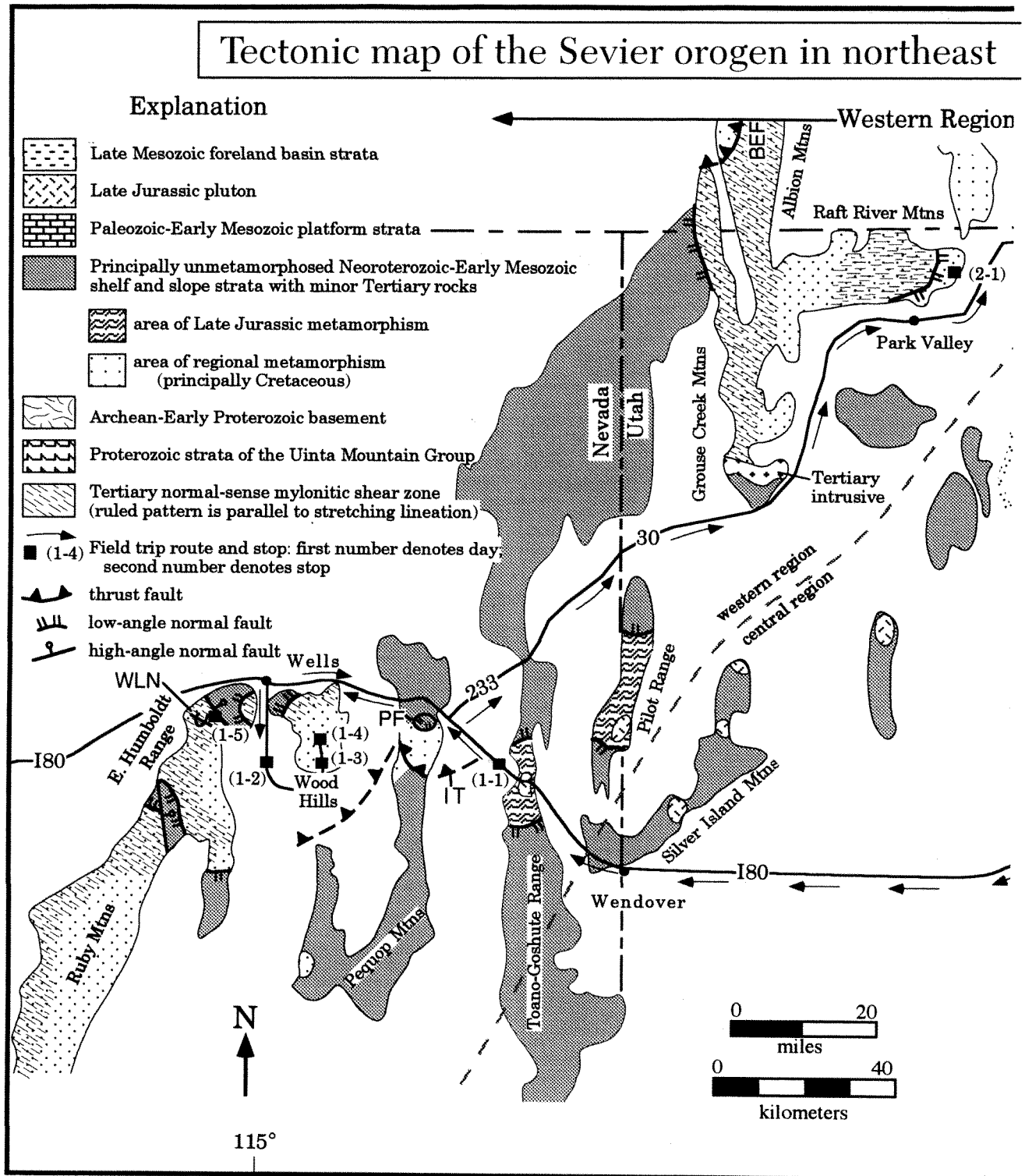


Figure 2. Simplified tectonic map of the Sevier orogen in northeast Nevada, northwest Utah, and southwest Wyoming showing location of field trip route and stops. Note that although the East Humboldt Range, Raft River, Grouse Creek, and Albion mountains contain exposures of Archean and Early Proterozoic basement, they are not shown on the map because they are too small to show at this scale.

Range-Wood Hills-Pequop Mountains region and the Raft River Mountains (stops 1-1 to 2-1, Fig. 2). Together, these traverses offer glimpses into the nature of ductile flow in the middle crust, the geometries of thrust faults, and the metamorphic architecture of the Sevier hinterland.

The East Humboldt Range, Wood Hills, and Pequop Mountains expose a large area of regionally metamorphosed strata that record at least two periods of Mesozoic top-to-the-southeast thrust faulting, and two subsequent phases of Late Cretaceous to mid-Tertiary normal faulting. The first phase of thrust faulting involved as much as 30 km of crustal thickening and 70 km of shortening during emplacement of a southeast tapering thrust wedge of slope-shelf strata above an inferred fault called the "Windermere thrust" (Camilleri and Chamberlain, 1997). Thermal relaxation during and or following emplacement of the thrust wedge resulted in Barrovian metamorphism and partial melting in deep levels within the footwall of the Windermere thrust. Thermal weakening of the footwall, coupled with the hanging wall load, induced predominantly ductile coaxial layer-parallel extension, development of bed-subparallel S and S-L (S_1 and L_1) tectonites, and consequent attenuation and collapse of the footwall during prograde metamorphism (Camilleri, 1994a,b). Geochronologic data suggest that peak metamorphism was attained at ~84 Ma and that emplacement of the thrust wedge preceded peak metamorphism probably between 153 Ma to 84 Ma (Camilleri and Chamberlain, 1997). Following the development of S_1 , the Pequop Mountains-East Humboldt Range region underwent a second phase of modest crustal thickening and shortening. Between 84 Ma and 75 Ma, the footwall of the Windermere thrust at intermediate structural levels was overprinted by the Independence thrust and a series of back folds, and during peak metamorphism between 70 Ma and 90 Ma, basement at deep structural levels underwent recumbent folding resulting in the formation of the Winchell Lake nappe (McGrew, 1992)(Fig. 2).

The latter phase of contraction was closely followed by as much as 10 km of crustal thinning along the west-rooted Pequop normal fault, which initiated prior to 75 Ma, and marked a fundamental change from large-scale crustal thickening to crustal extension in the hinterland. Continued Late Cretaceous to early Tertiary (?) slip on the Pequop fault and mid-Tertiary slip on the west-rooted Mary's River normal fault system accommodated collapse of the wedge above the Windermere thrust and exhumed the footwall of the thrust. The exhumed, metamorphosed footwall, along with parts of the unmetamorphosed Windermere hanging wall preserved above the low-angle normal faults, are exposed in the Pequop Mountains, Wood Hills, and East Humboldt Range.

The Raft River, Grouse Creek, and Albion Mountains expose a metamorphosed midcrustal section of shelf strata

that lies unconformably above Archean basement. These rocks record alternating episodes of late Mesozoic to early Cenozoic contraction and extension. Archean to Pennsylvanian rocks within the mid-crustal section were tectonically buried 12 to 18 km in excess of stratigraphic depths and metamorphosed sometime between late Jurassic and ~90 Ma. A preserved duplication of the miogeoclinal section above the complex Basin-Elba fault zone (Quartzite allochthon of Miller, 1980, 1983; Fig. 2) in the northern Albion Mountains may represent the remnants of a once areally extensive thrust sheet responsible for much of the structural burial.

Prior to 90 Ma, widespread bed-subparallel foliation developed within the footwall of the Basin-Elba fault zone, synchronous with prograde amphibolite-facies metamorphism that may have peaked at about 100 Ma (Wells et al., 1990). Resulting S and S-L tectonites record dominantly coaxial flattening and top-to-the-north-northeast shearing, interpreted to record orogen-parallel extensional flow of a thrust footwall following crustal thickening. These fabrics are overprinted by top-to-the-west, low-angle normal faults that accommodated several kilometers of crustal thinning, including the ~90 Ma Emigrant Spring fault, and Mahogany Peaks fault of probable latest Cretaceous age (Wells et al., 1990). Normal-sense slip on the Basin-Elba fault zone, which either reactivated or cut an earlier thrust fault, may also have occurred at ~90 Ma (Hodges and Walker, 1992). This extension was followed by another period of contraction, bracketed between 90 Ma and early Tertiary, with development of recumbent folds that deform the low-angle shear zones (Wells, 1997). Early Tertiary (~45–37 Ma) extension is recorded by a major amphibolite facies top-to-the-west-northwest extensional shear zone along the western flanks of the Raft River, Grouse Creek, and Albion mountains (Saltzer and Hodges, 1988; Wells and Snee, 1993). At higher structural levels, the west-rooted middle detachment fault (Compton et al., 1977), which juxtaposes middle greenschist facies Pennsylvanian and Permian rocks over upper greenschist to lower amphibolite facies older rocks, may represent a higher crustal level of this extensional system. These Late Mesozoic to early Cenozoic fabrics and faults are overprinted by two Miocene extensional systems of opposite sense of slip; a top-to-the-west system along the western flank of the Grouse Creek and southern Albion Mountains (Compton, 1983), and a top-to-the-east system within the eastern and central Raft River Mountains (Wells and Snee, 1993).

Although mid-crustal Mesozoic structures recorded in the Raft River Mountains region cannot be directly correlated with those in the East Humboldt Range-Pequop Mountains region, both areas share similar tectonic histories, including an episode of large-magnitude crustal thickening and Barrovian metamorphism that predates 90 Ma

in the north and 84 Ma in the south. Moreover, in both areas, crustal thickening culminated in layer-parallel extension and attenuation of stratigraphic units in tectonically buried and thermally weakened thrust footwalls. The Raft River region also experienced a phase of normal-sense shearing at ~90 Ma. Both regions subsequently experienced a second episode of Late Cretaceous modest crustal thickening that involved overturned to recumbent folding and sparse thrust faulting. Overall, the hinterland is characterized by an early large-magnitude crustal thickening event followed by late-stage episodes of contraction and extension that were synchronous with foreland shortening. We view these late-stage alternating episodes of contraction and extension in the hinterland as products of the complex interplay between positive buoyancy forces generated by overthickening of the crust, which tend to promote thinning of the crust, and compressional boundary stresses which promote thickening of crust (e.g., Platt, 1986; Dahlen and Suppe, 1988). Although protracted extensional collapse of the hinterland began in the Late Cretaceous in both regions, major crustal thinning and exhumation of mid-crustal rocks were accomplished by episodic extensional phases in the Tertiary.

Central Region

The central region of the wedge can be crudely divided into a western part with limited structural relief above a flat basal decollement, and an eastern part with greater structural relief associated with ramps near the leading edge of the Willard thrust system. On this trip we will focus on structural relations preserved in the Promontory Mountains in the western part and in the northern Wasatch Range in the eastern part (stops 2-2 to 2-6; Fig. 2).

From north to south, respectively, the Promontory Mountains expose an oblique section from the upper levels to the base of the Willard thrust sheet. Upper levels consist of upper Paleozoic strata imbricated by the Late Jurassic Manning Canyon decollement and shortened by a system of large-scale upright to inclined folds. Middle levels contain a gently dipping sequence of competent quartzite and carbonate that display limited internal deformation. Lower levels exposed to the south contain incompetent mica-rich strata that were metamorphosed to greenschist facies and internally deformed during concentrated layer-parallel extension and top-to-the-southeast simple shear, probably associated with Early Cretaceous slip on the Willard thrust. The footwall of the Willard thrust, which is exposed south of the Promontory Mountains on Antelope Island (Fig. 2), also displays Early Cretaceous low-grade metamorphism and internal deformation, with layer-parallel extension and top-to-the-southeast simple shear in incom-

petent strata and minor layer-parallel shortening within competent strata (Yonkee, 1992). Low-angle normal faults of uncertain age locally omit parts of the stratigraphic section in the Promontory Mountains and may record minor Late Cretaceous to early Tertiary extension and tectonic unroofing. Listric normal faults, which locally reactivated older thrusts, bound asymmetric grabens that contain tilted Eocene to Oligocene strata in this area, probably recording collapse and extension of the orogenic wedge after cessation of thrusting (Constenius, 1996).

The northern Wasatch Range exposes a wide range of structural levels in the eastern part of Willard thrust sheet. Here, the Willard thrust displays a ramp-flat geometry and has associated large-scale fault-bend and fault-propagation folds. The nature of internal deformation of the thrust sheet varies with structural level. Upper levels contain unmetamorphosed, competent carbonate and quartzite that display limited layer-parallel shortening. Lower levels contain incompetent mica-rich strata that underwent greenschist-facies metamorphism and concentrated layer-parallel extension plus top-to-the-east simple shear prior to and synchronous with slip on the Willard thrust, producing intense thrust-parallel foliation (Yonkee, 1992). The basal fault zone consists of mylonite and very fine-grained cataclasite that are cut by multiple vein sets and extended by minor, syntectonic normal faults. The veins and thrust-parallel foliation within the base of the Willard sheet probably record episodic high fluid pressures and rotation of the stress field adjacent to a weak fault zone. The footwall of the Willard thrust displays complex combinations of layer-parallel extension, imbricate thrusting, and folding, which record spatially and temporally overlapping extension and shortening. Internal deformation and metamorphism of the lower levels of the Willard sheet occurred from about 140 to 110 Ma (Yonkee, 1990). Large-scale top-to-the-east slip on the Willard thrust from 120 to 90 Ma resulted in uplift and erosion of the sheet with deposition of synorogenic deposits in the foreland basin to the east (DeCelles, 1994). Subsequently, the Willard sheet was passively uplifted, rotated, and eroded during slip on underlying thrusts between 90 and 50 Ma (DeCelles, 1994).

Eastern Region

The eastern region contains the basement-cored Wasatch anticlinorium, a series of Late Cretaceous to early Tertiary faults of the eastern thrust system, and synorogenic deposits that record the timing and erosional unroofing of thrust sheets. This part of the field trip will focus on the nature of basement deformation, thrust kinematics, and proximal foreland basin deposits exposed in north-central

Utah (stops 3-1 to 3-8; Fig. 2), providing a glimpse of the structural and depositional evolution of shallow crustal levels in the frontal part of the orogenic wedge.

The Wasatch anticlinorium, which is cored by Precambrian basement, developed synchronously with slip on the eastern frontal thrust system. The anticlinorium had a structurally complex and protracted history. Initial deformation of basement was accommodated by spaced shear zones that produced minor bulk subhorizontal shortening between 140 and 110 Ma (Yonkee, 1992). Major growth of the anticlinorium began by the early Late Cretaceous with slip along the roof and floor thrusts of the Ogden thrust system, which imbricated and rotated basement. Subsequent Late Cretaceous to early Tertiary slip on thrust faults underlying the Ogden thrust system produced basement duplexing, continued growth of the anticlinorium, and folding of the Ogden thrust system. Slip on basement thrusts in the anticlinorium was largely transferred to the east into slip in the eastern thrust system, with the progressive growth of the Wasatch anticlinorium producing wedge taper that helped drive slip on frontal thrusts (Yonkee, 1992; DeCelles, 1994; DeCelles and Mitra, 1995).

The eastern thrust system in north-central Utah imbricated platform and foreland basin strata, and like the anticlinorium, had a complex and protracted history. Initial deformation began with Early Cretaceous layer-parallel shortening, folding, and cleavage development associated with footwall deformation beneath the Willard thrust and transfer of slip to the east along detachments in Jurassic evaporites. Main thrusts of the eastern thrust system, which had basal decollements in Cambrian strata (Coogan and Royse, 1990; Coogan, 1992), developed from early Late Cretaceous to early Tertiary and locally merged into existing detachments in Jurassic strata. Thrusting progressed overall from west to east on the Crawford, Medicine Butte, Absaroka, and Hogsback thrusts, but some thrusts had multiple periods of movement. Development of the Uinta foreland uplift (Fig. 2) overlapped with the later stages of thrusting (Bryant and Nichols, 1988). Late Eocene to Oligocene collapse of the wedge was accommodated by listric normal faults that locally reactivated thrusts (Constenius, 1996).

Jurassic to early Tertiary synorogenic deposits in the eastern region preserve an excellent record of thrust-related erosion and deposition. Middle Jurassic strata may record initial influx of clastic material from the west and deposition in the distal back-bulge zone of the foreland basin system (DeCelles and Currie, 1996), possibly related to contractional deformation in central Nevada (e.g., Oldow, 1984; Speed et al., 1988). A Late Jurassic-Early Cretaceous unconformity in this area may record regional uplift during passage of the forebulge, synchronous with

deformation spreading into the hinterland in eastern Nevada and western Utah (DeCelles and Currie, 1996). Lower to lower Upper Cretaceous strata in this area record deposition in the increasingly proximal foredeep part of the foreland basin system, and by ~90 Ma, the front of the orogenic wedge had propagated into north-central Utah and coarse fan-delta and alluvial fan facies were deposited on top of the active frontal wedge (DeCelles, 1994).

SPATIAL AND TEMPORAL DEVELOPMENT OF THE SEVIER OROGENIC WEDGE

Characteristics of deformation, metamorphism, and sedimentation are synthesized below to develop a highly generalized model for development of the Sevier orogenic wedge. This model links events at various structural levels in the western, central, and eastern regions and provides a simplified conceptual framework for interpreting the dynamic evolution of the wedge in terms of idealized stages from the Early Jurassic (stage 1) to Late Eocene-Oligocene (stage 6) (Figs. 3 and 4). However, we submit this model with the following caveat: the timing of thrust faulting in the central and eastern regions of the orogenic wedge is well constrained but the timing of major thrust faulting and tectonic burial in the western region is not. In this model, we infer that major thrust faulting and tectonic burial in the western region was protracted from the Late Jurassic to the early Late Cretaceous.

Stage 1—Early Jurassic

By the early Jurassic an overall westward thickening sedimentary wedge had been deposited. The wedge consisted of a platform section containing a thin (<10 km thick) sequence of Paleozoic to lower Mesozoic strata deposited on stable basement, a shelf section containing a thicker (10 to 15 km thick) sequence of Neoproterozoic to lower Mesozoic strata deposited on thinned basement, and a slope-shelf section farther west that also included synorogenic material shed from the late Paleozoic Antler orogenic belt. We infer primary ramps along the slope-shelf transition and along the shelf-platform transition, and refer to these ramps as the western and eastern transition zones respectively (Fig. 3). In our model the initial geometry of the sedimentary wedge influenced later development of the orogenic wedge, with a basal decollement forming near the basement-cover contact and locally cutting into basement along ramps at both transition zones. A western thrust system developed in the slope-shelf section, a central thrust system developed in the shelf section, and an eastern thrust system developed in the platform section, with concentrated tectonic thickening and basement deformation along the two transition zones.

Stage 2—Late Jurassic

Development of the Sevier orogenic wedge in the Late Jurassic included: (1) initial tectonic burial and metamorphism in the western region beneath the leading edge of the western thrust system; and (2) early shortening and decollement faulting within the central region. Emplacement of thrust sheets at the leading edge of the western system, including the Windermere thrust and Quartzite allochthon, may have started at this time and produced initial tectonic thickening, with inception of footwall metamorphism and layer-parallel extension. Granitic plutons were locally intruded into the western region, producing metamorphic aureoles and minor extension. Within the central region the Manning Canyon decollement formed, and smaller-displacement thrust faults, folds, and foliation produced minor internal deformation. Development of topographic relief and heat from plutons to the west may have initiated regional fluid flow through the central region. Although a foredeep may have developed from isostatic flexure near the leading edge of the western thrust system, no synorogenic sediments are preserved, possibly due to subsequent uplift and erosion (Royse, 1993). A forebulge and associated Late Jurassic-Early Cretaceous unconformity developed in eastern Utah, and further east a backbulge basin developed and accumulated clastic material derived in part from the western thrust system.

Stage 3—Early Cretaceous

The Sevier orogenic wedge evolved during the Early Cretaceous with: (1) inferred tectonic burial and metamorphism in the western region; (2) major slip on the central thrust system and synorogenic sedimentation in an associated foredeep; (3) internal shortening of basement within the eastern transition zone; and (4) local layer-parallel shortening in the eastern region. Continued emplacement of thrust sheets at the leading edge of the western thrust system, including possible footwall under-thrusting and basement duplexing, produced significant crustal thickening along the western transition zone, with up to 30 km of tectonic burial, prograde metamorphism, and footwall layer-parallel extension. This extension produced subhorizontal foliation and low-angle shear zones, reflecting footwall collapse or adjustment of the orogenic wedge during periods of decreased horizontal stress. Although metamorphism in the western region did not peak until the early Late Cretaceous, much of this area probably experienced elevated temperatures through the Early Cretaceous. Major slip on the central thrust system, which included the Willard thrust, transported the shelf section eastward above a regional basal flat and up a ramp at the leading edge of the system. Complex internal deformation included minor layer-parallel shortening within competent strata at

upper levels, significant layer-parallel extension in incompetent strata at lower levels, and development of syntectonic minor normal faults along the main thrust, reflecting complex stress and fluid pressure variations along a weak base of the wedge. In this model the central thrust system developed a deeper western crustal ramp, and growth of topography and taper along the western transition zone helped drive emplacement of the central thrust system above a weak basal decollement. Basement in the eastern transition zone was internally shortened by networks of shear zones, and slip may have initiated on basement thrusts. The eastern region underwent local layer-parallel shortening and initial decollement faulting in Jurassic evaporite beds within the footwall of the central thrust system. A regional foredeep depozone developed by isostatic flexure east of the leading edge of the central thrust system, and accumulated several kilometers of synorogenic sediment (Jordan, 1981).

Stage 4—early Late Cretaceous

Development of the Sevier orogenic wedge during the early Late Cretaceous included: (1) attainment of peak metamorphic conditions and minor tectonic thickening in the western region; (2) passive transport and local uplift of the central thrust system; (3) imbricate faulting and growth of the basement-cored Wasatch anticlinorium along the eastern transition zone; and (4) initial slip on the eastern thrust system with synorogenic sedimentation in an associated foredeep. Within the western region temperatures remained high with some areas experiencing peak metamorphism, and medium-displacement thrusts, including the Independence thrust, back folds, and basement-cored folds, such as the Winchell Lake nappe, produced minor thickening. Locally, shortening was punctuated by extension along normal-sense shear zones, including the Mahogany Peaks and Emigrant Springs shear zones. The alternating periods of shortening and extension accommodated adjustments of the orogenic wedge in response to a fluxing stress regime in the middle crust. The main part of the central region was passively transported eastward above a regional basal flat, with local uplift and erosion farther east above the Wasatch anticlinorium. Propagation of the basal decollement into basement along the eastern transition zone resulted in emplacement and folding of basement-cored thrust sheets to form the growing Wasatch anticlinorium, which marked a site of concentrated thickening and increased taper that helped drive emplacement of the eastern thrust system. The basal decollement propagated eastward into the base of the platform section, and slip on basement thrusts was mostly transferred into the developing eastern thrust system, which included the Crawford thrust and a decollement in Jurassic evaporites

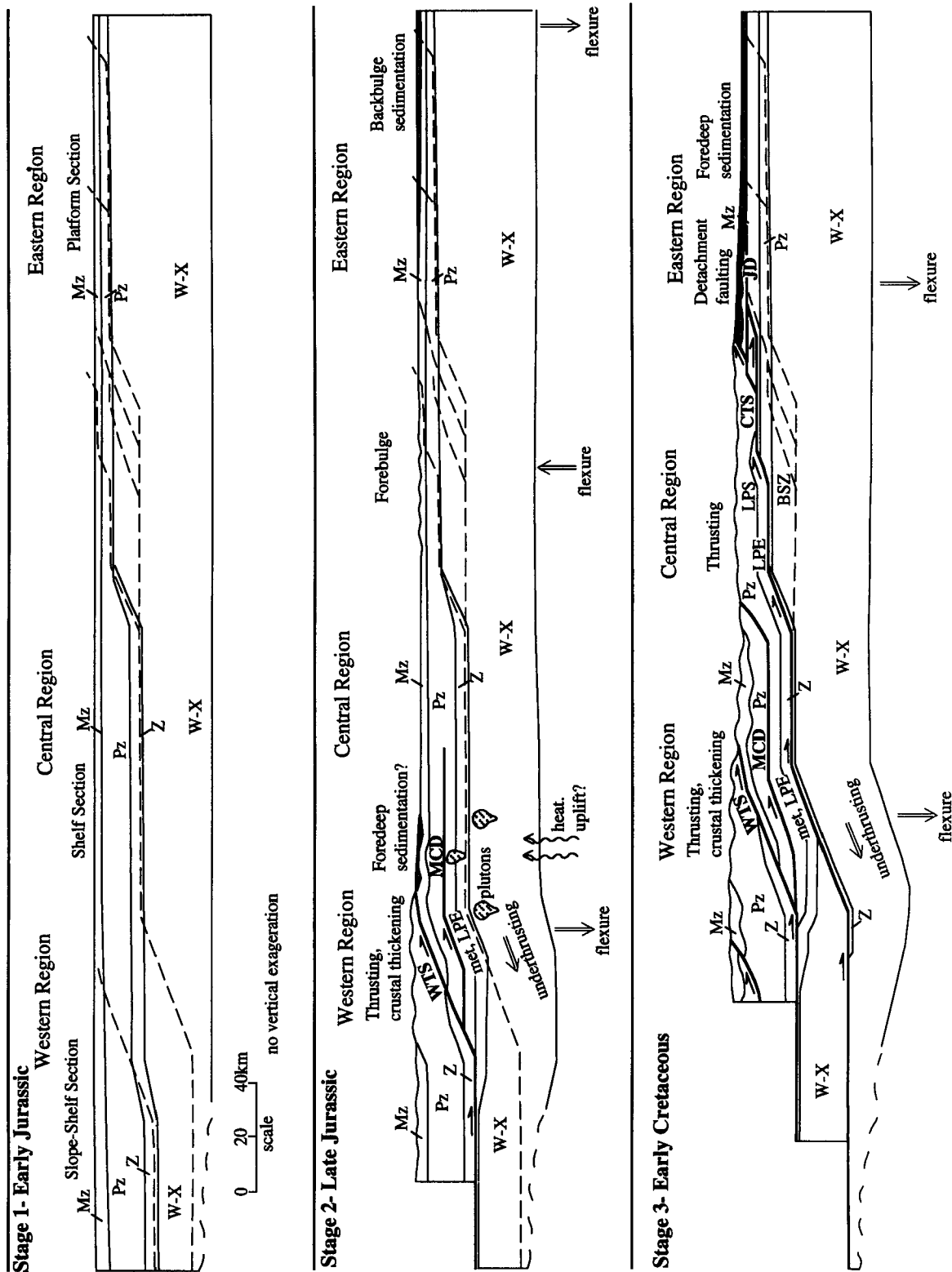
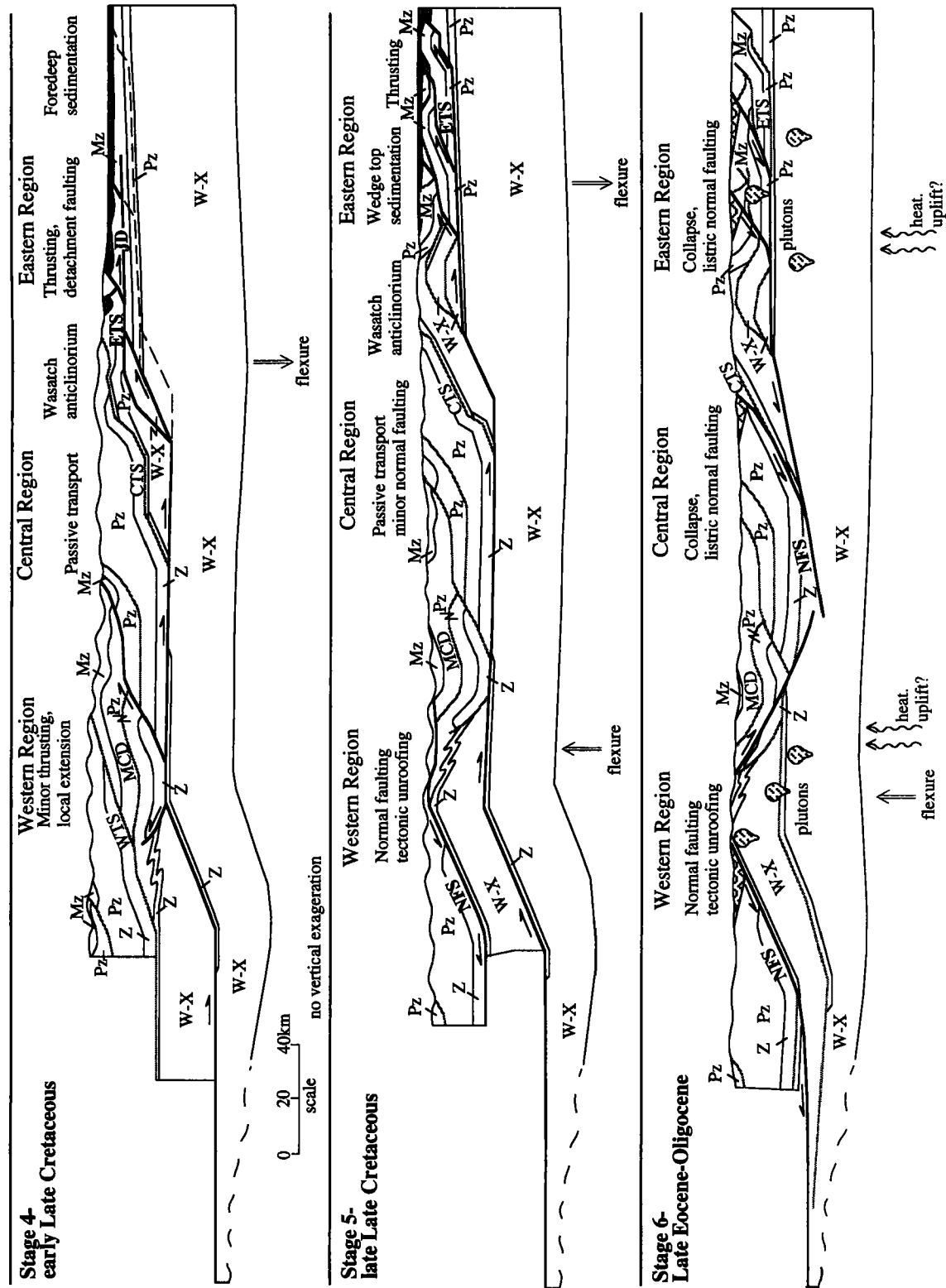


Figure 3. Simplified tectonic model for the evolution and subsequent collapse of the Sevier orogenic wedge. Note that it is unknown if large-magnitude crustal thickening in the western region was accommodated by a single or multiple thrust systems; for simplicity in this model we show a single thrust system (WTS). Active faults indicated by bold lines, inactive faults by gray lines, synorogenic sediments by dot pattern, and flexure from crustal thickening/thinning by arrows. W-X = Archean to Lower Proterozoic basement rocks; Z = Neoproterozoic



sedimentary and metasedimentary rocks, Pz = Paleozoic sedimentary and metasedimentary rocks; Mz = Mesozoic sedimentary rocks and synorogenic deposits; and Cz = post-thrusting Cenozoic deposits. WTS = western thrust system; MCD = Manning Canyon decollement, CTS = central thrust system; JD = decollement in Jurassic evaporites; and ETS = eastern thrust system. LPS = layer-parallel shortening; LPE = layer-parallel extension; met = metamorphism; BSZ = basement shear zones; NFS = normal fault system.

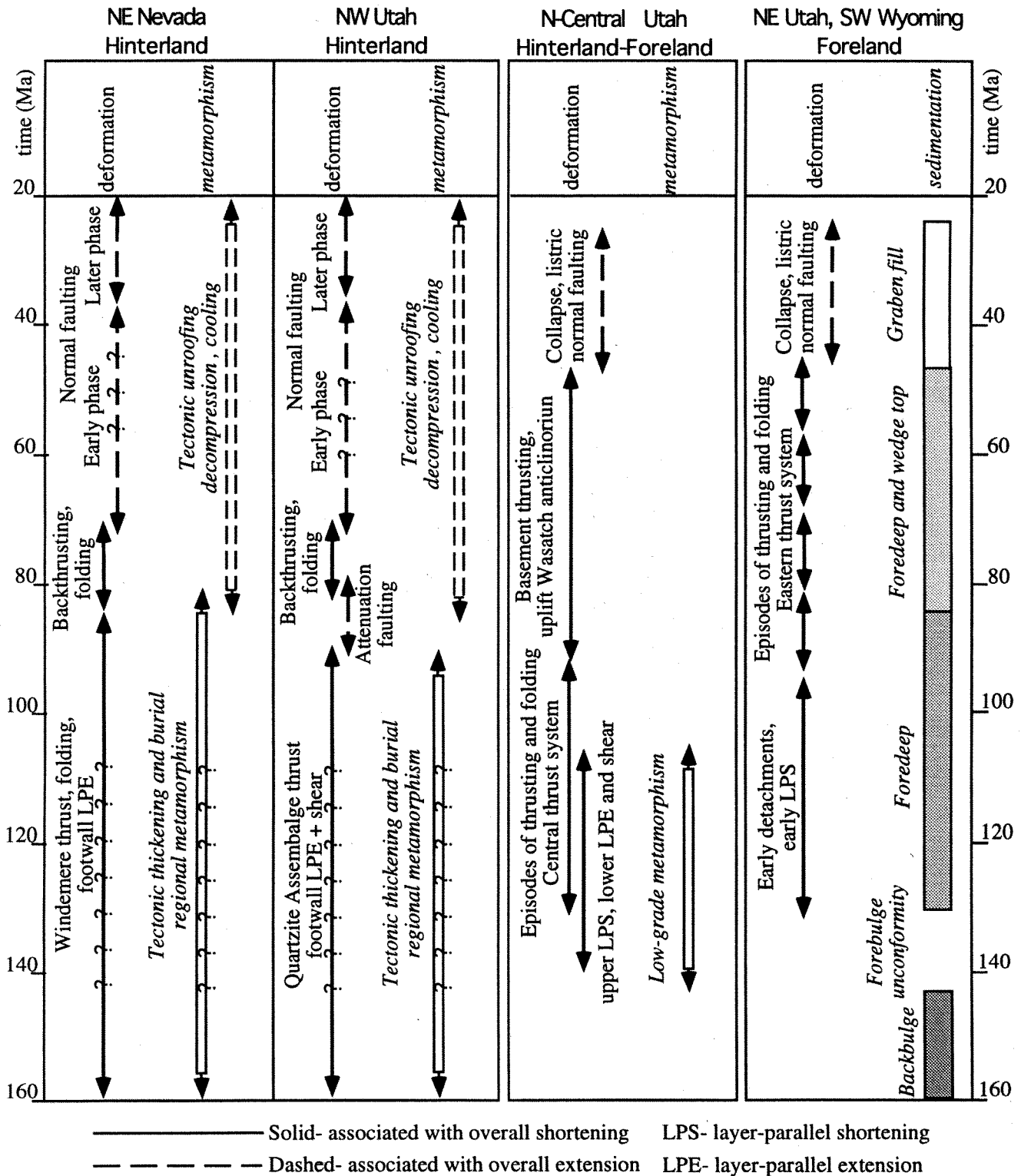


Figure 4. Chart illustrating the timing of deformational, metamorphic, and depositional events in various parts of the Sevier orogenic wedge.

that linked into the incipient Medicine Butte and Absaroka thrusts (Coogan and Royse, 1990; Coogan, 1992). Synorogenic deposits shed from the developing Wasatch anticlinorium and eastern thrust system accumulated proximally to growing thrusts and folds and within a foredeep to the east (DeCelles, 1994).

Stage 5—late Late Cretaceous to early Eocene

The Sevier orogenic wedge began to undergo significant changes during this stage, including: (1) initial tectonic unroofing in the western region; (2) passive thrust transport and local extension in the central region; (3) continued growth of the Wasatch anticlinorium; and (4) continued slip on the eastern thrust system with synorogenic wedge-top and foredeep sedimentation. The western region experienced widespread tectonic unroofing and cooling, especially in areas of previous tectonic thickening, with development of normal fault systems, including the Pequop and Basin-Elba faults. Evidence for deep synextensional basins is lacking, and relief may have been low or the entire area may have been elevated. Despite extension in the hinterland, thrust faults continued to develop in the frontal part of the Sevier orogenic wedge. Relations between the western projection of the basal decollement for the thrusts and the normal fault systems are uncertain. In this model, reverse slip along the deeper western crustal ramp in the basal decollement resulted in relative upward transport of mid-crustal rocks and transfer of slip eastward, simultaneous with upper crustal extension to reduce taper. Alternatively, extension may reflect adjustments of the hinterland to decreased horizontal stress, with listric normal faults rooting into a complex basal fault zone that included part of the thrust decollement (Constenius, 1996). The central region was passively transported above a regional flat, synchronous with development of low-angle normal faults to the west. The Wasatch anticlinorium continued to grow by incorporating basement thrust slices along the eastern transition zone, resulting in concentrated thickening that helped maintain taper. Slip from basement thrusts was largely transferred eastward into the eastern thrust system, in particular along the Absaroka and Hogsback thrusts, in an overall break-forward sequence. Minor fold-

ing and break-backward reactivation of thrusts produced internal thickening that also helped maintain taper of the wedge. Spacing between thrusts was closer, shortening was greater, and taper was probably higher within the thinner platform section compared to the thicker shelf section to the west, which had a weaker base. Synorogenic sediments derived from the frontal thrust sheets, Wasatch anticlinorium, and passively uplifted Willard thrust sheet were deposited proximally to growing thrust-tip folds on top of the wedge and in the foredeep depozone to the east.

Stage 6—Late Eocene to Oligocene

Thrusting within the Sevier orogenic wedge ceased and regional collapse of the frontal wedge began during Late Eocene (Constenius, 1996). Collapse involved development of listric normal faults, some of which reactivated earlier thrusts. In more eastern areas, asymmetric grabens and half grabens developed in the hanging walls of normal faults and accumulated thick clastic and volcanoclastic sequences. Low-angle normal shear zones in western areas uplifted and partially exhumed structurally deep metamorphic rocks. Widespread igneous activity also accompanied extension.

Much of the orogen was then overprinted by a final episode of Miocene to Recent extension during development of the Basin and Range Province. During this phase a series of widely spaced, generally moderate- to high-angle normal faults developed, resulting in further fragmentation of the orogen, as well as uplift of footwalls that expose partial crustal cross sections, providing us with a unique opportunity to view the architecture of the Sevier orogen.

ACKNOWLEDGMENTS

We thank Tim Lawton, Paul Link, Lon McCarley, and Wanda Taylor for constructive reviews of this manuscript. Camilleri acknowledges support of this project from the donors of the Petroleum Research Fund, administered by the American Chemical Society (ACS-PRF# 30860-GB2), and from an Austin Peay State University Tower Grant. Yankee acknowledges support from National Science Foundation grant EAR-9219809.

The Architecture of the Sevier Hinterland: A Crustal Transect through the Pequop Mountains, Wood Hills, and East Humboldt Range, Nevada

PHYLLIS CAMILLERI

Department of Geology and Geography, Austin Peay State University, Clarksville, Tennessee

ALLEN MCGREW

Department of Geology, University of Dayton, Dayton, Ohio

INTRODUCTION

The Pequop Mountains, Wood Hills, and East Humboldt Range region provides an exceptionally complete cross-section of the hinterland of the Mesozoic Sevier orogenic belt from the deep middle crust to upper crustal levels (Fig. 5). From east to west these ranges expose miogeoclinal strata representing progressively deeper structural levels of the polydeformed Mesozoic crust; from unmetamorphosed to greenschist facies rocks in the Pequop Mountains to ~5.5–6.4 kb amphibolite facies rocks in the Wood Hills and ~8.6 kb partially melted upper amphibolite facies rocks in the East Humboldt Range (Fig. 5). These metamorphic rocks lie structurally beneath, and were exhumed by, the west-rooted Cretaceous-Tertiary(?) Pequop normal fault and the Oligocene-Miocene Mary's River normal fault system (here taken in a broad sense to include the well-known Ruby Mountains-East Humboldt Range mylonitic shear zone and detachment fault as well as other normal faults in the area that we believe to be correlative [e.g., Snoke and Lush, 1984; Mueller and Snoke, 1993a,b]).

On this part of the field trip we will examine evidence for three major phases of Mesozoic deformation in the hinterland that were roughly coeval with deformation in the Sevier foreland. Older episodes of deformation no doubt affected this area, but their imprint is obscure. The first two phases of deformation discussed here are contractional and the last is extensional. The major phase of tectonic burial in this region occurred during the first phase of deformation due to emplacement of a southeast-tapering thrust wedge as much as 30 km thick above an inferred sole fault, the Windermere thrust (Camilleri and Chamberlain, 1997; Fig. 6F). The second phase of deformation involved (1) overprinting of the Windermere thrust footwall by the top-to-the-southeast Independence thrust at shallow structural levels and (2) emplacement of a basement-cored fold-nappe (the Winchell Lake nappe; Lush et al., 1988; McGrew, 1992) at deep structural levels (Figs.

6E and 7). Although the Winchell Lake nappe may have accommodated a large amount of shortening, the Pequop Mountains-Wood Hills-East Humboldt Range terrain did not significantly increase in depth of burial during this phase of deformation. The third phase of deformation resulted in as much as 10 km of crustal thinning accommodated by the Pequop normal fault (Fig. 6D).

PRESENT DISTRIBUTION OF STRUCTURES AND METAMORPHISM

Structural features produced during the three phases of Mesozoic deformation exist within the Pequop Mountains-Wood Hills-East Humboldt Range region (Fig. 8), although their present distribution in map-view is complex due to overprinting and exhumation by the Tertiary Mary's River fault system (see Fig. 6 A, B, and C). The vast tract of Barrovian style, regionally metamorphosed miogeoclinal rocks that lie beneath the Pequop and Mary's River low-angle normal faults are remnants of the metamorphosed to unmetamorphosed footwall of the Windermere thrust (Figs. 5 and 8). Metamorphic grade and pressure in the footwall increase toward the northwest (Fig. 5).

A remnant of the Pequop fault is exposed in the Pequop Mountains, and low-angle normal faults of the Mary's River fault system are present in the Wood Hills and East Humboldt Range (Fig. 8). These fault systems have been dissected by younger, Miocene to Holocene normal faults (Fig. 8). The Mary's River faults overlie a related top-to-the-WNW, normal-sense mylonitic shear zone with a WNW-trending stretching lineation (Snoke and Lush, 1984; Snoke and others, 1990). The mylonitic fabrics overprint Mesozoic fabrics and structures throughout the East Humboldt Range and locally in the northern part of the Wood Hills (McGrew, 1992; Camilleri 1994b; Fig. 5). The hanging walls of the low-angle normal faults contain unmetamorphosed Paleozoic strata, which are remnants of the

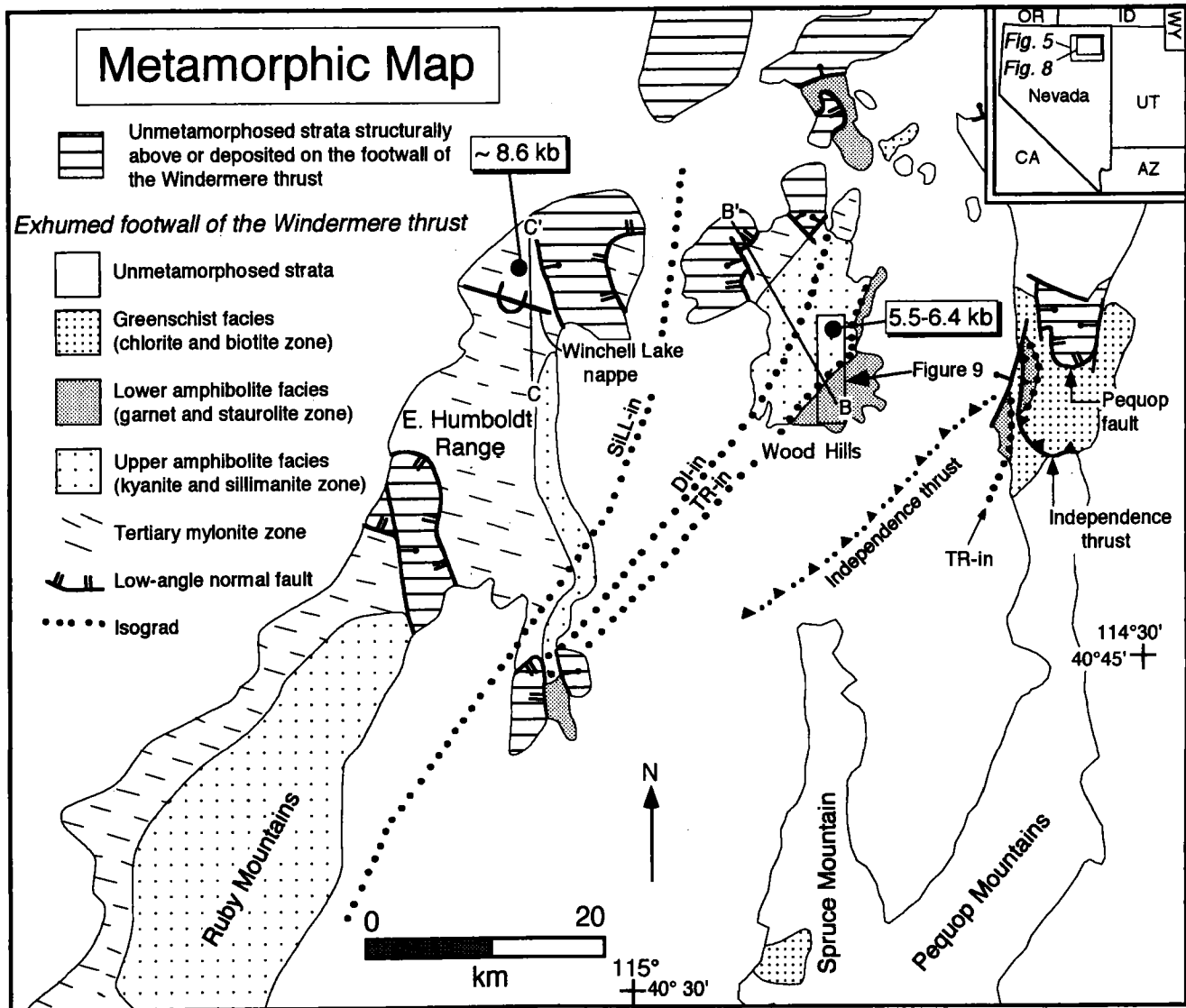


Figure 5. Metamorphic map of the Pequop Mountains, Wood Hills, and East Humboldt Range region. Modified after Camilleri and Chamberlain (1997). Barometric data shown in the Wood Hills are from Hodges *et al.* (1992) and in the East Humboldt Range from McGrew (1992) and Peters and McGrew (1994). SILL = sillimanite; DI = diopside; TR = tremolite.

Windermere thrust plate. In addition, hanging wall rocks of the Mary's River fault system also contain preextension Tertiary volcanic rocks and overlying synextensional sedimentary rocks (Humboldt Formation) (Fig 8; Mueller and Snoke, 1993a, b).

The Independence thrust and a series of NW-vergent back folds in its hanging wall are exposed in the Pequop Mountains and Wood Hills (Fig. 8). The back folds are cored by small displacement thrusts. Regionally, the folds have NE-SW trending axes. The fold geometry varies with metamorphic grade from predominantly kink folds in greenschist facies rocks in the Pequop Mountains to overturned

and recumbent folds in upper amphibolite facies rocks in the Wood Hills (Fig. 7A).

The Winchell Lake nappe is a recumbent fold with a WNW-trending axis exposed in the northern East Humboldt Range (Figs. 7B and 8). The nappe is cored by Archean and Proterozoic basement, which in turn is enveloped by a severely attenuated miogeoclinal section (Fig. 7B). An inferred premetamorphic fault separates basement rocks in the core from enveloping miogeoclinal strata. The nappe is bounded below by a premetamorphic fault that repeats the Paleozoic section at depth (Fig. 7B). Incomplete exposure of the nappe and intense overprinting by the Tertiary

extensional mylonitic shear zone make its original vergence and geometry uncertain.

STRUCTURAL EVOLUTION

In this section we illustrate the evolution of the Windermere and Independence thrusts, and Pequop and Mary's River faults utilizing a northwest-southeast reconstruction along A-A' (Figs. 6 and 8) by Camilleri and Chamberlain (1997). The cross sections (Fig. 6A to 6D) show sequential evolution of the Pequop Mountains-Wood Hills-East Humboldt Range region from the present to a time just after cessation of slip along the Independence thrust. We infer that the Winchell Lake nappe formed at approximately the same time as the Independence thrust, although the nappe as well as back folds in the hanging wall of the Independence thrust are too small to show at the scale of the cross sections. Figure 6F shows the sequence of metamorphic facies and isograds in the footwall of the Windermere thrust just before development of the Independence thrust.

Phase 1

The Windermere thrust (Fig. 6F) represents the first major phase of contraction that produced most of the tectonic burial in the region. The Windermere thrust is an inferred fault based in part on barometric constraints that imply structural burial of the metamorphosed footwall to levels deeper than stratigraphic depths and in part on the repetition of miogeoclinal strata across the younger, low-angle normal faults (cf. Camilleri and Chamberlain, 1997). For example, the Mary's River fault in the northwestern part of the Wood Hills and southern Windermere Hills contains an unmetamorphosed Devonian to Permian section in its hanging wall, which lies directly above regionally metamorphosed Devonian to Permian strata in its footwall (cf. Figs 5 and 8). These relationships require that the Mary's River fault cut two Paleozoic sections that were duplicated by thrust faulting prior to normal faulting.

Although inferred in the Wood Hills and Pequop Mountains, the Windermere thrust may be exposed in the northern East Humboldt Range where at least three different premetamorphic faults duplicate the miogeoclinal section. In addition, an early phase of small-scale isoclinal folding in the East Humboldt Range may date from this period (McGrew, 1992). The premetamorphic faults and small-scale folds have been so thoroughly overprinted by Late Cretaceous and Tertiary metamorphism and deformation that it is difficult to precisely reconstruct their kinematics.

Regional structural and thermochronologic data require that the Windermere thrust formed before 84 Ma (Camilleri and Chamberlain, 1997). Exactly when the Windermere thrust formed is uncertain, but regional relationships indi-

cate that contraction in this region began during the late Middle Jurassic (e.g., Miller and Allmendinger, 1991; Hudec, 1992; Click, 1987; Miller and Hoisch, 1992, 1995). Thus we infer the thrust formed at some time in/after the Jurassic but before 84 Ma. During and/or following emplacement of the thrust wedge, the footwall of the Windermere thrust underwent Barrovian metamorphism and partial melting at deep levels in response to burial. Thermochronologic data indicate that peak metamorphism at shallow structural levels in the Pequop Mountains was attained at ~84 Ma and at deep levels in the East Humboldt Range between 70 and 90 Ma (J.E. Wright, pers. comm.). Thermal weakening of the footwall during metamorphism, coupled with the hanging wall load, induced bulk ductile coaxial flow resulting in attenuation or collapse of the footwall and production of bedding parallel or nearly parallel prograde S-L (S_1 and L_1) and S-tectonites (Camilleri, 1994a,b). Collapse of the footwall probably facilitated sinking of the hanging wall with a consequent reduction in surface topography.

Due to subsequent extensional excision, little is known about the structural geometry of the Windermere thrust plate. We do not know whether burial of the footwall was accomplished by a series of structurally overlying imbricate thrust sheets or by an intact crustal wedge above the Windermere thrust. However, the presence of multiple supracrustal thrust faults that cut Paleozoic and Triassic strata (e.g., Coats and Riva, 1983) to the north and west of the Pequop Mountains-Wood Hills-East Humboldt Range terrain suggests that a polyphase imbricate thrust wedge is more likely.

Phase 2

The second phase of deformation involved development of the Independence thrust and back folds in its hanging wall (Figs. 6E and 7A), both of which are bracketed between 84 and 75 Ma (Camilleri and Chamberlain, 1997). The Winchell Lake fold-nappe (Fig. 7B) formed during regional migmatization and sillimanite zone peak metamorphism between 70 and 90 Ma (McGrew, 1992), approximately the same time as the Independence thrust. All of these structures formed after a phase 1 kyanite zone metamorphic event that records the tectonic burial of this region. Moreover, the nappe and Independence thrust deform the prograde metamorphic fabric (S_1), and we suggest that all are manifestations of a single continuum of contractional deformation developed at different structural levels. However, extensional tectonism represented by the Pequop normal fault may also have begun before 75 Ma (Camilleri and Chamberlain, 1997), so timing constraints are still too broad to allow definitive correlation of the Winchell Lake fold-nappe with the contractional episode that produced the

Independence thrust rather than the later Cretaceous extension. In either case, development of the Independence thrust and associated back folds marks a fundamental transition from bulk coaxial stretching of the middle crust during phase 1 to horizontal contraction during phase 2.

In support of the correlation between the Winchell Lake fold-nappe and the second phase of deformation that produced the Independence thrust, we note the similarity in deformational style between the fold-nappe and the north-west-vergent recumbent back-folds in the highest grade part of the Wood Hills (cf. Figs 7A and 7B). However, this correlation is rendered uncertain by the lack of continuous exposure between the Wood Hills and the East Humboldt Range and by a few important differences between the Winchell Lake fold-nappe and the folds in the Wood Hills. (1) Archean basement is involved in the core of the Winchell Lake fold-nappe but is not observed in the Wood Hills (although basement involvement at depth is a definite possibility). (2) The Winchell Lake fold-nappe is structurally detached whereas the folds in the Wood Hills are not. (3) The Winchell Lake fold-nappe has a WNW-trending hinge line and closes toward the south whereas the Wood Hills folds trend toward the northeast with a vergence toward the northwest. Differences (1) and (2) may merely reflect variations in deformational style with increasing structural depth and metamorphic grade. The third difference may be explained at least in part by transposition of the Winchell Lake fold-nappe in the Tertiary mylonitic shear zone that envelopes it. In support of this interpretation, we note that the hinge line of the fold-nappe is colinear with the Tertiary mylonitic stretching lineation that overprints it. We suggest that the nappe may originally have had a northeast trending hinge line similar to the folds in the Wood Hills, but that mylonitic shearing rotated it into parallelism with the Tertiary stretching lineation.

Phase 3

The Pequop normal fault marks a fundamental change from horizontal contraction to extension in the upper to middle crust of the Sevier hinterland in the Pequop Mountains-Wood Hills-East Humboldt Range region. Cross-cutting relationships indicate that the Pequop fault is younger than the Independence thrust, and that both the Independence thrust and Pequop fault postdate development of the 84 Ma (S_1) metamorphic fabric (Camilleri and Chamberlain, 1997). In addition, the Pequop fault must be older than 41–39 Ma (Brooks et al., 1995) because volcanic rocks of this age depositionally overlap both the hanging wall and the footwall of the Pequop fault in the Pequop Mountains (Fig. 8). Furthermore, thermochronologic data from metamorphic rocks in the footwall of the

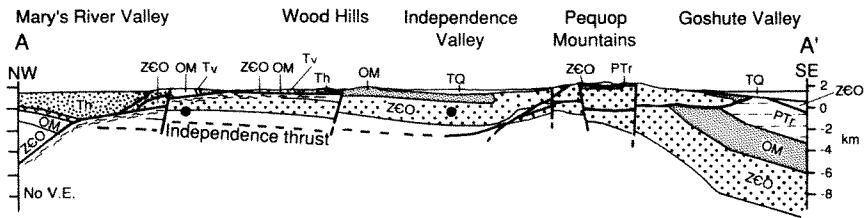
Windermere thrust in the Pequop Mountains and Wood Hills suggest that the rocks began cooling by ~75 Ma (Thorman and Snee, 1988; Camilleri and Chamberlain, 1997). We suggest that this early phase of cooling reflects partial exhumation of the metamorphic rocks by the Pequop fault. The implication is that the Pequop fault formed after 84 Ma but before initial cooling at 75 Ma. The duration of slip on the Pequop fault is unknown; activity could have continued until 41 Ma. Moreover, $^{40}\text{Ar}/^{39}\text{Ar}$ cooling ages on mica in the Wood Hills and hornblende in the East Humboldt Range suggest a cooling event in Paleocene to Early Eocene time (McGrew and Snee, 1994; Thorman and Snee, 1988). Final exhumation and cooling of the metamorphic rocks was accomplished by the Tertiary Mary's River fault system (Fig. 6 A, B, and C).

DAY 1: ROAD LOG FROM WENDOVER TO THE NORTHERN EAST HUMBOLDT RANGE, NEVADA

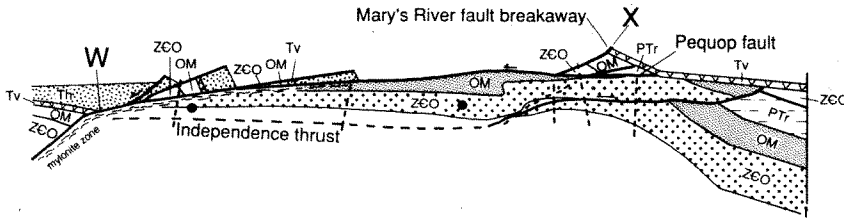
On day 1 of this field trip we will observe the metamorphic fabrics in the footwall of the Windermere thrust and examine structures developed during the second phase of Mesozoic deformation. At stops 1-1 and 1-2 we will view the Independence thrust and Winchell Lake nappe, respectively. At stop 1-3 we will observe prograde metamorphic fabrics in the footwall of the Windermere thrust in the southern part of the Wood Hills and at stop 1-4, in the northern part of the Wood Hills, we will observe these fabrics overprinted by an overturned back fold. Last, at stop 1-5 we will hike to and observe the Winchell Lake nappe.

MILEAGE		DESCRIPTION
Incre-	Cumu-	
mental	lative	
0.0	0.0	Road log begins at westbound entrance to Interstate 80 at the west end of Wendover. Proceed west on Interstate 80.
2.9	2.9	Toano-Goshute Range and the Pilot Range are in the foreground (see Fig. 2). Both of these ranges record mainly Late Jurassic plutonism, regional-contact metamorphism, and minor contractional deformation (Glick, 1987; Miller and Hoisch, 1992; 1995).
2.7	5.6	The Pilot Range is to the right. Much of Pilot Range in view is composed of Lower Paleozoic strata that underwent regional-contact metamorphism and southeast vergent folding during the Late Jurassic (Miller and Hoisch, 1992; 1995)

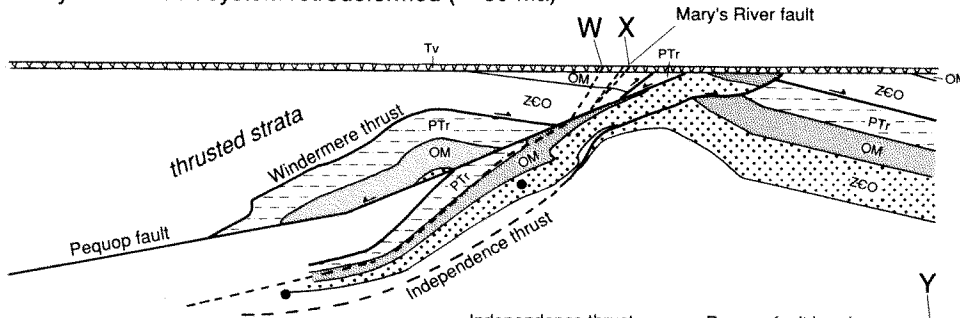
A. Present



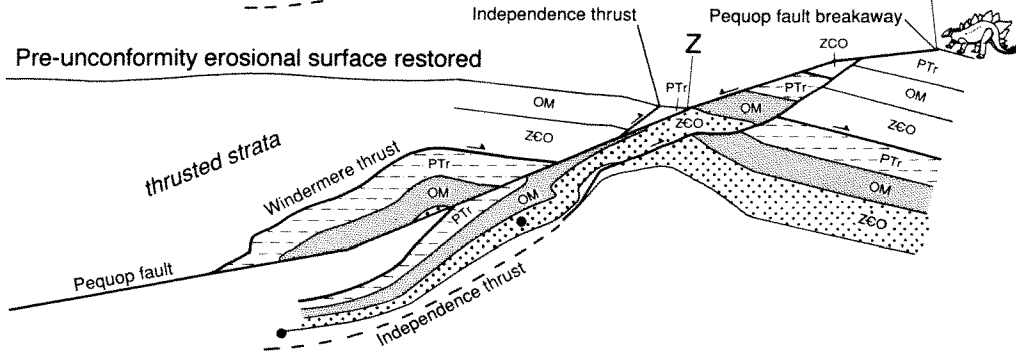
B. Minor high-angle faults retrodeformed and eroded units and structures projected into the line of section



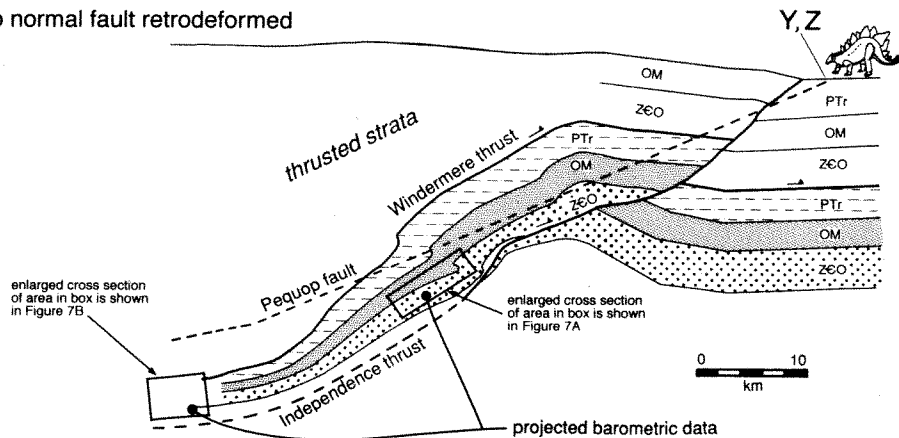
C. Mary's River fault system retrodeformed (~ 39 Ma)



D. Pre-unconformity erosional surface restored



E. Pequop normal fault retrodeformed



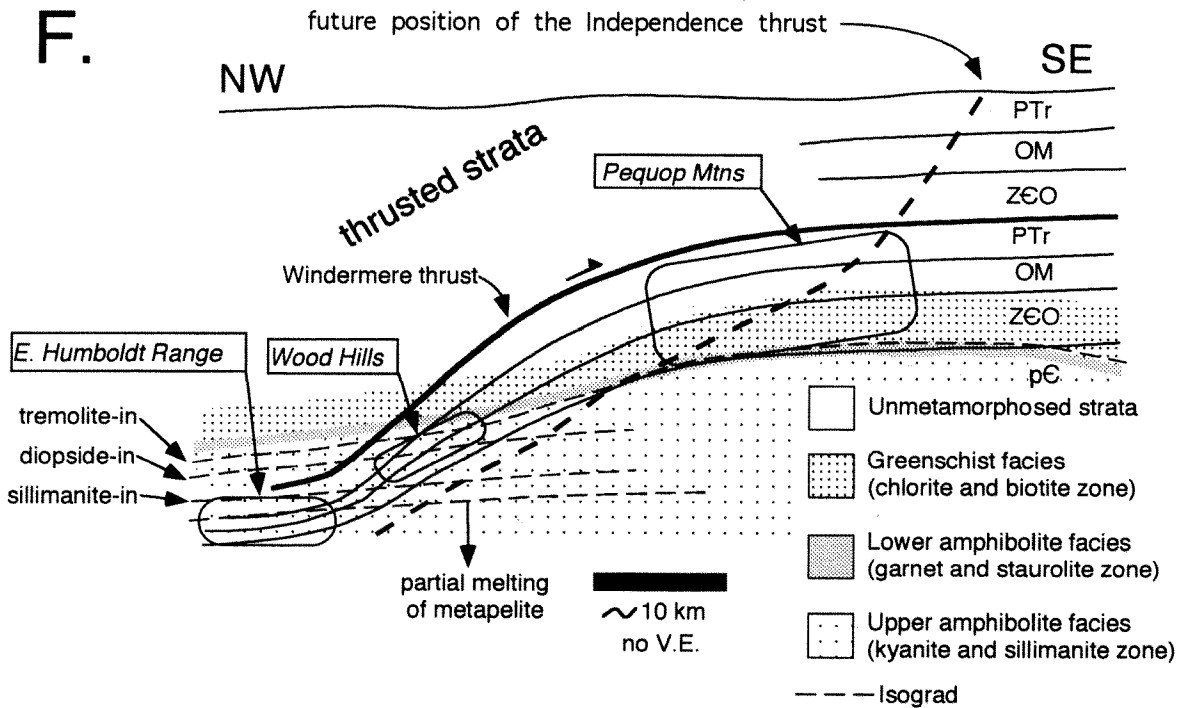


Figure 6. Northwest-southeast tectonic reconstruction along line A-A' (Fig. 8) from the present (A) to the Mesozoic (F). Cross sections A-C show the evolution of the Mary's River fault system. Cross section C shows the Mary's River fault retrodeformed at a time just after deposition of the 41–39 Ma volcanic rocks. Cross sections D and E show the evolution of the Independence thrust and Pequop fault following 84 Ma but prior to deposition of the volcanic rocks. Cross section E outlines the positions of the folds shown in figure 7, which are too small to show at the scale of this cross section. Cross section F shows the footwall of the Windermere thrust at ~84 Ma during peak metamorphism, and also shows those parts of the footwall that are presently exposed in the northern East Humboldt Range, Wood Hills, and Pequop Mountains. TQ = Quaternary and Tertiary surficial deposits; Th = Oligocene-Miocene Humboldt Formation; Tv = Eocene Volcanic rocks; PTr = Pennsylvanian, Permian, and Triassic strata; OM = Ordovician, Silurian, Devonian, and Mississippian strata; ZCO = Proterozoic, Cambrian and Ordovician strata; XZ = Proterozoic and Archean basement. W, X, Y, and Z are reference points. Barometric data from the Wood Hills and East Humboldt Range (Fig. 8) are shown projected into the cross sections. Modified after Camilleri and Chamberlain (1997).

11.8 17.4 Late Jurassic Silver Zone Pass pluton in the Toano Range is on your right. The Silver Zone Pass pluton intrudes lower Paleozoic strata that contain syn- to pre-plutonic metamorphic fabrics (Glick, 1987; Miller and Hoisch, 1992; 1995).

5.1 22.5 **STOP 1-1** (Fig. 2).

Get off the freeway at the Shafter exit and park in gravel lot south of the freeway. The Pequop Mountains are to the west. Unlike the Toano and Pilot Ranges, the Pequop Mountains, Wood Hills, and East Humboldt Range record mainly Cretaceous metamorphism and deformation.

The Pequop Mountains expose the lowest grade part of the exhumed footwall of the Windermere thrust. Metamor-

phic grade within the Pequop Mountains decreases up section from garnet zone Lower Cambrian strata to unmetamorphosed Mississippian and Pennsylvanian strata. Analysis of crystallographic preferred orientations of quartz c-axes in quartzite and textural analysis of poly-mineralic metamorphic rocks in the Pequop Mountains indicate a dominantly coaxial strain path during metamorphism (Camilleri, 1994a,b). A U-Pb sphene age from Cambrian meta-carbonate indicates a metamorphic peak at, and minimum age of the metamorphic fabric of, ~84 Ma (Camilleri and Chamberlain, 1997). The 84 Ma fabric is cut by the Late Cretaceous Independence thrust.

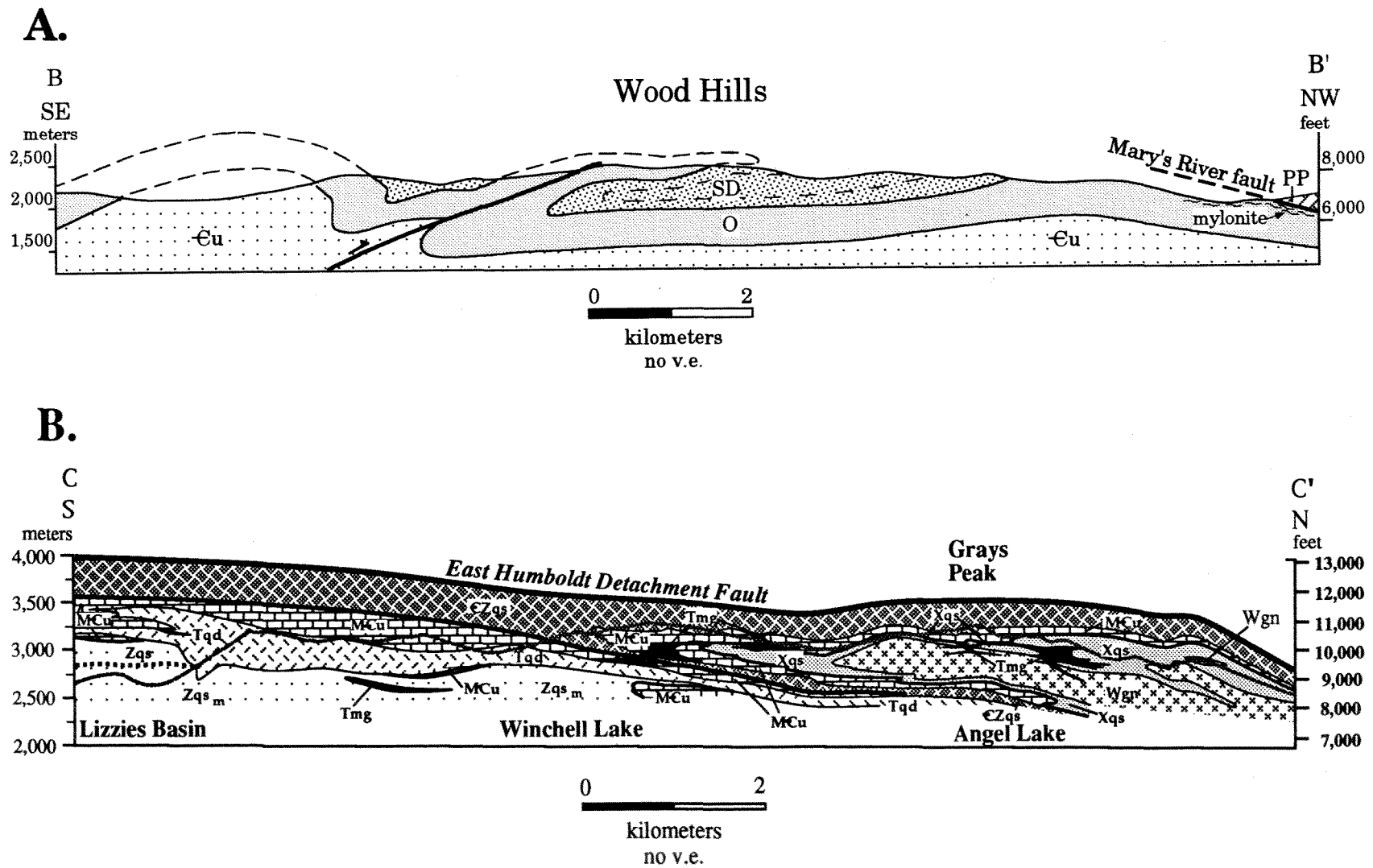


Figure 7. A. Simplified cross section of folds in the hanging wall of the Independence thrust in the Wood Hills. Cu = Cambrian metasedimentary rocks; O = Ordovician metasedimentary rocks; SD = Silurian and Devonian metasedimentary rocks; PP = unmetamorphosed Pennsylvanian and Permian strata. B. Cross section of the Winchell Lake fold-nappe. In this cross section the topographic surface is shown as a gray line, and units and structures are projected above the topographic surface. Wgn = Archean orthogneiss; Xqs = Early Proterozoic paragneiss; Zqs = paragneiss sequence of Lizzies Basin consisting of Neoproterozoic quartzite, schist, and marble (subscript "m" denotes leucogranite percentages > 65%); CZqs = Cambrian-Proterozoic quartzite and schist sequence; MCu = Mississippian to Cambrian marble and schist, undifferentiated; Tmg = 29 Ma biotite monzogranite. The inferred positions of the folds in the Wood Hills and the Winchell Lake nappe at their time of formation are shown in the reconstruction in Figure 6E. Locations of cross sections are shown in Figures 5 and 8.

To the south in the Pequop Mountains, at about 9:00, the trace of the Late Cretaceous Independence thrust (Fig. 8) is visible. The trace of the thrust lies near the base of the tree-covered slopes. In this locality, hanging wall rocks are metamorphosed (chlorite zone) Ordovician Pogonip Group and footwall rocks (barren slopes) are unmetamorphosed Mississippian Chainman Shale-Diamond Peak Formation.

- Return to the freeway and proceed west to Wells. As we cross the Pequop Mountains we will drive down-section through Pennsylvanian to Devonian carbonate and siliciclastic rocks in the hanging wall of the Independence thrust (Fig. 8).
- 11.1 33.6 Barren reddish brown slopes on both sides of the freeway are composed of Mississippian Chainman Shale-Diamond Peak Formation.
- 1.9 35.5 Tree covered slopes at 9:00 comprise the Mississippian Tripon Pass Limestone.
- 2.3 37.8 On both sides of the freeway gray, cliff-forming limestone of the Devonian Guilmette Formation is exposed.
- 1.7 39.5 Independence Valley and the Wood Hills are straight ahead.
- 7.6 47.1 High peaks immediately to the south are composed of metamorphosed Devonian Guilmette Formation.
- 2.0 49.1 Low-lying hills immediately to the south of the freeway are composed of Miocene Humboldt Formation (Thorman et al., 1990), which lies in the hanging wall of a segment of the Mary's River fault system (Fig. 8). Bedding within these rocks, although not visible from this vantage point, dips around 25–35° east (Thorman, 1970).
- 0.8 49.9 East-dipping Humboldt Formation is exposed in the roadcut on the south side of the freeway.
- 4.8 54.7 Unmetamorphosed Permian strata are exposed immediately to the south. These Permian rocks form part of an unmetamorphosed sequence of Devonian to Permian strata that are also part of the hanging wall of the Mary's River fault (Fig. 8). Devonian to Permian rocks are also exposed in the footwall of the Mary's River fault in this area but they are regionally metamorphosed (Fig. 8). The Mary's River fault in the northern Wood Hills is part of the Mary's River fault system (cf. Mueller

and Snoke, 1993a), which is primarily responsible for exhumation of the structurally deep regionally metamorphosed Paleozoic strata in the East Humboldt Range and Wood Hills. An important aspect of the Mary's River fault here is that it duplicates Paleozoic strata. This relationship requires that the Paleozoic section was duplicated by thrust faulting prior to normal faulting. Furthermore, this is one piece of evidence requiring the inferred Windermere thrust.

- 1.6 56.3 Take first Wells exit and proceed south on U.S. Highway 93.
- 1.0 57.3 The hills immediately due east expose unmetamorphosed Devonian to Permian strata in the hanging wall of the Mary's River fault (Fig. 8).
- 3.2 60.5 The metamorphic sequence of the Wood Hills is exposed to the east.
- 3.9 64.4 **STOP 1-2** (Fig. 8)
Turn left onto dirt road at the gravel pit, cross over the cattle guard, and park. View of East Humboldt Range and southern Wood Hills. To the east, in the southern Wood Hills, kyanite zone Ordovician Pogonip Group strata are exposed. To the west, in the northern East Humboldt Range, partially melted, sillimanite zone Archean basement and Proterozoic to Mississippian metasedimentary rocks are exposed. The sillimanite-in isograd is inferred to be concealed beneath the valley fill between the Wood Hills and northern East Humboldt Range (Fig. 5). From this vantage point we have an excellent view of the Late Cretaceous Winchell Lake nappe in the East Humboldt Range.

From the gravel pit, proceed east on the dirt road that veers to the right.

- 0.7 65.1 Dirt road bifurcates at the railroad tracks. Turn right and proceed south.
- 1.6 66.7 Spruce Mountain is at 1:00. The highest peak on Spruce Mountain is 10,076' and is composed of low-grade metamorphosed Ordovician Pogonip Group strata (Hope, 1972). The low-lying ridge or prong of Spruce Mountain extending to the north is composed of unmetamorphosed Pennsylvanian to Permian strata intruded by a Mesozoic or Tertiary hornblende diorite pluton (Hope, 1972).

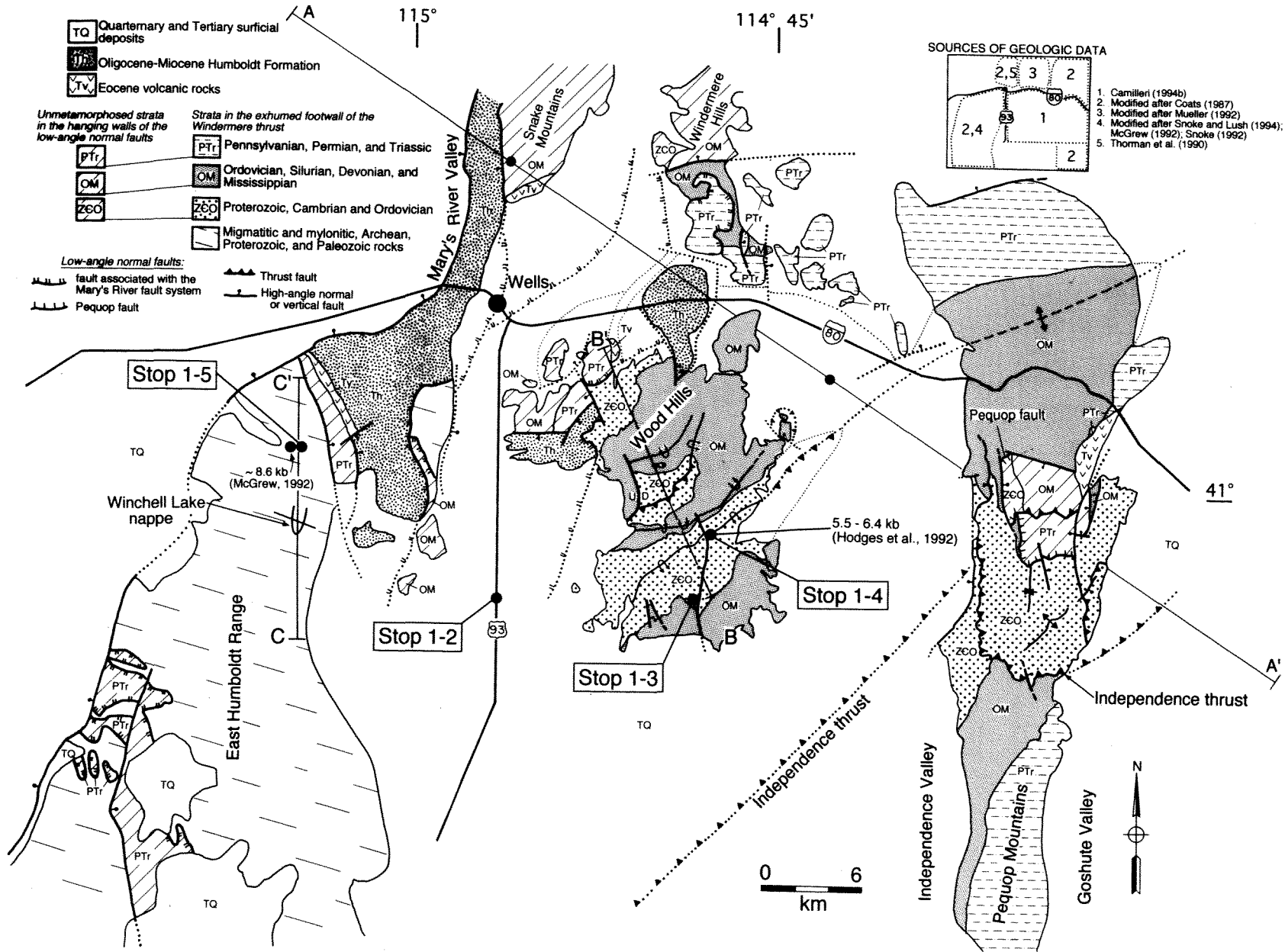


Figure 8. Simplified geologic map of the Pequop Mountains-Wood Hills-East Humboldt Range region. Fault and stratigraphic contacts are shown dotted where concealed by Quaternary and Tertiary surficial deposits. Modified after Camilleri and Chamberlain (1997).

- 3.8 70.5 Dirt road bifurcates. Take road to the left toward Warm Springs.
- 0.9 71.4 Cross railroad tracks. Immediately after crossing the tracks, the road we are traveling on splits into four dirt roads. Counting from the railroad tracks on your right take the third road (or second road from the tracks on your left).
- 1.4 72.8 The Pequop Mountains are straight ahead.
- 2.0 74.8 Turn left on dirt road that heads towards the southern Wood Hills.
- 1.0 75.8 Looking to the north in the Wood Hills, we can see southeast dipping gray Devonian to Ordovician dolomite. These rocks constitute the lowest grade rocks in the Wood Hills as well as part of the upright limb of a NW-vergent overturned anticline, a back fold in the hanging wall of the Independence thrust (Figs. 7 and 9).
- 0.8 76.6 On the left or east side of the canyon is the basal sandy (quartzose) dolomite of the Devonian Simonson Dolomite. Thin section examination of these rocks indicates that they are metamorphosed, although they lack a macroscopic metamorphic fabric, and upon close inspection cross-bedding is visible. As we proceed up the canyon from north to south we will traverse down-section through Devonian to Ordovician dolomite.
- Degree of recrystallization of dolomite and of fabric development increases down-section such that Ordovician to Silurian dolomite is a fine-grained marble and contains a well-developed bedding-parallel cleavage or foliation.
- 1.1 77.1 **STOP 1-3** (Fig. 9).
Park on dirt road. On this stop we will observe the prograde metamorphic S-L tectonite in Ordovician rocks. On the east side of the canyon, foliated and lineated Ordovician Lehman Formation, Eureka Quartzite, and Fish Haven Dolomite are exposed. From here we can see that foliation is approximately parallel to stratigraphic boundaries and we can observe a complete but plastically attenuated section of Eureka Quartzite. Here, the Eureka Quartzite is approximately 75' thick, whereas regionally the Eureka Quartzite is generally 200' thick or greater.

Hike up the hillside to observe S_1 fabric elements. At the base of the hill, fine-grained micaceous marble of the Lehman Formation is exposed. Foliation dips about 30° to the southeast and pronounced stretching lineations trend approximately 23° to the east-southeast. The overlying Eureka Quartzite has a well developed foliation, but lineation is less well pronounced. The Fish Haven Dolomite consists of dark gray dolostone with chert lenses and abundant tiny pelmatozoan fragments, and has a strong bedding-parallel foliation. Stretching lineations are poorly developed and are generally only visible on chert lenses. Petrofabric analyses of quartz c-axes from the Eureka Quartzite in this and other localities in the Wood Hills suggests predominantly coaxial plane strain accompanied metamorphism (Camilleri, 1994a,b).

Return to vans. Proceed north on dirt road.

2.8 80.5 **STOP 1-4** (Fig. 9).

Park on the side of the dirt road. At this stop we will hike up into the Dunderberg Shale [schist] in the core of the northwest-vergent overturned anticline (Fig. 9). We will observe the overprinting effects of the fold on S_1 . Bring lunch and water.

Hike up the hillside to the saddle on the north-trending ridge on the east side of the canyon. In the saddle the Upper Cambrian Dunderberg Shale [schist] is exposed in the core of the anticline. On the southern slope of the saddle, the Cambrian Notch Peak Formation (calcite marble) is exposed on the upright limb of the anticline and on northern slope of the saddle the Notch Peak Formation is exposed again in the overturned limb of the anticline.

The Dunderberg Shale contains porphyroblastic garnet, staurolite/kyanite, and biotite. Kyanite in these rocks is a by-product of the breakdown of staurolite by a reaction such as quartz + muscovite + staurolite = biotite + garnet + kyanite. The general metamorphic mineral assemblage is biotite-staurolite-kyanite-garnet-muscovite-quartz-plagioclase-allanite-rutile-ilmenite. Barometric analysis of this

EXPLANATION

- Qs Surficial deposits (Quaternary)
alluvium and colluvium
 - OSDd Fish Haven, Laketown, Sevy, and Simonson dolomite, undivided (Ord., Sil., and Dev.)
dolomitic marble/dolostone with a dolomitic quartz sandstone/quartzite at the base
 - Oe Eureka Quartzite (Ordovician)
 - Opl Lehman Formation (Ordovician)
micaceous calcite marble
 - Opc Unit C (Ordovician)
phyllite or schist near the top (= Kanosh Shale), micaceous calcite marble
in the middle and ~ 50' thick quartzite at the base
 - Opb Unit B (Ordovician)
micaceous calcite marble and calcite marble with minor phyllite or schist
 - Opa Unit A (Ordovician)
cherty, micaceous calcite marble
 - Enp Notch Peak Formation (Cambrian)
cherty calcite marble and calcite marble with dolomite marble and cherty
dolomite marble near the top
 - Eu Dunderberg Shale, Oasis and Shafter formations, undivided (Cambrian)
schist with minor micaceous calcite marble near the top (= Dunderberg Shale);
calcite marble, micaceous calcite marble, and minor dolomitic marble
(= Shafter and Oasis formations undivided)
- high-angle normal fault

— low-angle fault
- Pogonip Group

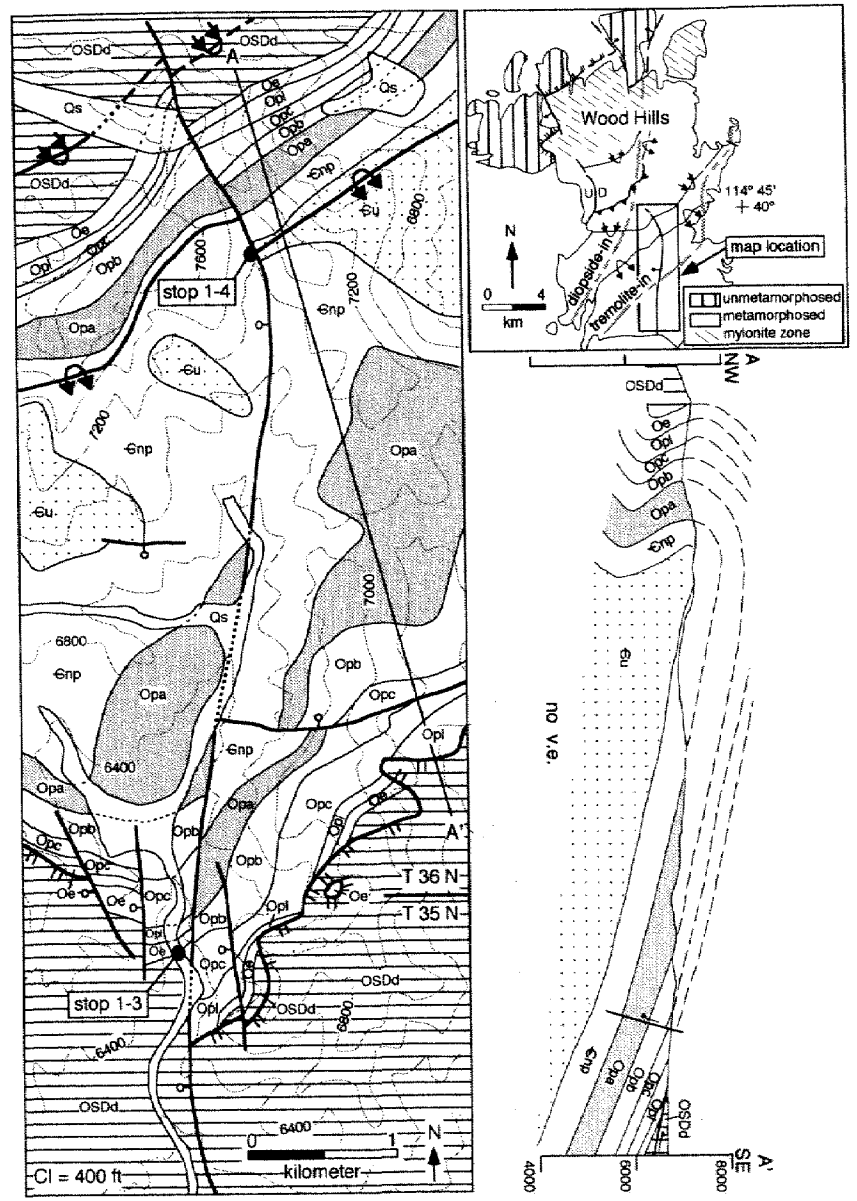


Figure 9. Simplified geologic map of the south-central part of the Wood Hills showing location of field trip stops 1-3 and 1-4.

is a good example of the outcrop style of this important lithology.

- 0.7 115.5 Trailhead to Winchell Lake on left.
 1.9 117.4 The road terminates in the Angel Lake parking area. Angel lake is an artificially enhanced cirque-lake directly beneath Grey's Peak (elev. 10,674 ft), the highest point in the northern part of the range.

STOP 1-5 (Fig. 8: see also geologic map in Figure 8 in Snoke et al., this volume).

At Stop 1-5 we will view the lower limb of the Winchell Lake fold-nappe, an inferred pre-metamorphic fault folded by the nappe, and the structurally deepest and highest grade (sillimanite zone) rocks in the region. We will be looking at some of the same units observed in the Wood Hills but the rocks here are migmatitic gneisses of higher grade than those of the Wood Hills.

Angel Lake Cirque exposes both limbs of the Winchell Lake fold-nappe, although the trace of the hinge surface of this fold is not clearly displayed in this area because it lies within the middle of the massive Archean orthogneiss sequence. However, the Greys Peak fold, a map-scale parasitic fold on the upper limb of the Winchell Lake nappe, is visible on the east cliff face directly beneath Greys Peak. Within Angel Lake Cirque the Tertiary mylonitic shear zone and its associated WNW-trending stretching lineation overprint the Winchell Lake nappe to varying degrees.

We will follow a transect across the lower limb of the fold-nappe to the base of the Archean orthogneiss sequence. This hike will require a steep climb with an elevation gain >600 ft over a distance of less than 0.5 mi (0.8 km). From bottom to top, the characteristic stratigraphic sequence that we will traverse on the lower limb of the fold-nappe is: (1) a quartzite and schist sequence of probable Early Cambrian to Late Precambrian age, (2) a thin sequence of calcite marble and calc-silicate gneiss that is probably Upper Cambrian and Ordovician in age, (3) a discontinuous, thin orthoquartzite layer (< 2 m thick) here inferred to correlate with the Ordovician Eureka Quartzite, (4) a sequence of dolomitic marbles pre-

sumed to correlate with the Ordovician to Devonian dolomites of the miogeoclinal sequence of the eastern Great Basin, (5) more calcite marbles which locally include isolated enclaves of intensely migmatized rusty-weathering graphitic schist of possible Mississippian age, (6) a sequence of severely migmatized quartzitic and quartzo-feldspathic paragneiss inferred to be of Early Proterozoic age, and (7) a thick sequence of Archean-aged striped monzogranitic orthogneiss. The contact between the Paleozoic (?) meta-sedimentary sequence (units 1-5) and the Early Proterozoic (?) paragneiss (unit 6) is inferred to be a pre-folding, pre-metamorphic fault. The contact between units (6) and (7) could be either tectonic or unconformable.

Throughout the transect you will notice sporadic small-scale folds and stretching lineations superimposed on the nappe. Fold hinge lines and stretching lineations show an average trend of approximately 5°, 295°, and small-scale fold hinge planes are approximately parallel to foliation, with an average orientation of 15°, 270°. However, considerably more dispersion exists in the small-scale structural data at deep levels than in the well-developed mylonites near the crest of the range, and locally a NNE-trending lineation of uncertain age is developed. Three dimensional constraints indicate that the map-scale folds (i.e., the Greys Peak fold and the Winchell Lake fold-nappe itself) show the same WNW-oriented trends as the smaller scale structures. The WNW-trending lineations and mylonitic microstructures superimposed on the nappe are constrained to be Tertiary in age because they also overprint a suite of 29-Ma biotite monzogranitic orthogneiss sheets (Wright and Snoke, 1993). In addition, some of the monzogranitic sheets are at least partially involved in small-scale folds.

Although some of the minor folds within the nappe are documented to be Tertiary in age, a variety of constraints indicate that most minor folds actually formed before Tertiary time. Many monzogranitic bodies clearly cut folds, and at map-scale the Winchell Lake fold-nappe itself is cut

by 29-Ma monzogranitic sheets. Furthermore, just east of Chimney rock the pre-metamorphic fault at the base of the fold-nappe is cut by a thick sill of 40-Ma hornblende biotite quartz dioritic orthogneiss. In Winchell Lake a few kilometers farther south, field relationships between the fold and synkinematic leucogranites indicate that it was emplaced during regional migmatization and sillimanite zone metamorphism between 70 to 90 million years ago (McGrew, 1992).

On our traverse we will stop at five localities, A through E, which can be located on the geologic map of Angel Lake cirque (Figure 8 of Snoke et al., this volume).

Locality A.

Hike around the south side of the lake to the gentle bedrock promontory labeled "A" on the geologic map (Fig. 8 of Snoke et al., this volume). These outcrops consist of coarse-grained severely migmatized quartzite, paragneiss, and schist here inferred to be Late Precambrian and Early Cambrian in age (correlating with the Prospect Mountain quartzite and perhaps also the upper part of the McCoy Creek Group). An outcrop of schist not far from this locality yielded an internally consistent PT estimate of 657°, 4.5 kb, but this probably reflects relatively late stage equilibration because other localities in the East Humboldt Range yield PT estimates as high as 790°C, 8.7 kb (McGrew and Peters, unpublished data). Pelitic mineral assemblages are similar throughout the northern East Humboldt Range, although rare relict assemblages of kyanite + staurolite survive only on the upper limb of the Winchell Lake fold-nappe. In addition, late stage muscovite and chlorite become increasingly prominent in the well-developed mylonitic rocks at relatively high structural levels. The most characteristic assemblage is biotite + sillimanite + garnet + quartz + plagioclase ± chlorite ± muscovite ± K feldspar ± rutile ± ilmenite.

Locality B.

Cross the small stream and proceed to point "B" on the map. Here we see more

of the Cambrian-Late Proterozoic quartzite and schist sequence, but here it includes some sparse amphibolitic bodies and more marble than the previous outcrops. These outcrops expose interesting small-scale fold and fault relationships, including a minor thrust fault, which is unusual because most shear surfaces in the northern East Humboldt Range show normal-sense displacement formed during Tertiary extensional tectonism. Proceed northward up the hill to point C.

Locality C.

At this locality we will observe quartzite and calcite and dolomite marble correlative with metamorphosed Cambrian to Devonian strata we observed at stops 1-3 and 1-4 in the Wood Hills. Pause at a layer of white quartzite approximately 1 m thick which probably correlates with the Ordovician Eureka quartzite. In nearby mountain ranges where Paleozoic strata are unmetamorphosed, the Upper Cambrian to Middle Ordovician limestone sequence is at least 1 km thick. Assuming the correlation is correct, here it is possible to walk through the entire section in a vertical distance of just 25 m! Overlying the ortho-quartzite layer is a few meters of dolomitic marble that probably correlates with Upper Ordovician to Devonian dolomites exposed in nearby ranges.

Marble and calc-silicate assemblages typically consist of calcite + diopside + quartz ± dolomite ± phlogopite ± plagioclase ± grossular ± scapolite ± K-feldspar ± sphene ± amphibole ± epidote. Peters and Wickham (1994) report that amphibole + grossular + epidote represent a secondary subassemblage that records infiltration of water-rich fluids under a metamorphic regime that proceeded from high temperature (600°–750°C) to lower temperature (< 525°C) conditions. The earlier, primary assemblages probably equilibrated at ≥ 6 kb, 550°–750°C with a relatively CO₂-rich fluid. Proceed westward, gaining elevation gradually to point D.

Locality D.

At this locality we will observe a thin raft of distinctive rusty-weathering graphitic

migmatitic paragneiss, inferred to correlate with the Mississippian Chainman Shale. These may be the youngest high grade metasedimentary rocks in the East Humboldt Range. Here, the rusty-weathering graphitic migmatitic paragneiss is completely encased in a mass of pegmatitic leucogranite, but on the upper limb of the fold-nappe this same rock type forms a continuous layer approximately 25 m thick that in general is only slightly migmatitic. Remarkably, the transition between these two contrasting outcrop styles occurs over a distance of <2 km as this unit is traced from the upper limb of the fold-nappe (where it typically contains <25% leucogranite) into the hinge zone of the fold-nappe above Winchell Lake where it contains >60% leucogranite. These meter-scale leucogranitic bodies are clearly folded around the nose of the fold-nappe, but the fact that isopleths of leucogranite concentration cut the fold-nappe implies that nappe emplacement and leucogranite segregation occurred at the same time. Moreover, relict kyanite also disappears over this same interval, being completely replaced by sillimanite on the lower limb of the fold-nappe. Consequently, it is inferred that a 70–90 Ma U-Pb zircon age on these leucogranitic rocks (J.E. Wright, pers. comm.) probably constrains both the timing of fold-nappe emplacement and the timing of migmatization and sillimanite zone metamorphism (McGrew, 1992). Proceed westward to point E.

Locality E.

In going from locality D to E we will traverse additional marbles overlying the graphitic schist unit and through the overlying Early Proterozoic (?) paragneiss sequence. Pause momentarily at the contact between the marble and the overlying paragneiss. By inference, this contact is a premetamorphic, pre-folding thrust(?) fault

of unconstrained but probably large displacement. Could this be the Windermere or a related thrust?

Continue across the Early Proterozoic paragneiss sequence to the exposures of the Archean orthogneiss at Point E. The Archean rocks occupy the core of the Winchell Lake fold-nappe and represent the only-known exposures of Archean basement in the state of Nevada. These rocks have a biotite monzogranitic composition and are generally grey in color with a distinctive striped appearance due to segregation of biotite. In addition, they commonly contain large augen of potassium feldspar. U-Pb zircon dating of a sample collected on the north side of the cirque yielded a minimum age of 2520 ± 110 Ma (Lush and others, 1988). Meter-scale amphibolite and garnet amphibolite boudins form a volumetrically small but distinctive and widespread component of both the Archean orthogneiss and the inferred Early Proterozoic paragneiss sequence. These bodies probably represent metamorphosed mafic intrusions and are rarely observed in the Late Proterozoic and Paleozoic metasedimentary sequence.

Return to the parking area, retrace route to Interstate 80, and proceed to Wendover. End of day 1.

ACKNOWLEDGEMENTS

This manuscript has benefited from reviews by Tim Lawton, Paul Link, Lon McCarley, and Wanda Taylor. This work represents an outflow of Ph.D. research conducted at the University of Wyoming and originally supported by University of Wyoming graduate fellowships and National Science Foundation research grant EAR 87-07435 awarded to A.W. Snoke. Camilleri acknowledges support of this project from the donors of the Petroleum Research Fund, administered by the American Chemical Society (ACS-PRF# 30860-GB2), and from an Austin Peay State University Tower Grant. McGrew acknowledges the support of a University of Dayton Research Council Seed Grant.

Large magnitude Crustal Thickening and Repeated Extensional Exhumation in the Raft River, Grouse Creek, and Albion Mountains

MICHAEL L. WELLS

Department of Geoscience, University of Nevada, Las Vegas, Nevada 89154

THOMAS D. HOISCH

LORI M. HANSON

EVAN D. WOLFF

Department of Geology, Northern Arizona University, Flagstaff, Arizona 86011

JAMES R. STRUTHERS

Department of Geoscience, University of Nevada, Las Vegas, Nevada 89154

INTRODUCTION

The Raft River, Grouse Creek, and Albion Mountains of northwestern Utah and southern Idaho lie in the hinterland of the Late Mesozoic to early Cenozoic Sevier orogenic belt (Armstrong, 1968a), to the west of the classic foreland fold and thrust belt (Armstrong and Oriel, 1965), and east of the outcrop belts affected by Paleozoic contractional orogeny. Following the cessation of Sevier orogenesis, this region experienced large-magnitude crustal extension and associated magmatism and metamorphism, episodically, from middle to late Eocene time to the present (Compton, 1983; Mueller and Snoke, 1993a; Smith and Sbar, 1974; Wells and Snee, 1993).

The kinematic role of the Sevier belt hinterland during Late Mesozoic to early Cenozoic Sevier orogenesis has been controversial, and the structural record apparently contradictory (e.g., Hose and Danes, 1973; Allmendinger and Jordan, 1984; Snoke and Miller, 1988). For example, Mesozoic contractional structures (e.g., Miller and Gans, 1989; Snoke and Miller, 1988; Camilleri and Chamberlain, 1997; Taylor et al., 1993) and Mesozoic extensional structures (e.g., Wells et al., 1990; Hodges and Walker, 1992) have both been reported in the northeastern Great Basin. Study of Neoproterozoic to Permian rocks of the Raft River, Grouse Creek, and Albion Mountains suggests alternating periods of contraction and extension in this region during Late Mesozoic to early Cenozoic time (Wells, 1997), including an episode of large-magnitude extension of Late Cretaceous age (Wells et al., 1990). Dynamic adjustments of topography and crustal thickness in the hinterland during

contraction in the foreland would explain these apparent kinematic inconsistencies (Wells, 1997).

In addition to the Raft River Mountains area, extension of Cretaceous age has been interpreted to have occurred at numerous other localities within the Sevier Belt hinterland (Hodges and Walker, 1992), leading to the suggestion that the hinterland was a region of substantial crustal thickening and topographic uplift. The documentation, however, for large-magnitude contraction in the hinterland, while compelling in some areas (Camilleri and Chamberlain, 1997) has remained elusive in many other regions, partly because Mesozoic structures were fragmented during Cenozoic extension and isotopic systems and metamorphic fabrics have been strongly overprinted during Tertiary metamorphism, uplift and cooling.

In this paper, we summarize the results of earlier work on the sequence and kinematics of Mesozoic to early Cenozoic deformations, based on observations from the eastern Raft River Mountains (Wells, 1997), and incorporate new results on metamorphic P-T paths and deformation kinematics from the western Raft River and northern Grouse Creek Mountains. The new data have bearing on the magnitude of crustal thickening and topographic development in the hinterland region of the Sevier orogenic belt, and on the timing of episodes of gravitational collapse.

TECTONOSTRATIGRAPHY OF THE RAFT RIVER MOUNTAIN, GROUSE CREEK, AND ALBION MOUNTAINS

Overprinting Mesozoic and Cenozoic deformations have produced an incomplete and greatly attenuated stratigra-

phic section in the Raft River, Albion, and Grouse Creek Mountains. A tectonically thinned sequence of metasedimentary units of Neoproterozoic to Triassic age overlies Archean basement over an area greater than 4000 km² (Fig. 10) (Armstrong, 1968b; Compton et al., 1977; Wells 1997). The Green Creek complex (Armstrong and Hills, 1967; Armstrong, 1968b) is composed of ~2.5 Ga gneissic monzogranite (metamorphosed adamellite of Compton, 1972) that intrudes schist and amphibolite (Compton, 1975; Compton et al., 1977). The Elba Quartzite unconformably overlies the Green Creek complex and forms the basal unit of a sequence of alternating quartzite and psammatic and pelitic schist. Anomalously high $\delta^{13}\text{C}$ values from marble interbeds within the structurally, and presumably stratigraphically highest quartzite of this sequence (quartzite of Clarks Basin of Compton, 1972, 1975) resemble those measured in other Neoproterozoic rock sequences in western North America, and suggest a Neoproterozoic age for the entire rock package (Wells et al., 1996). Structurally overlying the Neoproterozoic rocks along the Mahogany Peaks fault are upper greenschist-lower amphibolite facies Paleozoic metasedimentary rocks including Ordovician calcitic marble, phyllite, quartzite and dolomitic marble. These rocks are overlain by Pennsylvanian(?) marble along the Emigrant Spring Fault (Wells, 1996, 1997). Middle greenschist facies Pennsylvanian and Permian rocks of the Oquirrh Formation structurally overlie the amphibolite facies rocks along the middle detachment fault. Within the eastern Raft River Mountains, these rocks have been subdivided into three low-angle fault-bounded tectonostratigraphic units (Compton et al., 1977; Miller, 1980, 1983; Todd, 1980, 1983; Wells, 1992, 1997). From structurally lowest to highest, these are: (1) the parautochthon, (2) the lower allochthon, and (3) the middle allochthon (Fig. 10).

KNOWN AND INFERRED CRETACEOUS TO EOCENE DEFORMATIONS IN THE RAFT RIVER, GROUSE CREEK, AND ALBION MOUNTAINS

The pre-Oligocene deformation record of the Raft River, Grouse Creek, and Albion Mountains is best preserved within rocks that lie in the upper plate of the Raft River detachment fault in the eastern Raft River Mountains. This is primarily because: (1) upper-plate Neoproterozoic to Permian rocks were not overprinted by Neogene mylonitization and metamorphism that affected lower-plate Archean and Proterozoic rocks, and have resided at high structural levels since Late Cretaceous time (Wells et al., 1990); and (2) stratigraphically equivalent strata within the western Albion Range, western Raft River and Grouse Creek Mountains were at deeper structural levels in Paleogene time and are structurally overprinted by penetrative

top-to-the-west Paleogene mylonitic fabrics and locally thermally overprinted adjacent to Paleogene plutons (Compton et al., 1977; Todd, 1980; Saltzer and Hodges, 1988; Wells et al., 1994; Wells and Struthers, 1995). The metamorphic record, on the other hand, is better understood for the western Raft River and northern Grouse Creek Mountains than the eastern Raft River Mountains, in part due to the serendipitous preservation of metamorphic rocks with the appropriate bulk compositions for thermobarometric calculations that have not experienced extensive retrograde metamorphism. New quantitative thermobarometry is presented below for these areas that fill in an important, and to date missing, component in the tectonic evolution of this region.

Eastern and Central Raft River Mountains

Rocks in the upper plate of the Miocene Raft River detachment fault preserve a protracted sequence of deformations that predate Miocene extension. The discussion below will focus on the early part of the deformation sequence, developed during and probably immediately after Sevier orogenesis. A more detailed and complete description of the deformations can be found elsewhere (Wells, 1992, 1996, 1997).

The earliest and most pervasive fabric (D_1) in the lower allochthon is a penetrative foliation which is generally parallel to lithologic layering and inferred bedding. Lineation varies in degree of development, is not ubiquitous, and generally trends NE. Kinematic analysis suggests that the D_1 fabric resulted from a combination of pure shear flattening and NE-directed simple shear. Textural evidence suggests that the D_1 fabric in the lower allochthon is a prograde metamorphic fabric (Wells et al., 1990, Wells, 1997).

Shear zones at a low angle to bedding postdate the early foliation and record top-to-the-west translation and stratigraphic attenuation. The two principal shear zones of this age are the Emigrant Spring and the Mahogany Peaks faults. The Emigrant Spring fault places Pennsylvanian(?) calcitic marble over Ordovician dolomitic marble. This fault removes about 5 km of stratigraphic section, including Silurian, Devonian, and all but centimeter-scale slivers of Mississippian rocks in the eastern and central Raft River Mountains and in the northern Grouse Creek Mountains. In the central and southern Grouse Creek Mountains, Devonian and substantive thicknesses of Mississippian rocks are present and thicken towards the south. It is not known whether these southward thickening units appear in the hanging wall or footwall of the Emigrant Spring fault, or alternatively, along the structurally higher middle detachment fault. The Mahogany Peaks fault separates the Neoproterozoic schist of Mahogany Peaks and quartzite of

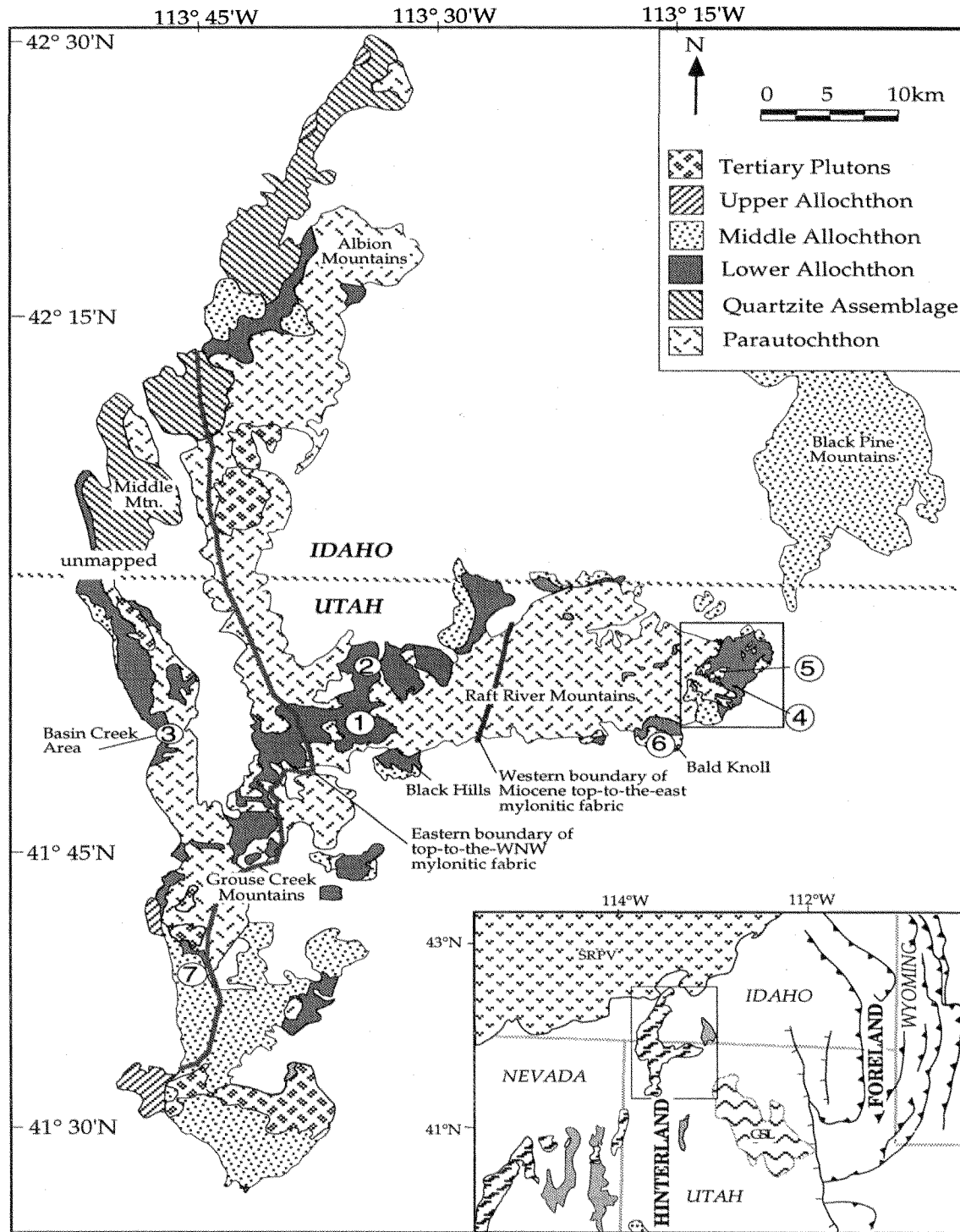


Figure 10. Tectonostratigraphic and sample location map of the Raft River, Black Pine, Albion, and Grouse Creek Mountains. Box in eastern Raft River Mountains indicates location of more detailed geologic map shown in Figure 14 of corresponding roadlog. Numbers indicate sample stations for calcite-dolomite and garnet-biotite thermometry, and conodont color alteration indices. Modified from Compton (1975), Compton et al. (1977), Todd (1980), Miller (1983), and Wells (1996). Inset, generalized location and tectonic map of the northeastern Great Basin illustrating location of hinterland metamorphic rocks (shown in diagonal wavy pattern). Barbed lines = thrusts of the Sevier belt, hachured lines = normal faults of the Wasatch system. SRPV, Snake River Plain volcanic rocks (shown in v pattern).

Clarks Basin from Ordovician carbonate rocks and crops out discontinuously throughout the Raft River, Grouse Creek, and Albion Mountains (Compton 1972, 1975; Compton and Todd, 1979; Crittenden, 1979; Miller, 1980; Wells, 1996; Wells et al., 1996). The Ordovician rocks of the hanging wall are metamorphosed at upper greenschist-lower amphibolite facies, as documented by calcite-dolomite geothermometry from the western Raft River Mountains (475–500°C, Fig. 11, sample stations 1 and 2 on Fig. 10), and oxygen isotopic geothermometry of quartz-muscovite and quartz-biotite mineral-pairs (490 to 510°C) and conodont color-alteration indices (CAI) >7 from the eastern Raft River Mountains (sample station 4, Fig. 10; Wells et al., 1990). In contrast, the Neoproterozoic schist of Mahogany Peaks in the footwall is of higher metamorphic grade, indicating a grade discordance across the Mahogany Peaks fault. The schist of Mahogany Peaks, at the locations of the Black Hills, Johnson Creek, Bald Knoll, and the east end of the Raft River Mountains, has mineral assemblages that indicate pressures and temperatures in excess of 6.5 kb and 550°C, respectively (Spear and Cheney, 1989; Bohlen et al., 1991). Garnet-biotite thermometry on schist with euhedral garnets and the assemblage garnet+biotite+muscovite+staurolite+quartz+paragonite yield temperatures of $\geq 590^\circ\text{C}$ (assuming minimally 6.5 kb burial) (Fig. 11). The metamorphic grade discordance of about 75–100°C that occurs across the fault is consistent with the omission of 3–4 km of section if the fault post-dated the peak of metamorphism. Because the fault places younger strata over older, and shallower (colder) over deeper (hotter) rocks, the fault is interpreted as extensional in origin.

The upper greenschist-lower amphibolite facies Ordovician through Pennsylvanian(?) rocks of the lower allochthon are deformed into tight to isoclinal recumbent folds with amplitudes greater than 1.5 to 2 km. The complex superposition of later deformations, however, precludes determination of original fold geometry. The youngest unit involved in recumbent folding is the Pennsylvanian(?) marble, which occupies the cores of recumbent synclines.

The middle detachment truncates the recumbent folds and is the youngest structure that is probably of Eocene age. The middle detachment fault can be traced discontinuously across the east-west extent of the Raft River Mountains and into the Grouse Creek and Albion Mountains. This fault was interpreted by Compton et al. (1977) to represent the principal detachment in these ranges. Kinematic study of the few outcrops of fault rocks indicates top-to-the-WSW shear (Wells, 1997), consistent with data from the Black Pine Mountains (Fig. 10) (Wells and Allmendinger, 1990). Middle greenschist-facies Pennsylvanian to Permian Oquirrh Formation rocks of the middle allochthon lie above upper greenschist-lower amphibolite-facies Ordovician and Pennsylvanian(?) rocks of the lower allochthon

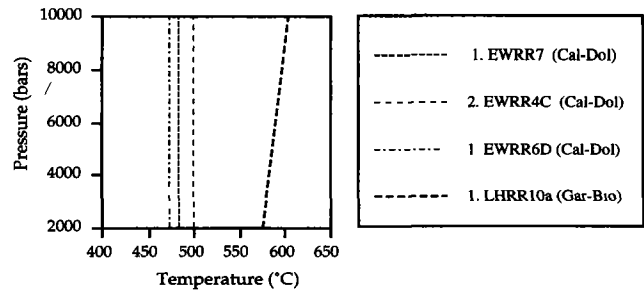


Figure 11. Calcite-dolomite geothermometry (Anovitz and Essene, 1987) of Ordovician carbonates from the hanging wall of the Mahogany Peaks fault (sample stations 1 and 2) and garnet-biotite geothermometry (Hodges and Spear, 1982) from the schist of Mahogany Peaks from the footwall (sample station 2). See Figure 10 for locations of sample stations.

along the middle detachment fault. The hanging wall limestones contain conodonts with CAI values of 5 (locations 5, 6, and 7), suggesting temperatures of $\sim 350 \pm 25^\circ\text{C}$ (assuming regional metamorphic time scales) (Epstein et al., 1977; Rejebian et al., 1987), in contrast to the higher metamorphic temperatures outlined above for the footwall rocks. The metamorphic discordance of $\sim 125\text{--}150^\circ\text{C}$ across this fault is consistent with removal of about 5–6 kilometers of structural section, and an extensional origin. However, quantitative thermometry for the Pennsylvanian marble tectonite in the hanging wall of the Emigrant Spring fault and footwall of the middle detachment has not been possible, so the data above should prudently be interpreted to indicate a temperature discordance of $\sim 125\text{--}150^\circ\text{C}$ that has been accomplished cumulatively by the two faults.

In the central and eastern Raft River Mountains, an amphibolite-facies fabric with generally NNW-trending elongation lineation and local top-to-the-NNW kinematics is preserved in the Elba Quartzite and older rocks, beneath the Raft River detachment and Miocene top-to-east shear zone. This fabric is also locally preserved in lenses of mechanically strong amphibolites within the Miocene shear zone that have escaped the younger deformation. This fabric is tentatively correlated to the D₁ fabric described above from the upper plate of the Raft River detachment fault.

Grouse Creek and Western Raft River Mountains

The west side of the Grouse Creek and Raft River Mountains expose a belt of mylonitic rocks that continues northward to Middle Mountain in the southern Albion Mountains of Idaho, where it has been termed the Middle Mountain shear zone (Saltzer and Hodges, 1988). In the northern Grouse Creek Mountains where we have concentrated our studies, the shear zone cuts down to the west across the

stratigraphy, including the Archean-Proterozoic unconformity. This shear zone contains WNW to W-trending lineation, generally flat-lying foliation and records top-to-the-WNW and top-to-the-W shear sense (Compton et al., 1977; Todd, 1980; Compton, 1983; Malavieille, 1987). Our work suggests at least two periods of generally west to northwestward shearing along the zone. The earlier shearing event is of higher temperature and records transport in the direction of N63W. The second shearing event is of lower temperature, deforms Oligocene granitoids (~27 Ma, Wells and Walker, unpublished data) and records transport in the direction of N87W. Three observations are significant in separating the two distinct events of ductile shearing: (1) the structurally deep rocks bear a lineation that trends N63W, while the structurally highest rocks, including the Oligocene granitoid rocks, have a lineation of N87W (Fig. 13). Intermediate structural levels show a bimodal distribution in lineation trend. (2) The Oligocene granitoid rocks, although they exhibit mylonite and locally ultramylonite near their roofs, are significantly less deformed as a whole by top-to-the-west-northwest shear than the surrounding country rock, regardless of the composition of the country rock. (3) The fabrics from the structurally deepest levels that carry more northwesterly-trending lineation are of higher temperature than the fabrics from the structurally highest levels. In the structurally lower rocks, microcline in Archean monzogranite has experienced extensive dynamic recrystallization. Well-developed core and mantle structure indicates recrystallization by subgrain rotation with minor grain boundary migration. Quartz exhibits moderate to high-T deformation features as well. Extensive grain-boundary migration recrystallization is associated with grain growth leading to an increase in grain size. Quartz lattice-preferred orientations exhibit maxima parallel to the Y axis of the finite strain ellipsoid, indicating dominantly prism $\langle a \rangle$ slip, which is a relatively high temperature slip system in quartz (Schmid and Casey, 1985), consistent with amphibolite facies deformation conditions. Pelitic schists show synkinematic growth of sillimanite in the pressure shadows of garnet. In contrast, deformation fabrics in the Oligocene granitoids and surrounding rocks from the higher structural levels exhibit only incipient plasticity and dominantly brittle deformation of K-feldspar, and abundant low-temperature, unrecovered quartz microstructures, suggesting greenschist facies deformation conditions. Thermochronological studies suggest an Eocene age for the early, higher-temperature shearing event (Wells and Snee, 1993; Wells et al., 1994).

Petrologic work on lesser strained samples of Neoproterozoic schist within the shear zone from the Basin Creek area (Fig. 10) have elucidated the earlier metamorphic and structural history that pre-dates Eocene extensional

shearing (Fig. 12). Numerical simulations of garnet zoning profiles based on the Gibbs method of Spear (1993) indicates a P-T path with an isothermal pressure increase of 2.5 kilobars (Fig. 12), indicating about 9 kilometers of rapid structural burial during garnet growth. Thus, the metamorphic conditions indicate tectonic loading, not thermal metamorphism at stratigraphic burial depths (in contrast to metamorphism in Pilot Range to the south, Miller and Hoisch, 1995).

Beneath the shear zone, an earlier fabric is present with generally flat-lying foliation and north-trending lineation that records top-to-the-north shear (Todd, 1980; Miller et al., 1983; Malavieille, 1987). Microstructural observations of the early fabric indicate that it developed at amphibolite facies conditions.

Albion Mountains

Two presumed Mesozoic deformations have been documented in the northern Albion Mountains (Miller, 1980). The earlier exhibits a NE-trending lineation (L_1 of Miller, 1980), with a component of top-to-the-NE shear (Malavieille, 1987), and the later a NW-trending lineation (L_2 of Miller, 1980) and top-to-the-NW shear (Malavieille, 1987). Hodges and Walker (1992) interpreted the L_2 fabric to record Cretaceous top-to-the-NW extensional shear. A third lineation, trending WNW, is present in the southwestern Albion Mountains within the Middle Mountain shear zone, a west-dipping extensional shear zone with top-to-the-WNW shear sense (Miller et al., 1983; Saltzer and Hodges, 1988). The Middle Mountain shear zone is younger than L_2 of Miller (1980), and metamorphic minerals that grew during shearing yield Late Eocene to Oligocene (K-Ar and $^{40}\text{Ar}/^{39}\text{Ar}$) cooling ages (Armstrong, 1976; Miller et al., 1983; Saltzer and Hodges, 1988).

DISCUSSION

Evidence for structural burial

The numerical simulations of garnet growth in the Neoproterozoic schist in the northern Grouse Creek Mountains (Basin Creek area, Fig. 12) provide conclusive evidence for rapid and substantial thrust burial. It is not possible to relate this P-T path to a specific rock fabric. However, it is interpreted that thrust burial, as recorded in the P-T path, preceded D_1 fabric development. Thrust burial may have developed lateral gradients in crustal thickness such as thrust culminations or localized duplexes, and subsequent thermal relaxation may have facilitated gravitational collapse parallel to the orogen, as recorded in the D_1 fabric.

A preserved thrust relationship in the northern Albion Mountains may represent the remnants of a once areally-extensive thrust nappe responsible for much of the burial

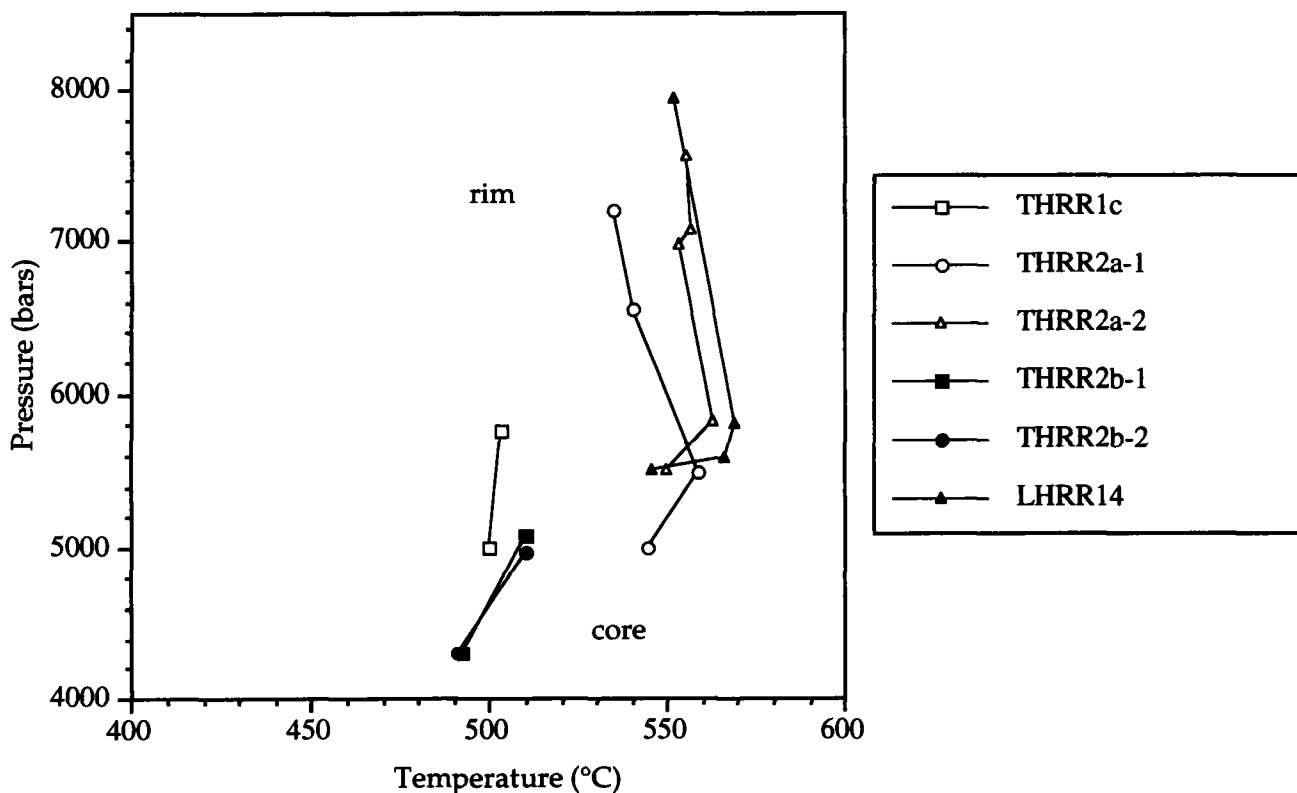


Figure 12. Pressure-temperature paths from numerical simulations of garnet growth based on the Gibbs method of Spear (1993). Samples are of pelite from the schist of Stevens Springs at Basin Creek (locality 3, Figure 10) from the northern Grouse Creek Mountains. The higher pressure endpoint of each P-T path represents the absolute conditions of metamorphism determined using garnet rims, the garnet-muscovite-biotite-plagioclase geobarometers of Hoisch (1991), and garnet-biotite thermometer of Kleemann and Reinhardt (1994). Consumption of the garnet rims and retrograde modification of the biotite compositions introduces much uncertainty in the absolute conditions, however, the shapes of the P-T paths are robust.

evident Raft River, Grouse Creek, and eastern Albion Mountains. At Mount Harrison in the northern Albion Mountains, an inverted sequence of Neoproterozoic rocks (Quartzite Assemblage, Fig. 10), unlike Neoproterozoic strata within the lower part of the Raft River Mountain sequence, structurally overlies Ordovician and older rocks of the Raft River Mountain sequence along the Basin-Elba fault zone (Miller, 1980, 1983; Armstrong, 1968b; Saltzer and Hodges, 1988). Late Cretaceous K-Ar cooling ages (Armstrong, 1976) from rocks within the Basin-Elba fault zone, combined with thermobarometric estimates, suggest that this structure is a Mesozoic thrust fault (Malavieille, 1987; Saltzer and Hodges, 1988). Hodges and Walker (1992) suggested that the stratigraphic juxtaposition was initially of thrust sense, and that the latest movement along the fault was of normal-sense in Late Cretaceous time. The middle detachment fault is interpreted to have removed the bulk of the thrust sheet responsible for burial.

Orogen-parallel extension interpretation of D_1

Similar deformation kinematics and conditions favor correlation of D_1 in the Albion Mountains (Miller, 1980), D_1 in the Grouse Creek Mountains (Todd, 1980), D_1 in the lower allochthon of the eastern Raft River Mountains (Wells, 1997), and the amphibolite-facies fabric present beneath the Raft River detachment and associated shear zone in the central and eastern Raft River Mountains. However, stretching lineations associated with these fabrics vary as much as 50° in azimuth. This proposed correlation is strengthened by recent study of Mississippian and Pennsylvanian rocks in the central Grouse Creek Mountains. Quartz and calcite pressure shadows around iron oxide that define L_1 show curving pressure shadow lineations when viewed on the foliation surface. Further study is needed to confirm the growth sense, but preliminary determinations indicate clockwise rotation from NW incre-

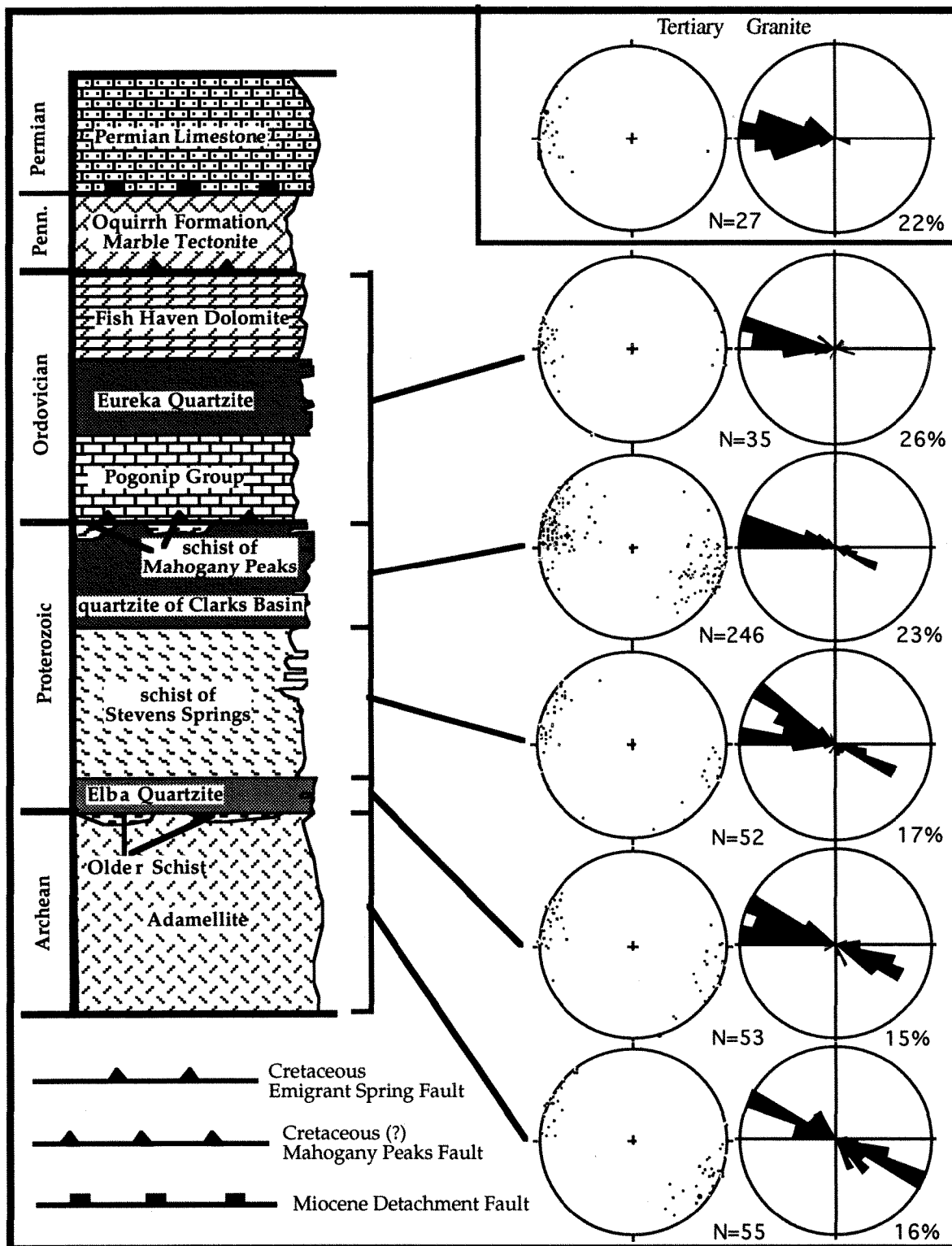


Figure 13. Tectonostratigraphic column for the northern Grouse Creek Mountains illustrating the variation in azimuth of elongation lineation within the top-to-the-WNW shear zone. Note change in mean orientations from N63W at deepest to N87W at highest, and bimodal azimuths at intermediate structural levels. Elsewhere, other schist and quartzite units lie between the Elba Quartzite and schist of Stevens Springs.

mental extensions to NE incremental extensions. In either case, this observation suggests that the orientation of extensional flow varied through time, and that the lineations documented in all three ranges, despite their variation in azimuth, have developed as part of one overall top-to-the-north shearing event.

The Sevier orogenic belt is dominated by east-west shortening and a N-S trend to the mountain belt. The orientation of northward shear at mid-crustal levels within the hinterland of the Sevier orogen indicates that the D_1 fabric records transport parallel to the orogen. Kinematic study of the D_1 fabric indicates combined distributed simple shear and vertical flattening strains (Wells, 1997). Thrusting of large magnitude perpendicular to the regional direction of shortening, as proposed by Malavieille (1987), is unlikely. Rather, this fabric is most compatible with an interpretation of orogen-parallel extensional flow. Gravitational collapse that is oriented parallel to the orogen has been documented in a number of orogenic belts (e.g. Ellis and Watkinson, 1987). Such extension commonly accompanies active convergence, such that the direction of extensional flow is limited to the orientation parallel to the orogen.

Seven Late Cretaceous K-Ar ages (biotite, muscovite, and hornblende) have been reported from rocks containing NE-trending L_1 lineations from the northern Albion Mountains (Armstrong, 1976; Miller, 1980). Three $^{40}\text{Ar}/^{39}\text{Ar}$ muscovite cooling ages from marble and schist from the lower allochthon in the eastern Raft River Mountains containing D_1 fabrics are Late Cretaceous (Wells et al., 1990). The D_1 fabrics are interpreted to have developed prior to cooling at ~ 90 Ma.

Late Cretaceous Extension

The west-directed Emigrant Spring and Mahogany Peaks faults place younger over older strata within the lower allochthon and are interpreted to represent normal faults (Wells et al., 1990; Wells, 1997). The preliminary geothermometry presented here from the hanging wall and footwall of the Mahogany Peaks fault indicates a discordance in metamorphic grade across the fault and confirms the interpretation of an extensional origin. The age of the Emigrant Spring fault is constrained by $^{40}\text{Ar}/^{39}\text{Ar}$ muscovite cooling ages of ~ 88 to 90 Ma from Ordovician rocks in the footwall, and from Pennsylvanian(?) marble tectonite within the Emigrant Spring fault zone (Wells et al., 1990). Faulting is interpreted to have occurred prior to or synchronous with cooling recorded by the muscovite cooling ages. The Mahogany Peaks fault may be younger than the Emigrant Springs fault and of Latest Cretaceous age.

Eocene Extension

The middle detachment fault may be related to the deeper level, high-temperature, top-to-the-west-north-

west extensional shear zone described above in the western Raft River, Grouse Creek, and Albion Mountains (Saltzer and Hodges, 1988; Wells and Snee, 1993; Wells and Struthers, 1995). A middle to latest Eocene age for the latter shear zone is suggested based on a reconstructed east-dipping monocline of middle Eocene age in the Proterozoic-Archean unconformity in the west-central Raft River Mountains. The east-dipping monocline, constrained by $^{40}\text{Ar}/^{39}\text{Ar}$ cooling ages of mica beneath the shear zone, is inferred to be related to footwall flexure resulting from tectonic denudation along the early top-to-the-west-north-west extensional shear zone (Wells et al., 1994). Additionally, $^{40}\text{Ar}/^{39}\text{Ar}$ cooling ages of muscovite from mylonitic rocks within the shear zone in the western Raft River Mountains range from 37 to 42 Ma (Wells et al., 1994; Wells and Snee, unpublished data).

ROAD LOG FOR PART 2 OF DAY 2: FROM MONTTELLO, NEVADA, TO RAFT RIVER MOUNTAINS AND SNOWVILLE, UTAH

by Michael L. Wells

Day two of this field trip consists of two parts. Part 1 is a transect through the deeply buried metamorphic rocks of the Raft River Mountains, and part 2 covers a traverse across the central section of the Sevier orogen, including vast exposures of lesser Mississippian and dominantly Pennsylvanian and Permian strata (inferred to overlie a regional flat in the basal decollement), and structures along the leading edge of the Willard thrust system at the shelf to platform transition. Stops in the Raft River Mountains will focus on the geometry, timing, and kinematics of Mesozoic to probable late Eocene structures within Neoproterozoic and Paleozoic rocks comprising the hanging wall of the Miocene Raft River detachment fault. We will view and discuss the evidence for large-magnitude extension of Late Cretaceous age, and probable contractional deformations which both post- and pre-date this extension. Additionally, we will view and explore the evidence for two later episodes of detachment faulting. For the additional background geologic information on this region, and the geologic map for the area of Stop 2-1, see Wells 1996 and 1997.

Day two of the field trip begins in Wendover, NV. The road log begins at the state line between Nevada and Utah, on Nevada State Highway 233-Utah State Highway 30, between Montello, NV, and Park Valley, UT. This road log contains excerpts from, and is in part modified from, a previous road log (Wells and Miller, 1992). See also Miller et al. 1983 for another road log of the Raft River, Grouse Creek, and Albion Mountains region.

MILEAGE		DESCRIPTION			
Incre-	Cumu-				
mental	lative				
68	68	Nevada-Utah state line, on Nevada State Highway 233 and Utah State Highway 30.	2.2	88.8	end cuts a thrust fault that duplicates part of the Ordovician section, and also cuts normal faults (Allmendinger and Jordan, 1984).
8.8	76.8	Crossroads; Grouse Creek to the left and Lucin to the right. Permian and Triassic strata are exposed in the nearby hills to the south and Miocene rhyolite plugs and minor related outflow volcanic rocks are exposed to the north.			Slow down but do not stop. For the next mile or so we will view the south end of the Grouse Creek Mountains. The high mountain mass is called Bovine Mountain and its geology has been studied in detail by Jordan (1983). It exposes an unusually thick sequence of the Oquirrh Formation that has been deformed broadly by folding on east-verging recumbent folds that predate or are coeval with an ~38-Ma pluton described below. The Oquirrh Formation is separated from Ordovician and Silurian strata (exposed in the low, dark outcrops that extend from a point near the highway for about one kilometer to the north) by a fault that parallels bedding in both fault blocks and that is folded by northeast-trending folds that predate the Immigrant Pass intrusion.
6.7	83.5	Small dirt road marked by a B.L.M. sign to Immigrant Pass and Rosebud Station. Four buttes to the northwest of the road are separate rhyolite plugs or thick flows that are cut by high shorelines of Lake Bonneville; the plugs were dated as 11.7 Ma (Compton, 1983, K-Ar on sanidine). The plugs intrude a thick sequence of middle Miocene tuff and interstratified sedimentary rocks that underlie the smooth-surfaced hills rising to the northeast of the road. The Miocene rocks are in fault contact with the older rocks of the range at the break in slope where the smooth hills meet the more jagged slopes of the southern Grouse Creek Mountains. The fault here dips approximately 25° WSW. The same fault has been mapped continuously for 24 miles to the north, and from that point it has been mapped discontinuously to the Idaho state line, a total distance of 39 miles. The Miocene rocks 4.8 miles to the north are tectonically intercalated with Permian ^(p) and Triassic rocks, and these rocks together comprise an upper plate of a detachment fault present along the western side of the Grouse Creek Mountains (includes the uppermost allochthonous sheet of Compton et al., 1977).	4.4	93.2	The craggy outcrops around 9:00 are granodiorite which makes up the Immigrant Pass intrusion. This approximately 38 Ma pluton intrudes the Oquirrh Formation. The pluton extends for 3 miles to the north, and 8.5 miles to the west, and was dated by R. Zartman as approximately 38 Ma by the Rb-Sr method (Compton et al., 1977). Also visible are the high wave-cut benches of Lake Bonneville and a level-topped gravel beach that extends from the mountain from northeast to a low, craggy spur exposing granodiorite.
			4.6	97.8	Historic Marker
			8.6	106.4	Muddy Ranch Road. Light-colored outcrops to the right are Miocene strata of the Salt Lake Formation.
1.6	85.1	White Miocene vitric water-laid tuff is well exposed in outcrops and in a quarry on the left (north) side of the road. The beds are broadly folded on roughly west-trending axes and dip at low angles (12 to 20°) to the north and south.	3.4	109.8	Hills on the right are just above the high stand of Lake Bonneville. They contain Miocene tuffaceous siltstone and vitric tuff of the Salt Lake Formation. On the left, the Grouse Creek Mountains form the skyline. The central and western Grouse Creek Mountains expose a top-to-the-west and west-northwest extensional shear zone that partially unroofed the central and western Raft River Mountains. The youngest movement on the shear zone deforms Oligocene granites. Beneath this shear zone the earliest deformation fabric,
1.5	86.6	Pidgen Mountain at 2:00 is composed of Permian and Triassic strata juxtaposed by several thrust faults. In the distance are the Newfoundland Mountains. The Late Jurassic Newfoundland stock at the north			

top-to-the-north shearing, is well preserved. To the southeast are the Matlin Mountains, which consist of a complex allochthon that was emplaced in the same approximate time span (middle to late Miocene) as the upper allochthon of the Grouse Creek Mountains (Todd, 1983). The Matlin Mountains were islands in the northwestern part of Lake Bonneville and are surrounded by, and partly covered by, lacustrine sedimentary deposits. They exposed a sequence of five thin displaced sheets that consist of upper Paleozoic and Mesozoic strata (Todd, 1983).

As we drive north, note the white, south-facing dip slopes in the Raft River Mountains, composed of the Proterozoic Elba Quartzite that overlie darker slopes within the canyons formed on Archean rocks. At the base of the range, many exposures of Paleozoic and Proterozoic rocks overlie the Elba Quartzite along the Raft River detachment fault. Detachment fault-bounded klippen on top and on the flanks of the mountains presumably were once part of a continuous extensional allochthon. The Raft River detachment separates Proterozoic and Archean rocks in the footwall (parautochthon) from Neoproterozoic and Paleozoic rocks in the hanging wall or upper plate. The detachment is parallel to lithologic contacts and the mylonitic foliation in the underlying parautochthon, and the morphology of the detachment is well expressed because of the lateral continuity of the resistant Elba Quartzite in the footwall. The Miocene extensional shear zone records top-to-the-east shearing and is developed within the Elba Quartzite and the overlying schist unit. The top of the shear zone is the Raft River detachment fault, and the base of the shear zone lies within the upper 10 to 30 meters of the Archean rocks. The western extent of the shear zone lies just east of the upper plate exposure of the Black Hills at 11:00. Similarly to the Grouse Creek Mountains, an earlier deformation fabric is preserved beneath the Cenozoic shear zone in the Raft River Mountains that records generally top-to-north shearing.

The upper plate of the Raft River detachment is composed of a lower allochthon of Neoproterozoic, Ordovician, and Pennsylvanian (?) rocks, and a middle allochthon of Pennsylvanian and Permian rocks. The pre-Miocene structural history of the Neoproterozoic through Permian rocks of the upper plate includes: (1) early NE-directed interbed plastic flow, (2) top-to-the west attenuation faulting, (3) recumbent folding of the attenuated strata and low-angle faults of the lower allochthon, (4) emplacement of the middle allochthon of Pennsylvanian and Permian (Oquirrh Group) rocks over the folded lower allochthon along a low-angle fault localized in the Mississippian Chainman Shale, and (5) folding of both the lower and middle allochthon into upright, open folds.

The principal stop for today (Ten Mile Canyon, see Figs. 14 and 15) will feature a traverse through the lower and middle allochthons of the Raft River detachment upper plate, including overviews of the geometry of F_5 upright folding, examination of the middle detachment fault, outcrop study of the D_1 fabrics, and D_2 attenuation faulting, and overview of the geometry of F_3 recumbent folds. Also, we will traverse down across the Raft River detachment fault through cataclases and mylonites developed during Miocene extension.

- | | | |
|-----|-------|--|
| 8.2 | 118.0 | Intersection of Palmer Ranch/Montgomery Ranch Road. |
| 1.3 | 119.3 | Rosette |
| 4.6 | 123.9 | Park Valley, one of the quarrying locations for the micaceous quartzite flagstone of the Elba Quartzite occurring in the Raft River Mountains. |
| 1.9 | 125.8 | The north-trending ridge ahead and to the left of the microwave tower is composed of Miocene tuffaceous mudstone, sandstone, and conglomerate of the Salt Lake Formation. |
| 9.0 | 134.8 | Basalt flows cut by Bonneville lake terraces are exposed north and south of the highway. White deposits in the valleys are composed of calcareous silt (white marl) from the floor of Lake Bonneville, derived from tuffaceous Miocene strata underlying the basalt. |

- 1.0 135.8 Turn left (north) onto the Cedar Creek Road, a dirt road that heads north along the eastern margin of the Raft River Mountains and connects with Utah State Highway 42.
- 0.9 136.7 Turn left just after crossing fence line, and drive west along fence line road on north side of fence.
- 0.2 136.9 Bear right at "Y" road intersection
- 0.9 137.8 Drive straight through fence line gate.
- 0.2 138.0 Drive through metal gate.
- 0.2 138.2 Turn left at the corral.
- 0.1 138.3 Proceed through the fence, then bear right.
- 1.3 139.6 Cross the wash.
- 0.1 139.7 Turn left at "T" intersection.
- 0.8 140.5 Bear right as road comes in from left.
- 0.3 140.8 Drive straight through gate. Enter mouth of Ten Mile Canyon. Exposures of the Neoproterozoic quartzite of Clarks Basin on slope to left (south), are overlain by marbles of the Ordovician Garden City Formation. The contact between these units is the Mahogany Peaks Fault. A metamorphic grade discordance across this fault is consistent with the removal of 3 to 4 kilometers of section, including the entire Cambrian section. As we proceed up Ten Mile Canyon, we are driving through the Archean rocks of the parautochthon (Fig. 15). Note the exposures of brown-weathering, muscovite-biotite-quartz schist (older schist of Compton, 1972), and blocky, dark outcrops of amphibolite interpreted to represent metamorphosed gabbroic intrusions into the older schist.
- 3.1 143.9 The road crosses the canyon bottom and heads up a long switch back on the north canyon wall. Here we drive through the easternmost exposures of the Archean metamorphosed adamellite unit of Compton (1972,1975). The base of the Miocene shear zone is displayed within the upper 15 meters of the exposures of the adamellite. The adamellite exhibits a gradient in strain, from undeformed in the structurally lower outcrops, to mylonitic in the uppermost structural levels. Structurally above the adamellite unit lies the older schist of Compton (1972, 1975) into which the adamellite intrudes. Further up section lies the Proterozoic Elba Quartzite, which lies unconformably on the Archean basement. The Raft River detachment

fault lies just above the dark schist member of the Elba Quartzite, and here places either Ordovician or Pennsylvanian-Permian rocks on Proterozoic rocks. Elsewhere, the detachment fault places Proterozoic rocks on Proterozoic rocks.

- 0.4 144.3 Turn right onto a faint dirt road that heads just south of the salt lick. Proceed up the road onto a ridge.

- 0.3 144.6 Park in the saddle.

Stop 2-1 (Figs. 14 and 15) Traverse through Cretaceous to Miocene contractional and extensional structures from Crystal Peak to Ten Mile Canyon, eastern Raft River Mountains.

The hike from here will be a one-way traverse. The drivers will backtrack down into Ten Mile Canyon, and meet us on the traverse. We will be climbing about 320 feet, and descending about 1,690 feet, into the bottom of Ten Mile Canyon where lunch will be waiting. This hike will take about 3–3.5 hours. Boots are highly recommended.

Follow the ridge up to Peak 7620, noting fusulinids in Oquirrh Formation sandstone along the way. From this vantage point we have a clear view to the east of a prominent stripe of 2-meter thick quartzite unit running across the slope on the south flank of Crystal Peak. Directly above this stripe of attenuated Eureka quartzite lies the middle detachment which here places Pennsylvanian Oquirrh Group rocks over Ordovician rocks. Beneath the Eureka quartzite lies an upright sequence of rocks, including the Swan Peak Formation and the underlying Garden City Formation. The Garden City Formation forms the grey-colored craggy slopes down the slope, and the basal Swan Peak Formation (a phyllite, Kanosh shale equivalent) forms the grass covered slopes directly above. Both the middle detachment fault and the underlying stratigraphy are folded about an upright, open fold whose axis is oblique to our vantage point. We can make out the southeastern limb as defined by discontinuous outcrops of Eureka Quartzite defining the trace of the middle detachment, and the underlying Ordovician stratigraphy. The fold and the middle

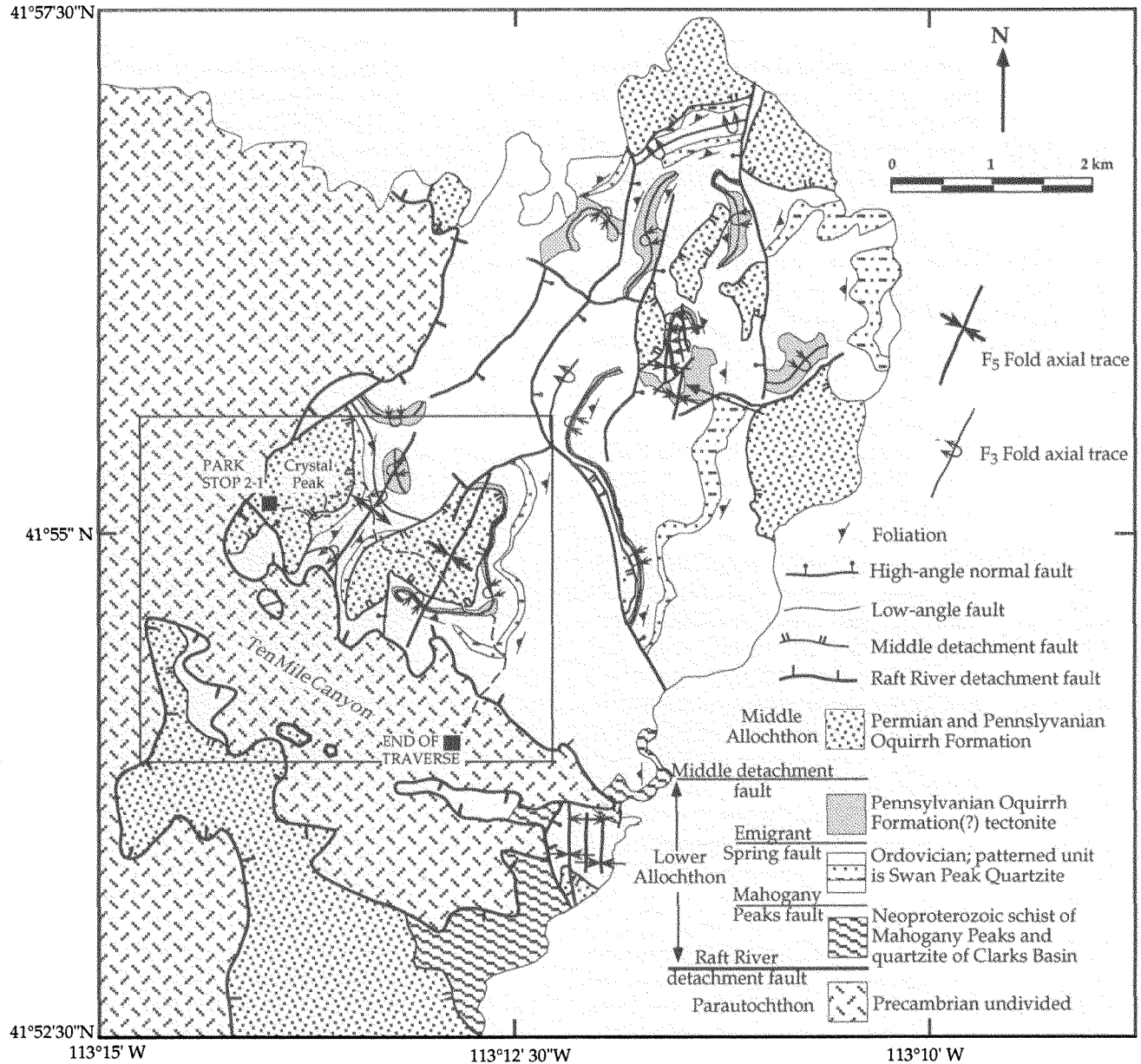


Figure 14. Generalized geologic map of the eastern Raft River Mountains, indicating locations of principal faults and rock units, and axial traces of F₃ recumbent folds and F₅ open folds. Note that Pennsylvanian(?) marble commonly occurs within the cores of recumbent synclines. Location of traverse for stop 2-1 is north of Ten Mile Canyon. The outlined box indicates location of more detailed map of Figure 15. Modified from Wells (1997).

detachment fault are cut by high-angle faults which sole into, or are cut by the Raft River detachment fault, such as the fault with down-to-the east offset seen in the foreground. Looking to the west, the domal morphology of the range is highlighted by the resistant Elba Quartzite. Scattered klippen of Ordovician and Penn-

sylvanian rocks are visible along the crest of the range.

Our next stop will be the Cedar-topped outcrops ~100 feet below the band of Eureka Quartzite. Proceed east across the saddle, over the quartzite ledge and down to the outcrops of the Swan Peak limestone. Walk along the base of the Swan

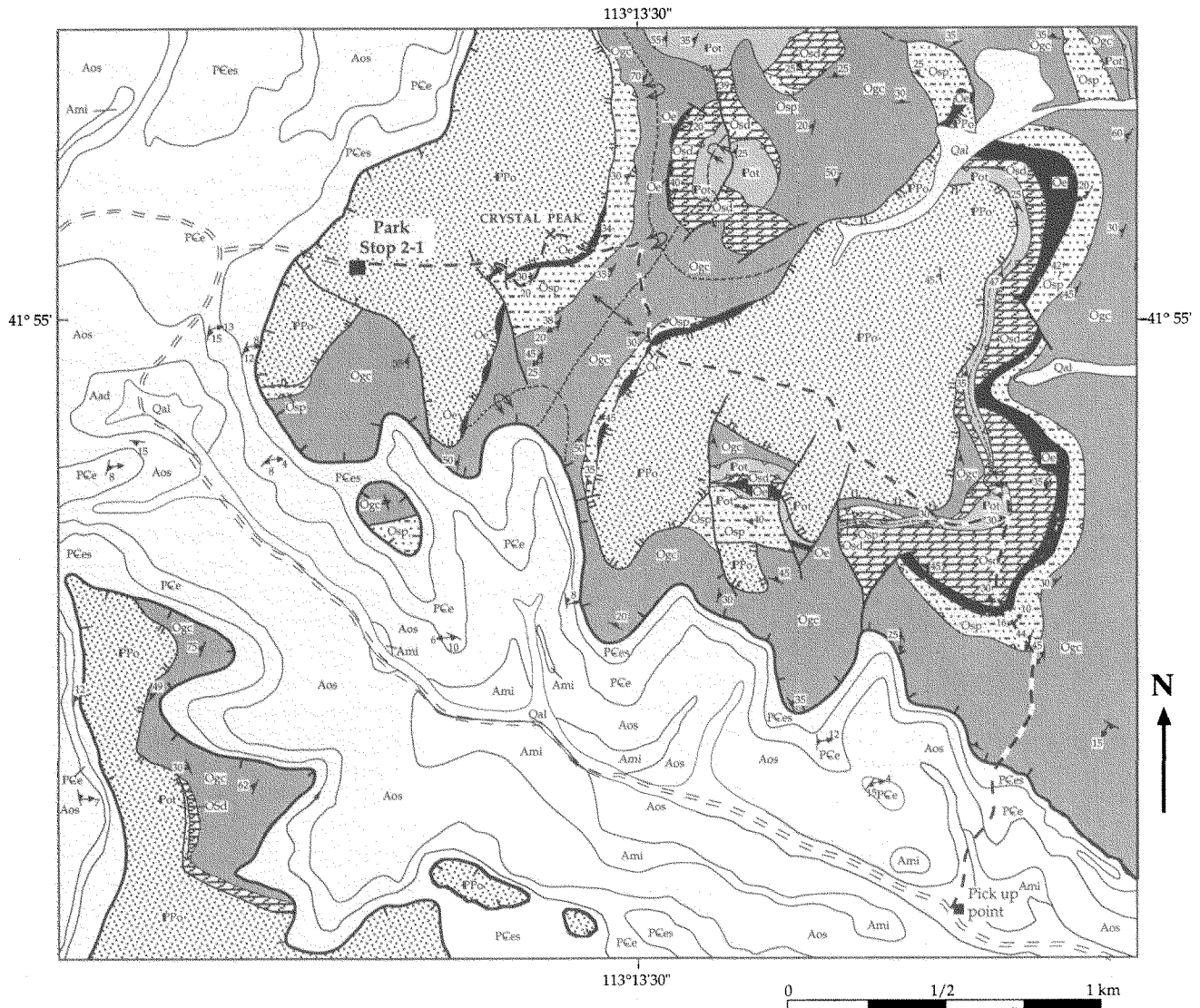


Figure 15. Detailed geologic map of the Crystal Peak area, eastern Raft River Mountains. Note Emigrant Spring fault, separating Pennsylvanian marble (Pot) from Ordovician rocks. Traverse of stop 2-1 is indicated by bold, dashed line.

Peak limestone outcrop from west, uphill to the east, to best view the array of structures. At this locality, D_1 fabrics are well-developed. Here, both bedding and D_1 foliation are discernible and are at a much larger angle to each other than is usual. D_1 foliation dips westward relative to a highly transposed bedding. Stretching lineations are defined by white-calcite streaking and calcite and quartz pressure shadows around pyrite. Foliation is axial planar to the principal small-scale recumbent folds and fold axes are sub-

parallel to the stretching lineation. Foliation intersects a highly transposed bedding at variable angles, forming higher angles in the sandy horizons, and lower angles in the dominantly calcite-rich horizons. Interestingly, foliation is not only refracted between layers but is apparently back-rotated.

Proceed uphill to the band of Eureka Quartzite. The Eureka here is internally brecciated, and within this fault zone above the Eureka occurs minor dolomite (remnants of the Fishaven Dolomite) and minor

Chainman Shale (only apparent as sooty soil) beneath the Oquirrh Group. Oquirrh Group from the top of Crystal Peak yield conodonts with CAI values of 5 indicating metamorphic temperatures of 350 to 400°C, whereas metamorphic temperatures in the footwall are 490 to 520°C, as indicated by oxygen isotopic geothermometry and CAI values >7 from the Swan Peak Formation (Wells et al., 1990; J. Repetski, personal communication, 1988). Therefore, the middle detachment accomplishes a metamorphic grade discordance in temperature of about 125–150°C, with colder rocks over hotter rocks.

Proceed uphill to the top of Crystal Peak (elev. 7770 feet) for a panoramic view including the Raft River Valley to the north and the Black Pine Mountains. To the north-northeast lie the Black Pine Mountains. The southern Black Pine Mountains are composed of three major bedrock units; the Devonian Guilmette Formation, Upper Mississippian and Lower Pennsylvanian Manning Canyon Shale, and the Pennsylvanian and Permian Oquirrh Group (Smith, 1982; Smith, 1983, Wells and Allmendinger, 1990). The Guilmette Formation is the structurally lowest allochthon and its basal contact is not exposed. In general, low-angle faults separate these stratigraphic units and place younger rocks over older rocks. Generally, no significant thickness of section is missing across these faults, with the exception of the fault which places Chesterian Manning Canyon Shale on Devonian Limestone; there, slivers of Kinderhookian limestone occur along the fault contact locally.

Five metamorphic and/or deformational events are recorded in the Black Pine Mountains (Wells and Allmendinger, 1990). From oldest to youngest these include: (1) static metamorphism (M_1) to 350–400°C recorded by pre-tectonic chloritoid porphyroblasts in the Manning Canyon Shale and conodont color alteration indices of 5 to 5.5, possibly synchronous with emplacement of Late Jurassic sills; (2) east-west layer-parallel elongation of 160% associated with synkinematic metamorphism (M_2) and growth of white mica

along cleavage; (3) generally west-vergent low-angle faulting and overturned to recumbent folding; and (4) and (5) doming, and high-angle normal faulting.

Within the Raft River Basin, approximately 1700 meters of upper Cenozoic deposits are present (Williams et al., 1982). Many of these volcanic and volcanoclastic deposits are well exposed in the Jim Sage Mountains, the first range we see to the west of the Black Pine Mountains across the valley. Within the central part of the basin, subsurface studies based on drilling show that these faulted and tilted Cenozoic deposits lie structurally above a relatively flat fault on metamorphosed PreCambrian rocks equivalent to those exposed within the Raft River Mountains. These and other Tertiary deposits within the Raft River Basin are west-dipping, interpreted to relate to down-to-the-east faulting in the upper plate of the detachment fault which floors this structural basin (Covington, 1983). At Strevell, Tertiary basin-fill deposits only reach to a depth of 340 meters, where they overlie Oquirrh Formation.

Walk down the NW-trending ridge to the Swan Peak-Garden City Formation contact, and then contour across to the northeast to outcrops of Garden City Formation at the top of a steep slope with calcite marble exposures. From this vantage point we can look into Crystal Hollow for an overview of upright and overturned stratigraphy and the Emigrant Spring normal fault, that is presently folded. The smooth weathering slopes on the north-west-trending ridge to the southeast are underlain by the Pennsylvanian and Permian Oquirrh Formation of the middle allochthon. The middle allochthon is in fault contact with metamorphosed Pennsylvanian rocks of the Oquirrh Formation of the lower allochthon, the prominent, cliff-forming blue-grey band projecting westward into Crystal Hollow. The Pennsylvanian marble structurally overlies a greatly attenuated Ordovician dolomite section, not visible from this vantage point. The fault separating the Ordovician dolomite from the Pennsylvanian marble, the Emigrant Spring Fault, is interpreted to

represent a Late Cretaceous normal fault of large displacement that omits Silurian, Devonian, and Mississippian section. In addition to the exposures of this fault in the eastern Raft River Mountains, this attenuation fault has been mapped on the highest klippe 7 km to the west and on the west side of Vipont Mountain in the northern Grouse Creek Mountains. Muscovite that defines the foliation within the marble mylonite adjacent to this fault yields a $^{40}\text{Ar}/^{39}\text{Ar}$ plateau age of 88.5 ± 0.3 Ma (Wells et al., 1990). The Ordovician dolomite is underlain by Eureka Quartzite which forms the prominent flat-lying bench along the ridge. Beneath the Eureka Quartzite lies the Swan Peak and Garden City Formations, together, comprising an upright stratigraphic section.

We are standing on uppermost Garden City Formation which is overlain by the Swan Peak Quartzite and an attenuated Eureka Quartzite. Down slope, structurally beneath the Garden City Formation, are white to tan outcrops and float of the Ordovician dolomite, and discontinuous slivers of Eureka Quartzite occur between these units. Below the Ordovician dolomite is Pennsylvanian marble. This overturned section beneath us, together with upright strata to the northwest, comprise a recumbent anticline, with the axial surface within the Garden City Formation. The Cretaceous normal fault is folded about this recumbent fold, which is in turn cut by the middle detachment.

Proceed back to the ridge crest to the south, and cross the middle detachment into the sandstone of the Oquirrh Formation. At the join of two ridges, proceed downhill to the east (~560 meters), bearing right at the next fork in the ridge at elevation 7,200'. Continue down ridge for another 500 meters until you cross the middle detachment fault again. Drop down the slope to the south several meters, until you see a banded, blue-grey and white marble unit. At other localities, there are bits of brown-weathering quartzite and phyllite along the contact between this marble and the Ordovician rocks that represent the remnants of the entire Mississippian section. This marble tec-

tonite is interpreted to be Pennsylvanian Oquirrh Formation within the lower allochthon, and displays fabrics associated with D_2 top-to-the-west shearing. The kinematics of shearing for this unit are not readily apparent from outcrop study, and were determined by study of calcite lattice-preferred orientation. Note few isoclinal folds, and the map pattern indicating that this unit crops out in the core of a recumbent isoclinal syncline. The ridge to the north provides a view of the relationship between the middle detachment and the underlying isoclinal fold in the lower allochthon.

Continue along the ridge to the south, as it winds its way across outcrops of Ordovician dolomitic marble. Proceed through the Eureka Quartzite, and into the heterogeneous Swan Peak Formation. Note the well-developed northeast-trending lineation defined by quartz and calcite pressure shadows. When the Garden City Formation is reached, proceed down slope to the south to the Raft River detachment and Elba Quartzite. Aim for the ridge just east of the prominent drainage that joins Ten Mile Canyon. When you cross the detachment fault, note the indurated dark-grey to black flinty cataclastite that locally overlies the Elba Quartzite, and the mylonitic fabrics within the Elba Quartzite. Also, locally you may find high-angle kink bands that record down-dip-side-up shear, interpreted to result from the passage of a rolling hinge (Manning and Bartley, 1994). Proceed down-slope to the vehicle for lunch.

Retrace route back down Ten Mile Canyon

- | | | |
|-----|-------|---|
| 3.9 | 148.5 | Through gate at canyon mouth. Retrace our route to the Cedar Creek Road. |
| 4.1 | 152.6 | At the intersection with the Cedar Creek Road, turn right through fence line, then an immediate left, and follow dirt road to the intersection of the paved Highway 30. |
| 0.3 | 152.9 | Intersection with paved State Highway 30. Turn left onto Highway 30. |
| 7.6 | 160.5 | Curlew Junction. Junction between State Highway 30 and 42. Turn right(east) on highway 42, heading towards Snowville, Utah. About 8 kilometers east and south- |

east from here three wells encountered Devonian, Mississippian and Pennsylvanian rocks (Pease, 1956). Within the Black Pine Mountains, Devonian and up to 2000 meters of Mississippian strata (thickened by folding) are present (Smith, 1982). This is in marked contrast to the absence of Mississippian and Devonian rocks in the eastern Raft River Mountains ten kilometers to the west-southwest. As we drive across the Curlew Valley, we can see recent mining activity along the east flank of the Black Pine Mountains. The roads on the east flank are within the newly redeveloped Black Pine mining district. Exploration by Noranda has defined five sepa-

rate orebodies totaling 5.2 million tons of 0.06 opt gold (Hefner et al., 1990) within Pennsylvanian and Permian Oquirrh Group rocks.

15.2 175.7 Junction of Interstate 84 and Highway 30, just west of Snowville Utah. Optional stop in Snowville. Proceed onto Interstate 84, heading towards Ogden, UT.

ACKNOWLEDGMENTS

This research was supported by the National Science Foundation (grant EAR-9317387 to Wells and grant EAR-9317044 to Hoisch). We thank D. M Miller for his continued help and encouragement in these studies. Reviews by T. Lawton, and editor P. Link are appreciated.

Kinematics and Mechanics of the Willard Thrust Sheet, Central Part of the Sevier Orogenic Wedge, North-central Utah

W. A. YONKEE

Department of Geosciences, Weber State University, Ogden, Utah 84408

INTRODUCTION

This paper and accompanying road log focus on structural relations of the Willard thrust sheet, which forms part of the central thrust system of the Sevier orogenic wedge. An integrated analysis of the large-scale structural geometry, style of internal deformation, and characteristics of fault rocks along the Willard thrust provide insights into the kinematics and mechanics of this very large and far-travelled thrust sheet. Specifically on this part of the trip we will examine evidence for significant thrust-parallel extension at the base of the sheet, development of a weak fault zone with high fluid pressures, and importance of footwall deformation.

Regional Setting of the Central Thrust System

The central thrust system of the Sevier orogenic belt carries a thick package of shelf (miogeoclinal) rocks, shares a basal decollement in Upper Proterozoic strata, and accommodated significant ESE-directed slip. Within northern Utah the central system is represented by the Willard thrust, which branches northward into the Paris and Meade thrusts in southeastern Idaho. The Willard thrust had about 50 km of top-to-ESE slip, and to the north displacement is divided into about 20 km of slip on the Paris thrust and 30 km of slip on the Meade thrust. Large-scale folds within these thrust sheets produced additional shortening, and lower levels were internally deformed by foliation, minor folds, and minor faults. The central system can be crudely divided into a western part above a flat decollement (preserved in the Promontory Mountains area) and an eastern part where the basal decollement ramped up (preserved along the Wasatch Front; Fig. 16). The western part is characterized by a thick section of Pennsylvanian to Permian Oquirrh Basin strata that were folded and transported eastward above the Late Jurassic Manning Canyon detachment (Allmendinger et al., 1984), and by development of low-angle normal faults that omit strata. The eastern part contains more widespread large-scale folds and imbricates, and was locally uplifted during growth

of the underlying basement-cored Wasatch anticlinorium.

The central thrust system experienced several episodes of major slip (DeCelles et al., 1993). The Neocomian (?) to Aptian (≈ 130 – 115 Ma) lower part of the Gannett Group and equivalent lower part of the Kelvin Formation to the south record the start of major slip and erosion of the Willard and Paris thrust sheets. Deposition of the Aptian to Albian (≈ 115 – 100 Ma) upper part of the Gannett Group and equivalent middle part of the Kelvin Formation record slip on the Meade thrust and renewed slip on the Willard thrust. A Cenomanian to Turonian (≈ 100 – 90 Ma) phase of erosion from the Willard and Meade sheets is recorded by conglomeratic facies of the Frontier Formation and equivalent strata to the north (Schmitt, 1985). Muscovite grains from syntectonic veins near the base of the Willard sheet have $^{40}\text{Ar}/^{39}\text{Ar}$ ages between 140 and 110 Ma, recording internal deformation that partly predated and was partly synchronous with major thrust movement (Yonkee, 1990).

Large-scale Structural Geometry of the Willard Thrust Sheet

The Willard thrust sheet is well exposed in north-central Utah where younger tilting and erosion has exhumed a wide range of structural levels, providing an excellent down-plunge view of this large, far-travelled thrust sheet (Figs. 16 and 17). The Willard sheet carries a thick package of rocks that includes from bottom to top: a 2- to 3-km-thick Upper Proterozoic section of mica-rich strata and micaceous quartzite; a 2- to 3-km-thick section of Upper Proterozoic and Lower Cambrian quartzites; and a 5- to 7-km-thick carbonate-rich section of Middle Cambrian to Permian strata that thicken westward. Mesozoic strata have been eroded and their original thickness is uncertain. By comparison, the footwall contains a distinctively thinner package of Paleozoic to early Mesozoic platform strata that overlie Lower Proterozoic high-grade metamorphic and igneous basement rocks (Bryant, 1984).

The main Willard thrust has a ramp-flat geometry, with a western hangingwall flat in mica-rich Upper Proterozoic

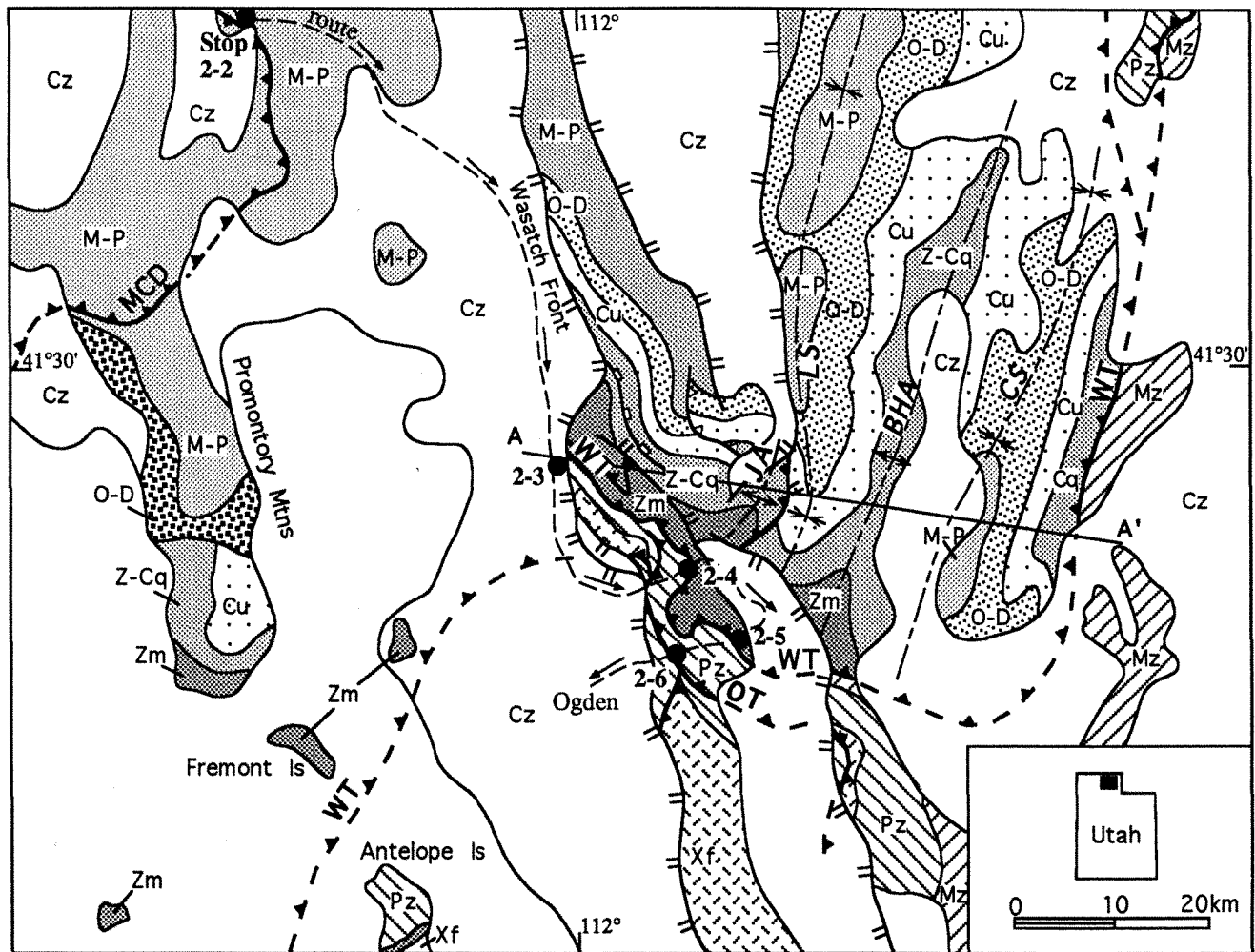


Figure 16. Index map of north-central Utah showing main structural features of the Willard sheet. Units in hanging wall of Willard thrust are: Zm—Upper Proterozoic mica-rich rocks and micaceous quartzites (also locally includes thin slices of Lower Proterozoic basement); Z-Cq—Upper Proterozoic and Lower Cambrian quartzites; Cu—Middle and Upper Cambrian strata; O-D—Ordovician to Devonian strata; and M-P—Mississippian to Permian strata. Units in footwall of Willard thrust are: Xf—Lower Proterozoic crystalline basement; Pz—Paleozoic strata; and Mz—Mesozoic strata. Cz—Cenozoic strata. Major faults are Manning Canyon decollement (MCD), Willard thrust (WT), and Ogden thrust system (OT). Major folds are Causey syncline (CS), Browns Hole anticline (BHA), Logan Peak syncline (LS), and James Peak anticline (JA). Modified from Hintze (1980). General line of cross section in Figure 17, and location of route and stops indicated.

strata and an eastern ramp in quartz-rich Upper Proterozoic to Lower Cambrian strata (Fig. 17). The thrust also has a western footwall flat in Cambrian shale and limestone, a central ramp, and an eastern flat in Jurassic argillaceous limestone and evaporites. A footwall imbricate appears to continue east from the eastern flat and is associated with a belt of folding and layer-parallel shortening in Jurassic strata. The Willard sheet is also deformed by a major imbricate, referred to as the upper branch of the Willard. Translation of the thrust sheet over ramps and

flats produced broad, open, upright folds including the Logan Peak syncline, Browns Hole anticline, and Causey syncline (Fig. 17). A tight, overturned anticline, referred to here as the James Peak anticline, probably formed during propagation of the upper branch.

Although the upper part of the Willard sheet is unmetamorphosed, the lower part underwent widespread greenschist-facies metamorphism with development of muscovite, chlorite, chloritoid, and biotite. Fluid inclusion data, combined with thermal modeling suggest peak temperatures

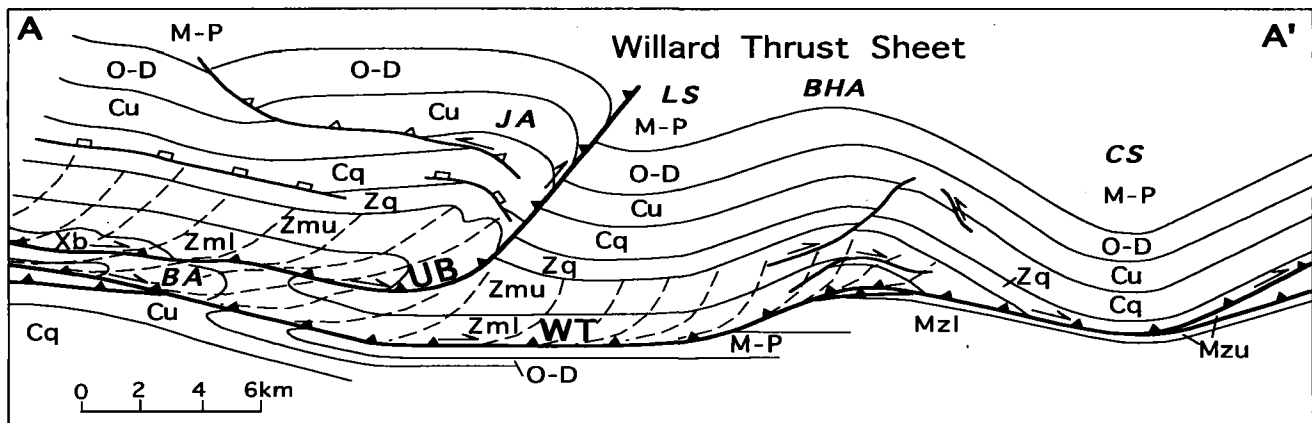


Figure 17. Generalized cross section A-A' of eastern part of Willard thrust sheet, drawn incorporating down-plunge projection of data, with effects of Cenozoic normal faulting removed. Units are same as Figure 16 except lower part of sheet divided into: Xb—Lower Proterozoic basement of Facer Formation; Zml—Upper Proterozoic mica-rich rocks; Zmu—Upper Proterozoic micaceous quartzites; Zq—Upper Proterozoic quartzites; and Cq—Lower Cambrian quartzites. Major faults and folds same as in Figure 16 and UB—upper branch of Willard thrust. General foliation trajectories indicated by dashed lines.

of about 300 to 450°C within the lower part of the Willard sheet at depths of 10 to 15 km, with elevated, temporally variable fluid pressures (Yonkee et al., 1989).

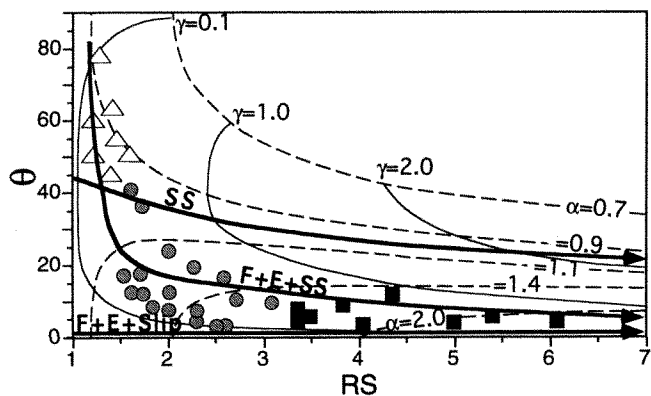
Kinematics of Internal Deformation

The thrust sheet was internally deformed during and prior to large-scale slip, and the style of internal deformation varies with lithology and structural level (Yonkee, 1994, 1996). Rocks in the upper and eastern parts of the thrust sheet are relatively undeformed, but the western, lower part of the sheet displays widespread foliation, minor folds, and minor faults. Foliation is generally absent in Paleozoic carbonates and quartzite at far distances from the thrust. Foliation is weakly to moderately developed and overall moderately dipping in Upper Proterozoic micaceous quartzite at intermediate distances from the thrust, and is strongly developed and gently dipping in Upper Proterozoic mica-rich strata near the thrust, defining a classic asymptotic pattern.

Finite strain has been estimated from changes in shapes and positions of quartz grains in quartzite and polymineralic clasts in diamictite using the R_f/ϕ and normalized Fry methods for several areas in the Willard sheet, including the Promontory, Willard Peak and Lewis Peak areas (stops 2-2 to 2-5; Yonkee, 1994). These areas show overall consistent strain patterns (Fig. 18A). X-Z axial ratios in quartzites away from the thrust are mostly <1.3:1, recording very limited strain. Micaceous quartzites at intermediate distances have X-Z axial ratios mostly from 1.3:1 to 2:1 and X-Y planes that generally dip at moderate to high angles to the thrust. Mica-rich strata in the lower part of the sheet

have axial ratios mostly from 2:1 to 8:1, with the highest ratios in a high-strain zone adjacent to the thrust. X-Y planes are gently dipping and rotate into parallelism with the thrust in the high-strain zone. Most samples display apparent flattening with principal E-W extension and minor to significant N-S extension.

Thrust sheets internally deform by varying combinations of simple shear, thrust-parallel extension and shortening, volume loss, and discrete slip. Relations between X-Z strain ratios, R_s , and the angle between X-Y planes and the thrust, θ , constrain the relative contributions of these components, although complexities may occur (Fig. 18; Sanderson, 1973). Ideal simple shear results in slowly decreasing θ with increasing R_s , but to produce thrust-subparallel foliation ($\theta < 5^\circ$), requires $R_s \gg 10:1$, inconsistent with observed strain patterns in the Willard sheet. Rather, observed patterns are consistent with a combination of thrust-parallel extension and simple shear at deeper levels, moderate layer-parallel shortening and shear at intermediate levels, and minor shortening at higher levels. In the simple model of heterogeneous simple plus thrust-parallel extension and perpendicular flattening shown in Figure 18B extension increases downward and simple shear increases both downward and toward the rear to the sheet to maintain strain compatibility. This model produces patterns similar to observed data, with asymptotic foliation trajectories, modest increases in strain ratios at the base of the sheet, and an increase in simple shear and total displacement toward the rear of the sheet. However, other factors, such as volume loss and discrete slip on minor faults, also need to be considered to develop a more com-



plete model. The overall strain pattern is consistent with rotation of strain axes (and probable complex rotation of stress orientations) in the base of the sheet. These rotations may be related to the presence of a weak fault zone that refracts stress trajectories or to isostatic adjustments within a weaker lower part of a sheet during thrust loading.

Fault Rocks and Fault Zone Mechanics

Rocks along the main Willard thrust are relatively well exposed at several locations, including the Willard Peak, North Ogden Pass, and Lewis Peak areas (stops 2-3 to 2-5; Yonkee, 1996). A composite traverse across the fault zone reveals overall consistencies and some differences with three general divisions: (1) a high strain zone in the base of the hanging wall; (2) a central fault core; and (3) a zone of variably concentrated footwall deformation (Fig. 19). Together, these three intervals can be viewed as a large brittle-ductile shear zone. The base of the hanging wall

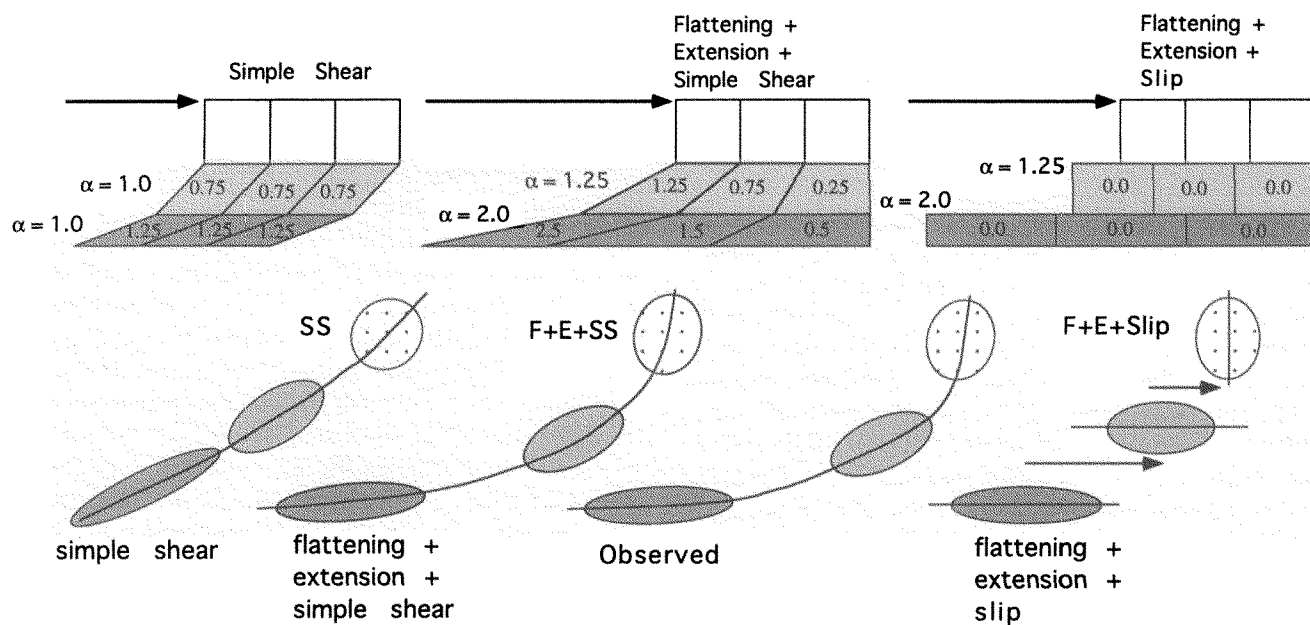


Figure 18. General strain model for Willard sheet.

A. Sanderson (1973) diagram illustrating relations between X-Z strain ratios, R_s , and angles between X-Y strain planes and Willard thrust, θ , for samples in the Willard thrust sheet. Values of thrust-parallel shear, γ and thrust-parallel extension, α are contoured. Samples in the high-strain base of the sheet (< 100 m from the thrust) indicated by black squares, mica-rich samples in lower levels of the sheet (about 100 to 500 m above the thrust) indicated by gray circles, and micaceous quartzite samples at intermediate levels (about 500 to 1000 m above the thrust) indicated by triangles. Strain values for combinations of thrust-parallel simple shear (SS), thrust-parallel extension and flattening plus simple shear (E+F+SS), and thrust-parallel extension and flattening plus discrete slip (E+F+Slip) indicated. Strain data are consistent with some combination of thrust-parallel extension, flattening, simple shear, and discrete slip.

B. Cartoon illustrating simple models for internal deformation of a thrust sheet. Average values of thrust parallel extension, α , and simple shear labeled, and resulting strain ellipses and foliation trajectories indicated. Observed strain ellipses and foliations trajectories are similar to those for thrust-parallel extension and flattening plus shear. Note, shear and slip increase downward and toward the back of a thrust sheet that undergoes thrust-parallel extension.

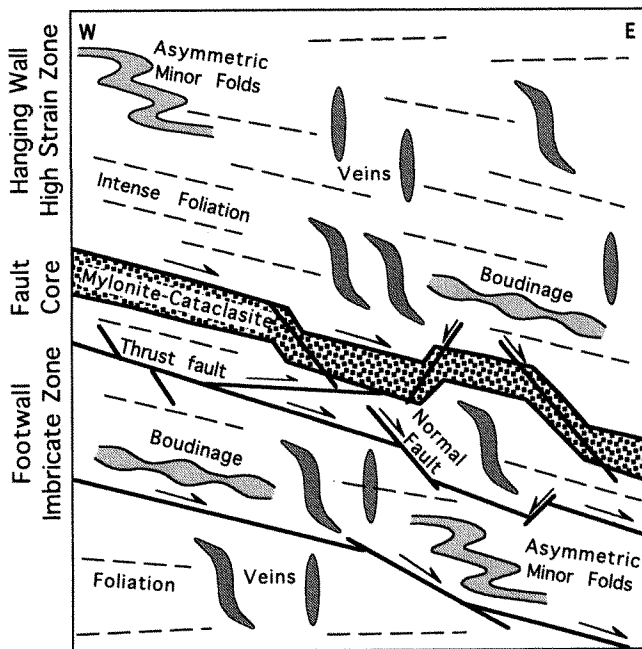


Figure 19. Cartoon of Willard thrust fault zone in Willard Peak area. The overall fault zone consists of a hanging wall high-strain zone, a central core, and a footwall imbricate zone. The fault zone is locally extended by minor normal faults and rocks display various combinations of foliation (dashed lines), veins, asymmetric folds, and boudinaged competent layers.

displays intense thrust-parallel foliation, multiple sets of variably deformed cross cutting veins, asymmetric minor folds, and boudinaged competent layers subparallel to the thrust. The fault core consists of phyllonite, ultramylonite, and cataclasite, with the amount of cataclasite and overprinting brecciation increasing with decreasing structural depth. The fault core is also locally cut by minor normal faults with similar mylonitic textures, indicating that normal faulting and thrust-parallel extension overlapped with large-scale thrusting. The style of footwall deformation varies with structural level. Deeper western levels display complex imbricate thrusts and folds that thicken strata, detachment faults that omit strata, foliation at varying angles to bedding, and complex vein networks. Higher levels display less pervasive, more brittle deformation, with development of contraction faults and some minor folds.

Deformation textures and interpreted deformation mechanisms vary across the overall fault zone. The base of the hanging wall displays highly flattened quartz grains with recrystallized margins, mica with strong preferred orientation, microveins, and quartz-mica fibers around competent grains recording widespread crystal-plastic and diffusive mass transfer deformation (Fig. 20A). The fault core contains abundant fine-grained, recrystallized micaceous matrix,

variably flattened breccia fragments, complex microvein networks, and discrete fractures, recording overlapping crystal-plastic deformation, brittle fracturing, and sealing with periods of high fluid pressure (Fig. 20B). Footwall limestone at deeper levels underwent extensive plastic recrystallization, but carbonates at shallow levels deformed mostly by brittle processes (Evans and Neves, 1993).

These overall patterns have important implications for the strength of the fault zone, and for the mechanics of the Willard thrust sheet (Yonkee, 1996). Concentrated thrust-parallel extension accompanied large-scale thrusting, with extensional and shear strains on the order of 0.1 to 1 increasing towards the thrust. These strains accumulated over time intervals on the order of 3 to 30 Ma, giving estimated average strain rates on the order of 10^{-14} to 10^{-16} s^{-1} . Widespread veins probably formed by hydrofracturing, requiring the local effective minimum stress to equal the tensile strength of the rock. Although stresses were probably spatially variable and partly controlled by local stress concentrators, large-scale vein geometries and fluid inclusion characteristics require significantly elevated fluid pressures. Minor normal faulting of more competent strata and sealed fault rocks also accompanied large-scale thrusting that was concentrated within a fine-grained micaceous fault core. A highly simplified model for stress conditions along the fault zone based on these observations is given in Figure 21. Plastic deformation of mica- and wet-quartz-rich material is consistent with low deviatoric stresses on the order of several MPa for the estimated strain rates. A Mohr stress circle for such low effective stress intersects the frictional failure criteria for a pre-existing mica-rich fault zone at low θ (corresponding to the maximum compressive stress at high angles to a weak fault), intersects the shear failure criteria for intact rock at higher θ , and intersects the tensile failure criteria due to high fluid pressures. Interestingly this pattern allows for roughly simultaneous development of thrust-subparallel foliation, veins, minor normal faults in intact or sealed rock, and large-scale thrusting along a mica-rich fault core. Thus large-scale emplacement of this very thick and far travelled thrust sheet appears to have been related to the presence of a very weak fault zone that experienced high fluid pressures.

Road Log for Part 2 of Day 2: Transect from Raft River Mountains to Wasatch Range, Utah

0.0	175.7	Begin part 2 of day 2 road log at junction of I-84 and Utah 30 near Snowville, UT. Large areas of Permian to Pennsylvanian strata of the Oquirrh Formation are poorly exposed in low ranges to the east of Snowville.
-----	-------	---

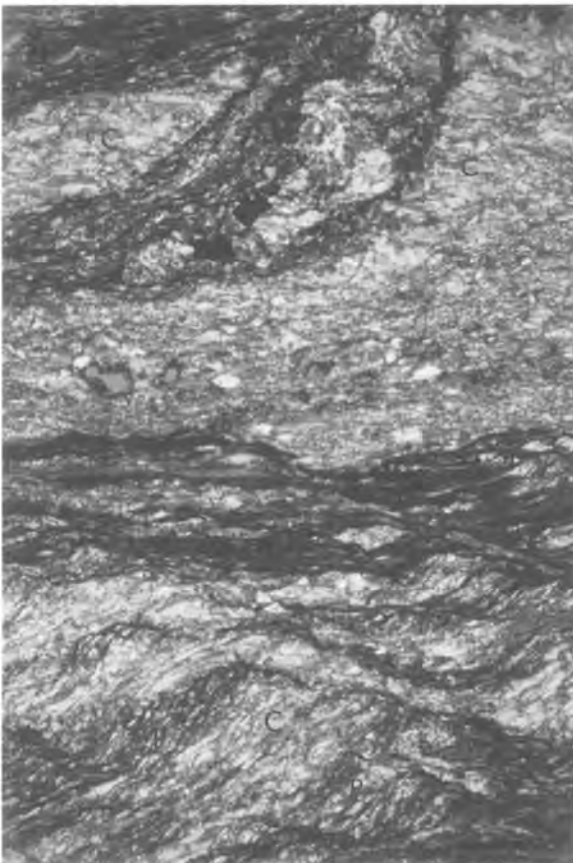


Figure 20. Photomicrographs of fault zone textures in the Willard Peak area. Bases of photographs represent 2 mm length.

A. Phyllonite from high strain zone contains abundant fine-grained, recrystallized micaceous matrix (M) and displays intense foliation that is refolded, crenulated, and cut by multiple sets of variably folded and recrystallized quartz-mica veins (V and xv).

B. Tectonite from fault core. Fragments of phyllonite (P) and calc mylonite (C) are tectonically mixed and variably recrystallized, flattened, and dissolved along dark seams.

11.0 186.7 Hansel Valley. This valley is bounded on the east by a normal fault, which had a magnitude 6.6 earthquake in 1934 and produced a small surface rupture to the south.

10.0 196.7 **Stop 2-2.** Overview of the structural style of Willard thrust sheet in the Promontory Mountains. Take Howell exit, pull over to side of exit ramp for discussion, and return to I-84.

The Promontory Mountains, visible to the south, expose overall northerly plunging structures along an oblique section from upper levels to the base of the Willard thrust sheet. Upper levels exposed in the northern part of the range consist of Permian to Mississippian strata imbricated by the Late Jurassic Manning Canyon decollement and shortened by a system of large-scale upright to inclined

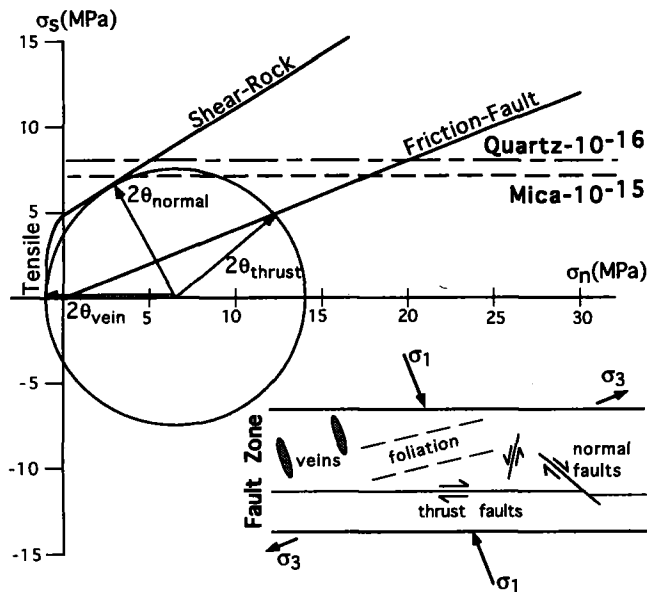


Figure 21. Model for possible effective normal stress (σ_n) and shear stress (σ_s) conditions at base of Willard sheet. Flow laws for muscovite and wet quartz at strain rates of $10^{-15} s^{-1}$ and $10^{-16} s^{-1}$ represents plastic deformation of mica-rich strata and quartzite. Solid lines represent frictional slip along a pre-existing micaceous fault zone (based on data for muscovite), shear failure of intact rock (based on a typical Byerlee's law), and tensile vein formation, with values of 2θ indicated. Inset shows resulting simultaneous formation of foliation, veins, normal faults, and thrust faults in a weak fault zone in which the maximum compressive stress, σ_1 , is rotated to steep angles.

folds (Crittenden, 1988). Middle levels contain a gently dipping sequence of competent quartzite and carbonate that display limited internal deformation. Lower levels exposed in the southern part of the range and on Fremont Island to the south contain Upper Proterozoic strata that were metamorphosed to greenschist facies and internally deformed by widespread foliation, minor folds, and vein arrays. Foliation is moderately to weakly developed in strata at moderate distances from the Willard thrust and becomes intensely developed at low angles to the thrust in the base of the sheet on Fremont Island (Fig. 22). Finite strain patterns for samples from the base of the sheet record concentrated thrust-parallel top-to-SE simple shear and thrust-parallel extension (Yonkee, unpublished data). The footwall, exposed further south on Antelope Island, also displays low-grade metamorphism and internal deformation, with foliation at low angles to bedding in mica-rich Upper Proterozoic strata, whereas Cambrian quartzite displays upright minor folds and moderately to steeply dipping foliation. Low-angle normal faults of uncertain age locally omit parts of the stratigraphic section in the

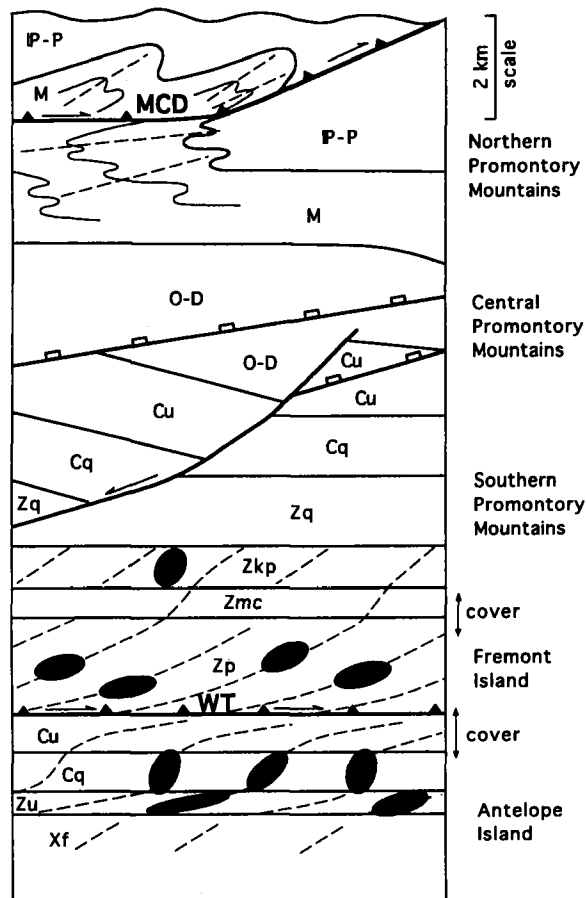


Figure 22. General structural column for Promontory Mountains south of stop 2-2. Overall foliation trajectories shown by dashed lines, and X-Z strain ellipses for selected samples indicated. Units are: Zp—mica-rich strata of formation of Perry Canyon; Zmc—micaceous quartzite of Maple Canyon Formation; Zkp—argillite and quartzite of Kelley Canyon and Papoose Creek Formations; Zq—Upper Proterozoic quartzites; Cq—Lower Cambrian quartzite; Cu—Middle and Upper Cambrian strata; O-D—Ordovician to Devonian strata; M—Mississippian strata; P-P Pennsylvanian to Permian strata; Zu—Upper Proterozoic strata undivided, and Xf—basement of Farmington Canyon Complex. WT—Willard thrust and MCD—Manning Canyon decollement. Column based on geology from Crittenden (1988) and Yonkee (unpublished data).

Promontory Mountains and may record minor Late Cretaceous to early Tertiary extension and unroofing (Fig. 22). Listric normal faults, that locally reactivated older thrusts, bound asymmetric grabens with tilted Oligocene strata within surrounding areas, probably recording initial collapse of the Willard sheet after cessation of thrusting (Constenius, 1996).

19.8 216.5 View to east of the Wasatch Range, where a thick sequence of Cambrian to Pennsylvanian strata is spectacularly exposed.

An overall northerly plunge to structures, combined with uplift in the footwall of the Cenozoic Wasatch normal fault, has resulted in exposure of an oblique section across upper levels in the Willard sheet. Internal deformation at upper levels is limited, with development of minor contraction faults, rare minor folds, and very rare weak cleavage. A series of E- to NE-striking, steeply dipping faults also cut the strata. Slip on these faults decreases eastward away from the mountain front, and these faults may be partly related to differential uplift and tilting within the footwall of the Wasatch fault.

- 16.1 232.6 Junction with U.S. 91. Bear right onto exit to Brigham City, take left at stop sign, and proceed east on U.S. 91. View to east of Wasatch Range, where a thick sequence of Cambrian to Upper Proterozoic quartzite is exposed in the Willard sheet.
- 2.1 234.7 Junction with U.S. 89. Turn right and proceed south on U.S. 89.
- 3.0 234.7 View to east of Perry Canyon where a thick sequence of Upper Proterozoic micaceous quartzite, argillite, and diamictite is exposed in the lower part of the sheet.
- 3.0 237.7 **Stop 2-3.** Overview of Willard thrust sheet in Willard Peak area (Fig. 16). Turn left onto Center Street, proceed east two blocks, turn right and proceed south one block to City Park. Pull over for discussion. After stop retrace route back to U.S. 89.

The Willard thrust system is well exposed to the north along Willard Canyon. Here the thrust consists of two branches: an upper branch that repeats Proterozoic rocks and a main branch that places Proterozoic rocks over Cambrian strata. Both branches dip east here due to tilting along the east limb of the underlying basement-cored Wasatch anticlinorium. The trace of the main branch continues southward along the Wasatch Range from Willard Peak to Ogden Canyon (Crittenden and Sorensen, 1985a, 1985b; Davis, 1985). The Willard sheet, which carries a distinctly thick package of Upper Proterozoic to Paleozoic rocks, is also exposed on Fremont Island, visible to the southwest, and in the Promontory Mountains, visible to the west.

In the Willard Peak area the main branch has a hangingwall flat in mica-rich Upper Proterozoic strata with local slices of Lower Proterozoic basement and a footwall flat in imbricated and tectonized Cambrian strata (Fig. 23).

An isoclinal, recumbent syncline with a complexly deformed hinge zone is developed between the two branches. Foliation is generally absent at higher levels in Upper Proterozoic quartzite away from the thrust, and limited deformation is produced mostly by minor faults. At intermediate levels in argillite and micaceous quartzite of the Kelley Canyon and Maple Canyon Formations foliation is weakly to moderately developed and overall moderately dipping. At lower levels in mica-rich strata of the formation of Perry Canyon foliation is well developed and overall gently dipping. Foliation rotates into subparallelism with the upper branch, and is approximately parallel to the two branches in the isoclinal syncline.

Finite strain, estimated using the R_f/ϕ and normalized Fry methods, varies systematically with structural level (Fig. 23). Strain ratios in quartzites away from the thrust are mostly less than 1.3:1, indicating only limited penetrative deformation. Within micaceous quartzite and argillite at intermediate levels X-Z axial ratios range mostly from 1.3:1 to 2.0:1 and X-Y planes dip steeply to moderately subparallel to foliation. Within mica-rich strata at deeper levels X-Z axial ratios range mostly from 2:1 to 5:1 with the highest ratios adjacent to the main branch, and X-Y planes dip gently, subparallel to the thrust branches. Most samples display apparent flattening with principal E-W extension and variable N-S extension. Strain patterns record minor layer-parallel shortening and simple shear at higher levels, and a combination of concentrated thrust-parallel extension and top-to-E simple shear at deeper levels, although complexities occur.

The main branch of the Willard thrust is relatively well exposed at several nearby locations and can be viewed as part of a larger brittle-ductile shear zone that includes the highly strained base of the hanging wall, a fault core with concentrated slip, and a footwall imbricate zone (Fig. 19). The base of the hangingwall displays intense thrust-parallel foliation, multiple vein sets, asymmetric minor folds, and boudinaged quartz-rich layers, recording thrust-parallel extension and shear, as well as repeated episodes of high fluid pressure, fracturing, and sealing. The fault core is generally 2 to 5 m thick in this area and consists of ultramylonite, phyllonite, and cataclasite composed of tectonic mixtures of hanging wall and footwall material. The fault core displays evidence for overlapping brittle deformation with discrete fracturing and brecciation, ductile deformation with plastic recrystallization and flattening of breccia fragments, and diffusive mass transfer with development of multiple vein sets at high fluid pressures (Fig. 20; Yonkee, 1996). The imbricate zone consists of slices of Cambrian strata and some hangingwall phyllite that are bounded by 0.1 to 2-m-thick mylonite and cataclasite zones. Argillaceous limestone within the imbricate slices displays thrust-parallel foliation, variably deformed veins, asymmetric

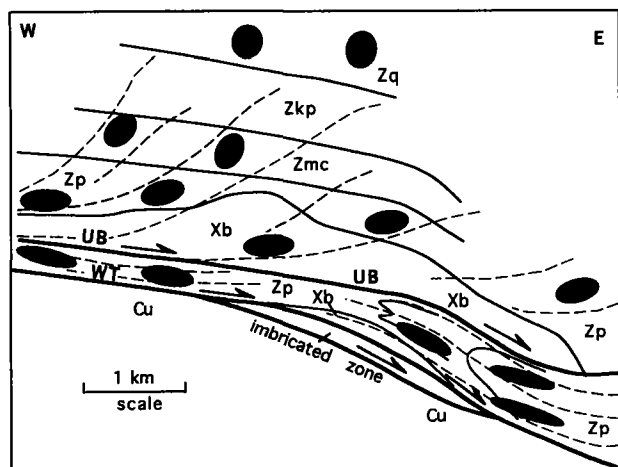


Figure 23. Down-plunge projection of Willard Peak area near stop 2-3. Overall foliation trajectories shown by dashed lines, and X-Z strain ellipses for selected samples indicated. Units are: Xb—basement of Facer Formation; Zp—mica-rich strata of formation of Perry Canyon; Zmc—micaceous quartzite of Maple Canyon Formation; Zkp—argillite and quartzite of Kelley Canyon and Papoose Creek Formations; Zq—Upper Proterozoic quartzites; and Cu—Cambrian strata. WT—main branch of Willard thrust and UB—upper branch of the Willard thrust.

minor folds, and boudinaged competent layers, similar to patterns in the hanging wall although details are more complex. Interestingly the fault core and imbricate zone are locally cut by minor normal faults that appear to have overlapped with large-scale thrusting. Along the north side of Willard Canyon the imbricate zone is unusually thick and consists of tightly folded, strongly foliated Cambrian limestone and shale, which form a wide zone of penetrative footwall deformation.

3.3. 241.0 Dark-colored granitic gneiss of the Precambrian Farmington Canyon Complex is well exposed along lower parts of the Wasatch Range to the east within the east limb of the Wasatch anticlinorium beneath the Willard thrust. The overlying Cambrian section consists of tan-colored Tintic Quartzite and brown to gray tectonized shale and limestone of the Ophir and Maxfield Formations. Willard Peak, the high point, is capped by light-colored Lower Proterozoic Facer Formation in the Willard sheet.

1.8 242.8 Roadcut in Tintic Quartzite at the southwest end of the Pleasant View bench. The bench consists of complexly faulted bedrock with discontinuous Holocene fault scarps, and is bounded on the southwest

- and northeast by major splays of the Wasatch fault zone (Crittenden and Sorensen, 1985a; Personius, 1988).
- 0.2 243.0 Turn left and head east on Pleasant View Drive.
 - 2.0 245.0 Bear left onto Elberta Drive and continue heading east.
 - 1.5 246.5 Turn left at stop sign and head north on 450 East.
 - 0.4 246.9 Turn right and head east on North Ogden Drive (3100 North).
 - 1.0 247.9 Junction with 1050 East. Continue heading east on North Ogden Drive.
 - 1.0 248.9 Cross approximate trace of Wasatch fault and start climb into the Wasatch Range. Complexly folded and imbricated Cambrian Tintic, Ophir, and Maxfield Formations, visible beneath Ben Lomond Peak to the north, form part of a footwall duplex beneath the Willard sheet. The Ogden thrust, visible to the southeast, repeats tan-colored quartzite of the Tintic Formation. The thrust branches further southward and imbricates basement and cover rocks within the Wasatch anticlinorium.
 - 0.5 249.4 Fractured Tintic Quartzite is exposed along road cuts to north. Limestone ledges in the Cambrian Ophir and Maxfield Formations are exposed to the south on the downdropped side of an east-striking normal fault near the base of the canyon.
 - 1.2 250.6 Cross approximate trace of north-striking normal fault that downdrops east side. An isoclinal, recumbent syncline is developed within middle to upper Cambrian gray carbonates beneath a klippe of the Willard thrust sheet along the ridge to the northeast.
 - 0.8 251.4 North Ogden Pass. View to east of Ogden Valley, which is an asymmetric graben partly filled with east-tilted late Eocene to Oligocene volcanic and volcanoclastic rocks. Early development of the graben may record initial collapse of the Sevier wedge after cessation of thrusting (Constenius, 1996).
 - 0.6 252.0 Cross approximate trace of detachment fault that omits section and places tectonized Maxfield Limestone on the east over Tintic Quartzite on the west.

- 0.4 252.4 Highly fractured carbonates of the Maxfield Limestone exposed along this series of roadcuts lie within an east-dipping horse beneath the Willard thrust.
- 0.4 252.8 **Stop 2-4.** Willard fault zone and footwall deformation in North Ogden Pass area (Fig. 24). Pull over into small parking area where road makes a sharp bend to the right.

The Willard thrust dips about 20° to 40° NE here and places graywacke and argillite of the Upper Proterozoic formation of Perry Canyon over Cambrian Maxfield Limestone in the road cut. Within the hangingwall strata are folded into an east-verging anticline and display strong, gently dipping axial planar foliation at low angles to the thrust (Fig. 24). Finite strain data record X-Z axial ratios from 3:1 to 5:1, gently dipping X-Y planes at low angles to the thrust, and flattening strains, consistent with a combination of thrust-parallel extension and top-to-E simple shear at the base of the Willard sheet (Yonkee, unpublished data).

Part of the Willard fault zone is exposed in the road cut, including: intensely foliated phyllite with shear bands in the base of the hanging wall; a 1- to 3-m-thick zone of cataclasite and breccia composed of phyllonite, mylonitic limestone, and vein fragments; and a 3- to 5-m-thick zone of tectonized limestone and dolostone in the footwall. Quartz in phyllite displays widespread plastic deformation, calcite in limestone underwent extensive plastic recrystallization, and dolomite deformed mostly by microcracking. Minor structures near the thrust include small shear zones that record heterogeneous top-to-east shear and net-vein systems that probably record high fluid pressures. Rocks 20 to 100 m below the thrust are overall less deformed.

The footwall consists of complexly imbricated Cambrian rocks and includes: a lower horse of Cambrian carbonates that are rotated into a recumbent, isoclinal syncline and bounded below by a detachment fault that omits section; and an upper horse of east-dipping Tintic Quartzite and Cambrian carbonates bounded below by a major footwall imbricate and above by the Willard thrust (Fig. 24). The footwall imbricate locally truncates the lower horse and associated syncline, and a smaller-displacement reverse fault cuts the imbricate, recording a complex history of faulting. The syncline fold axis plunges gently N, subparallel to the Willard thrust and subperpendicular to the interpreted eastward regional transport direction. Foliation is well developed in Cambrian limestone, and forms a partial fan within the syncline of the lower horse, and is at acute angles to subparallel to bedding in the upper horse. These complex patterns probably record overlapping footwall folding and imbricate faulting that thickened the section, detachment faulting that thinned the section, and foliation

development that both thinned and thickened bedding depending on location, all associated with major slip on the Willard thrust.

- 0.7 253.5 Continue east and reach floor of Ogden Valley. The valley floor is mostly covered by Quaternary deposits, but volcanic and volcanoclastic rocks of the late Eocene to Oligocene Norwood Tuff are locally exposed along the flanks of the valley (Sorensen and Crittenden, 1979). These strata dip about 30° east, probably due to rotation above a listric normal fault that bounds the east side of the valley.
- 0.7 254.2 Junction. Continue heading east on Utah 162.
- 0.2 254.4 Enter Liberty. Bear right and continue south on Utah 162.
- 3.1 257.5 Junction with Utah Highway 158. Turn right and head west on Utah 158. Upper Proterozoic to Cambrian strata in the Willard sheet are exposed in the mountains to the east, and in the Wasatch Range to the west.
- 0.6 258.1 Junction with spur. Continue southwest on Utah 158.
- 2.6 260.7 Gently east-dipping argillite and grit of the formation of Perry Canyon exposed in road cuts display gently dipping foliation that increases in intensity southwest toward the Willard thrust.
- 0.6 261.3 **Stop 2-5.** Willard fault zone and internal deformation in the eastern part of the Lewis Peak area (Fig. 16). Pull over into large parking area on south side of highway.

The Willard thrust is exposed in a large road cut along the north side of the highway. The thrust dips 20 to 30° east here and places diamictite, quartzite, and argillite of the Upper Proterozoic formation of Perry Canyon over limestone, dolostone, and sandstone of the Mississippian Humbug Formation (Sorensen and Crittenden, 1979). Structural relations in this area further illustrate the structural style of the Willard sheet. The thrust has a hanging-wall flat in Upper Proterozoic mica-rich strata and a foot-wall ramp and isoclinal, recumbent syncline from Cambrian to Mississippian strata (Fig. 25). The nature of internal deformation varies with structural level, with patterns generally similar to those in the Willard Peak area (compare Figs. 23 and 25). Foliation is weakly to moderately developed and overall moderately dipping in micaceous quartzite of the Maple Canyon Formation at intermediate distances from the thrust. However, foliation is steeply dipping and east-striking within some narrow zones, pos-

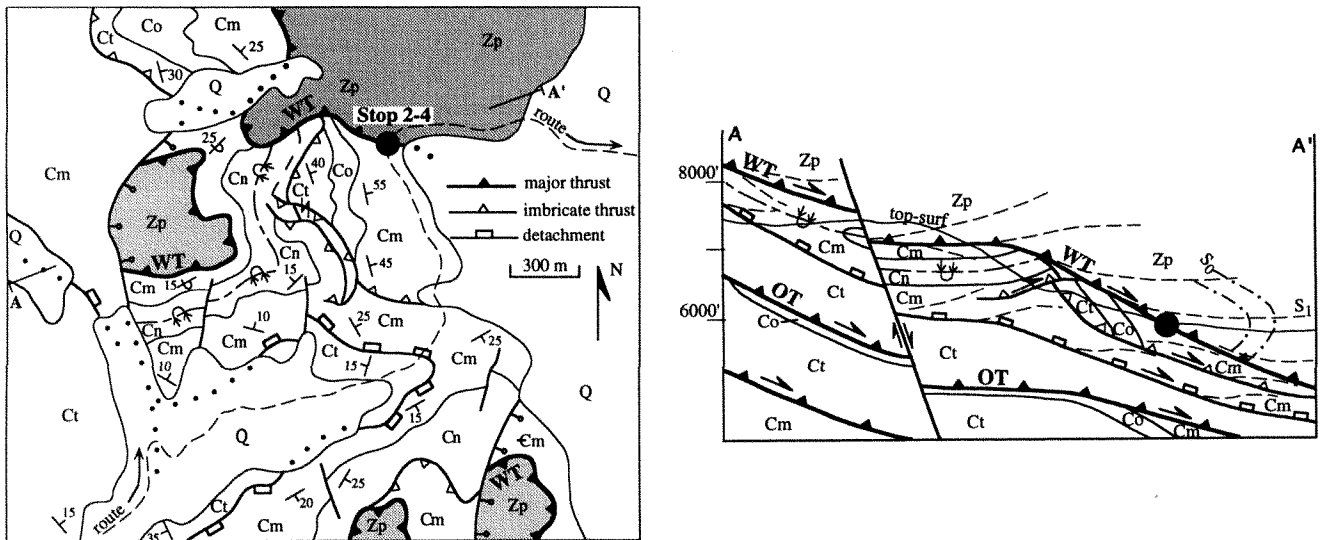


Figure 24. A. Geologic map of the North Ogden Pass area near stop 2-4. Units are: Zp—formation of Perry Canyon, Ct—Cambrian Tintic Quartzite, Co—Ophir Shale, Cm—Maxfield Limestone, Cn—Nouan and St. Charles Formations, and Q—Quaternary deposits. WT—Willard thrust. Adapted from Crittenden and Sorensen (1985a), Evans and Neves (1993), and Yonkee (unpublished data). B. Cross section of the North Ogden Divide area incorporating down-plunge projection of data. Units are same as above. OT—Ogden thrust system. Topographic surface (top surf) along line of section indicated.

sibly related to wrench shear. Foliation becomes strongly developed in the formation of Perry Canyon toward the thrust, and rotates into subparallelism with the thrust, defining an asymptotic pattern. Stretching lineations and tensile veins record principal E-W extension, and fibers on shear veins record generally top-to-E simple shear.

Finite strain, estimated using the R_f/ϕ and normalized Fry methods, also varies systematically with distance from the thrust (Fig. 25). Within micaceous quartzite at intermediate distances from the thrust X-Z axial ratios range mostly from 1.5:1 to 2.5:1, and X-Y planes are generally moderately dipping, although some samples have steeply dipping, east-striking X-Y planes within dextral, east-striking shear zones. Within mica-rich strata of the formation of Perry Canyon X-Z axial ratios range mostly from 2:1 to 5:1, with ratios increasing overall toward the thrust, and gently dipping X-Y planes rotate into parallelism with the thrust at the base of the sheet. Most samples display apparent flattening with principal E-W extension and variable N-S extension. The strain patterns record minor to moderate shortening and simple shear at intermediate levels, and a combination of concentrated thrust-parallel extension and top-to-E simple shear at deeper levels.

The Willard fault zone here includes: strongly foliated phyllite, diamictite and quartzite at the base of the hanging wall locally cut by brittle deformation zones; a central core of highly weathered ultracataclasite, brecciated and

net-veined mylonite and phyllonite, and rare limestone protomylonite; and a narrow footwall zone of brecciated and highly veined carbonate and sandstone. The style of hanging wall deformation is broadly similar to that at Willard Peak, although cataclasis and overprinting brecciation are more widespread here. The style of footwall deformation, however, is much different, being more brittle and concentrated compared to the thick zone of penetrative footwall deformation near Willard Peak (Evans and Neves, 1993). The Willard thrust ramps obliquely upsection toward the southeast in its footwall, and the higher level exposed here, combined with differences in lithology, may have precluded widespread plastic deformation of footwall rocks.

- | | | |
|-----|-------|--|
| 0.3 | 261.6 | Road cut in gently east-dipping Mississippian Humbug Formation. Contraction faults with both top-to-E and top-to-W slip cut bedding at low angles and produce minor footwall thickening. |
| 0.3 | 261.9 | Junction with Utah Highway 39. Turn right and head west on Utah 39. |
| 0.1 | 262.0 | Footwall deformation beneath the Willard thrust produced several dramatic structures along Ogden Canyon including the "Z-fold" visible on the north side of the highway. This fold probably developed from shortening and top-to-E shear below |

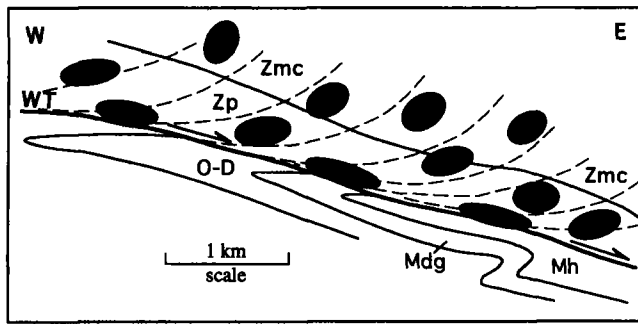


Figure 25. Down-plunge projection of eastern part of Lewis Peak area near stop 2-5. Overall foliation trajectories shown by dashed lines, and X-Z strain ellipses for selected samples indicated. Units are: Zp—formation of Perry Canyon, Zmc—Maple Canyon Formation, Mh—Mississippian Humbug Formation; Mdg—Deseret and Gardison Formations; and O-D—Ordovician to Devonian strata. WT—Willard thrust.

Willard thrust (Crittenden, 1972). A recumbent, isoclinal, east-vergent syncline is developed to the northwest beneath the Willard thrust, and also records top-to-E shear and significant footwall deformation where the Willard thrust ramped from Cambrian to Mississippian strata (Fig. 25; Sorensen and Crittenden, 1979).

- 0.4 262.4 Mississippian Gardison Formation is exposed in cliffs northwest of highway. Successively deeper levels of the Paleozoic section are encountered heading west.
- 0.3 262.7 Devonian Bierdneau Formation is exposed in quarry north of highway.
- 0.4 263.1 Small road cut in Ordovician Fish Haven Dolomite. Cambrian St. Charles and Nounan Formations are exposed in slopes to northwest.
- 0.4 263.5 Exposures of argillaceous limestone of the Maxfield Limestone.
- 0.6 264.1 Bridge across Ogden River. A tight, recumbent anticline is developed in the Ophir and Maxfield Formations. These formations display extreme variations in thickness associated with disharmonic folds, imbricate thrusts, detachment faults, and foliation at varying angles to bedding. Here strata are tectonically thickened by folding and imbricate thrusting, but to the west the Ophir Shale is highly thinned and locally omitted along detachment faults (Fig. 26).

- 1.1 265.2 Tintic Quartzite in road cut. An upper branch of the Ogden thrust, exposed along the draw to the northwest, dips east and juxtaposes the Tintic Quartzite over the Ophir Shale.
- 0.3 265.5 Cross approximate trace of lower branch of Ogden thrust. Fractured Nounan Dolomite is in road cut.
- 0.2 265.7 **Stop 2-6.** Ogden thrust system in the Ogden area (Fig. 26). Turn left, park at Coldwater trailhead along south side of highway, and hike southwest to small quarry.

The lower branch of the Ogden thrust, visible on the north side of Ogden Canyon, dips east and places Tintic Quartzite over Nounan Dolomite (Crittenden and Sorensen, 1985b; Yonkee, 1992). Secondary folds and cleavage are locally developed in the Maxfield and Ophir Formations in the footwall of the Ogden thrust. Beds of the upper Maxfield Limestone exposed in the quarry are cut by vein arrays and by contraction faults at low angles to bedding.

To the south, the Ogden thrust system branches into a lower floor thrust and an upper roof thrust (Fig. 26; Yonkee, 1992). The floor thrust ramps down laterally southward from upper Cambrian strata to Precambrian crystalline basement in the footwall, and from Tintic Quartzite to basement in the hanging wall. Stratigraphic separation reaches >4 km to south, and estimated slip reaches >15 km. The roof thrust ramps laterally upsection in its footwall from the Ophir Shale to Nounan Dolomite, and ramps laterally down section in its hanging wall from Cambrian strata to basement rocks further southeast. Basement in the Ogden area is also cut by widely spaced minor shear zones that accommodated top-to-E shear in the lower parts of the Ogden thrust sheet. The cover is deformed by gently N- to NW-plunging folds, NE-plunging minor folds at low angles to lateral ramps, cleavage in shale and argillaceous limestone, and complex minor faults. Cleavage is gently dipping in most areas, but cleavage is steeply dipping near lateral ramps in the Ogden thrust system. Finite strain estimated from deformed ooids in Cambrian limestone records spatially variable combinations of thrust-parallel shear, wrench shear parallel to lateral ramps, layer-parallel shortening, and extension (Yonkee, 1992). Note, the Ophir Shale represents a detachment horizon and displays extreme variations in thickness, possibly related to spatially and temporally varying components of shear, extension, and shortening. The style of deformation along the Ogden thrust system is similar to the style of the imbricate zone in the footwall of the Willard thrust, and initial deformation along the Ogden system may have overlapped with slip on the Willard thrust.

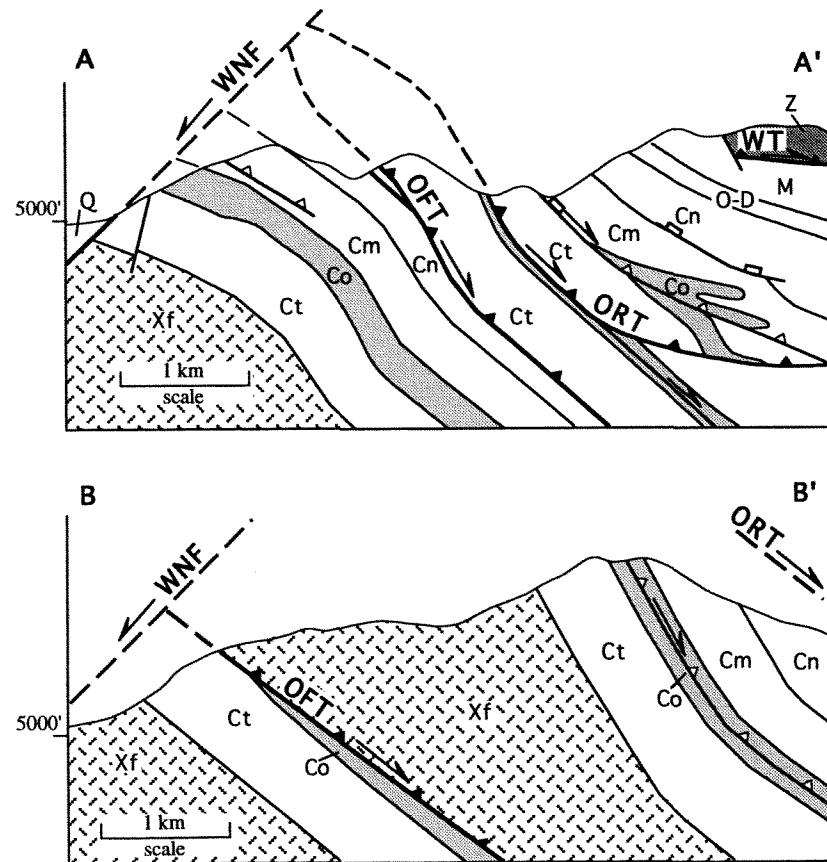
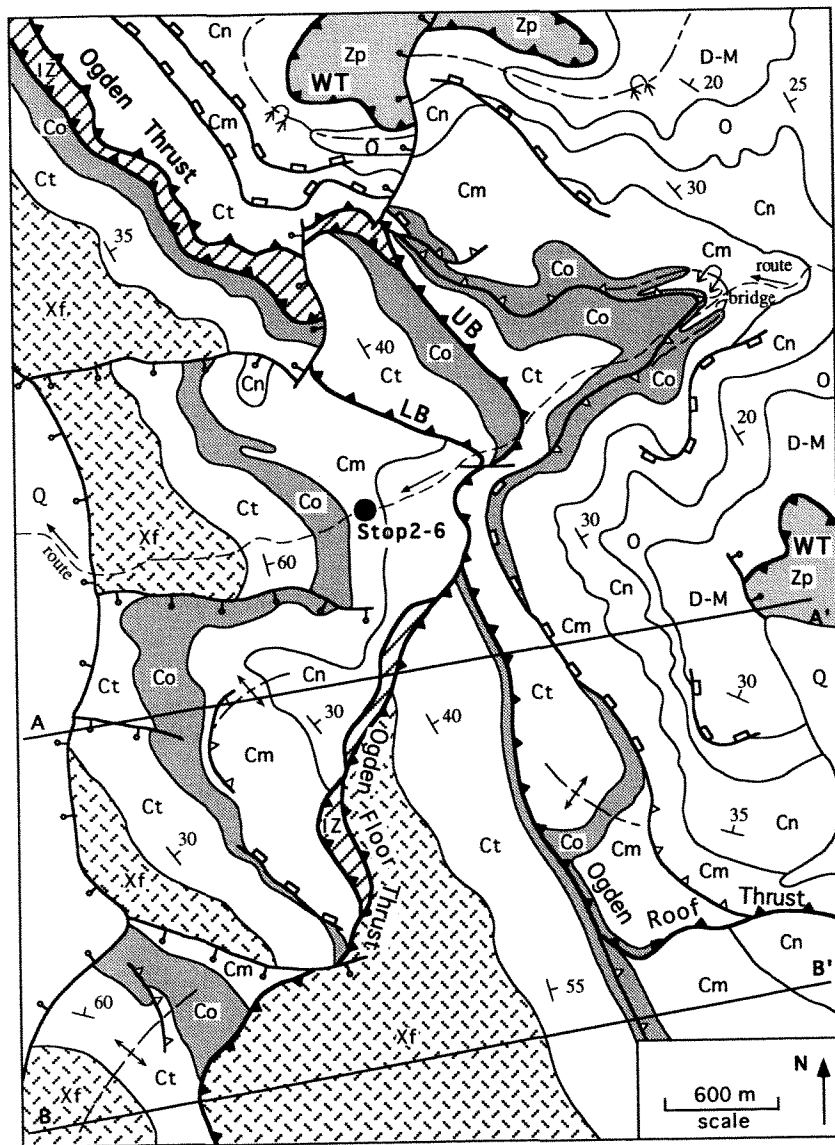


Figure 26. A. Geologic map of the Ogden thrust system near stop 2-6. Basement and cover are imbricated by the Ogden thrust system and klippe of the overriding Willard thrust sheet (WT) are preserved locally. Units are: Xf-Precambrian crystalline basement, Z-Upper Proterozoic rocks of Willard sheet, Ct-Tintic Quartzite, Co-Ophir Shale, Cm-Maxfield Limestone, Cn-Noman and St. Charles Formations, O-Ordovician strata, DM-Devonian to Mississippian strata, IZ-imbricated Paleozoic and Precambrian rocks, and Q-Quaternary deposits. Symbols same as in Figure 24. Locations of cross sections A-A' and B-B', and route indicated. LB-lower branch of Ogden thrust and UB-upper branch of Ogden thrust. B. Cross sections A-A' and B-B' of Ogden thrust system. The Ogden thrust system dips overall eastward and the floor thrust ramps laterally down section to the south and imbricates basement and cover rocks. OFT-Ogden floor thrust and ORT-Ogden roof thrust. Units same as above.

0.3	266.0	Ophir Shale displays cleavage and minor folds in road cut.			60 km in the Wasatch Range, and lie within the east limb of the Wasatch anticlinorium, which will be examined in more detail during day 3.
0.1	266.1	E-dipping beds of Tintic Quartzite form cliffs. This quartzite is relatively undeformed in most areas, and the overlying Ophir Shale is detached and strongly deformed in many areas.	0.7	267.1	Cross approximate trace of Weber segment of the Wasatch fault zone at mouth of Ogden Canyon.
0.3	266.4	Unconformity between Tintic Quartzite and underlying granite gneiss of the Precambrian Farmington Canyon Complex. High-grade metamorphic and igneous rocks of the Farmington Canyon Complex crop out over a north-south distance of	1.0	268.1	Junction with Utah 203. Turn left and proceed south on Utah 203 (Harrison Boulevard).
			2.8	270.9	Weber State University. End road log for part 2 of day 2.

Kinematics and Synorogenic Sedimentation of the Eastern Frontal Part of the Sevier Orogenic Wedge, Northern Utah

W. A. YONKEE

Department of Geosciences, Weber State University, Ogden, Utah 84408

P. G. DECELLES

J. COOGAN

Department of Geosciences, University of Arizona, Tucson, Arizona 85721

INTRODUCTION

The general kinematic and chronologic development of regional structures in the frontal part of the Sevier orogenic belt is relatively well constrained, making this an excellent area to study the dynamics of an orogenic wedge (e.g. Royse et al, 1975; Dixon, 1982; Lamerson, 1982; Coogan, 1992; Royse, 1993; Yonkee, 1992; DeCelles, 1994; DeCelles and Mitra, 1995). Major structural features in this part of the wedge include: (1) the basement-cored Wasatch anticlinorium and associated Ogden thrust system; (2) the eastern thrust system; and (3) associated foreland basin deposits (Fig. 27). Specifically we will examine the large-scale geometric development of the Wasatch anticlinorium and characteristics of basement fault and shear zones; kinematics of the eastern thrust system, including relations to early detachment faulting and shortening; and characteristics of synorogenic strata that record progressive changes from backbulge to foredeep to wedgetop deposition. This integrated tectonic analysis will help in understanding interactions between basement deformation, fault zone mechanics, transfer of slip between thrust systems, and synorogenic sedimentation. Importantly, the geometry, ages, and lithologic characteristics of preserved synorogenic deposits allow progressive reconstruction of the orogenic wedge over time, providing an excellent opportunity to constrain the evolution of the frontal part of the Sevier orogenic wedge (DeCelles and Mitra, 1995).

WASATCH ANTICLINORIUM

Precambrian crystalline basement forms the core of a regional anticlinorium, which has a major culmination in northern Utah and continues in the subsurface into southern Idaho (Figs. 27 and 28; Yonkee, 1992). The anticlinorium is asymmetric with a steeply east-dipping eastern limb preserved in the Wasatch Range and a gently dipping west-

ern limb preserved on Antelope Island (Fig. 27). This regional fold represents a complex antiformal stack that developed over a protracted history of internal shortening and large-scale imbrication by the Ogden thrust system. Deformation within the anticlinorium produced significant tectonic thickening that may have increased wedge taper and helped drive slip on the eastern thrust system (DeCelles and Mitra, 1995).

Basement in the anticlinorium was internally deformed by networks of shear zones that accommodated 10 to 15% bulk shortening between about 140 and 100 Ma, mostly prior to large-scale thrusting (Yonkee, 1992). Shear zones form conjugate sets that bound relatively undeformed lozenges of basement, and foliation is about parallel to the acute bisector of conjugate sets. Within the gently dipping western limb foliation is overall steeply dipping and bisects steeply dipping conjugate sets that have reverse slip. Within the steeply dipping eastern limb foliation is gently dipping and bisects gently to moderately dipping sets. Foliation and shear zone sets thus define a partial fan about the anticlinorium, reflecting rotation during large-scale folding (Fig. 28B).

Slip on the Ogden thrust system produced large-scale imbrication of Precambrian basement and the sedimentary cover in the anticlinorium between about 100 and 50 Ma (Schirmer, 1988; Yonkee, 1992; DeCelles, 1994). In detail, the Ogden system displays complex lateral variations: to the north a main thrust that repeats Cambrian strata, but to the south structural relief increases and the system branches into a floor thrust that places basement over Cambrian strata and a roof thrust that repeats Cambrian strata. The floor thrust ramps laterally down section to the south and has greater than 15 km of top-to-east slip. The roof thrust also ramps down to the south and has about 5 km of top-to-east slip. The Ogden thrust system was rotated to easterly dips on the east limb of the anticlinorium

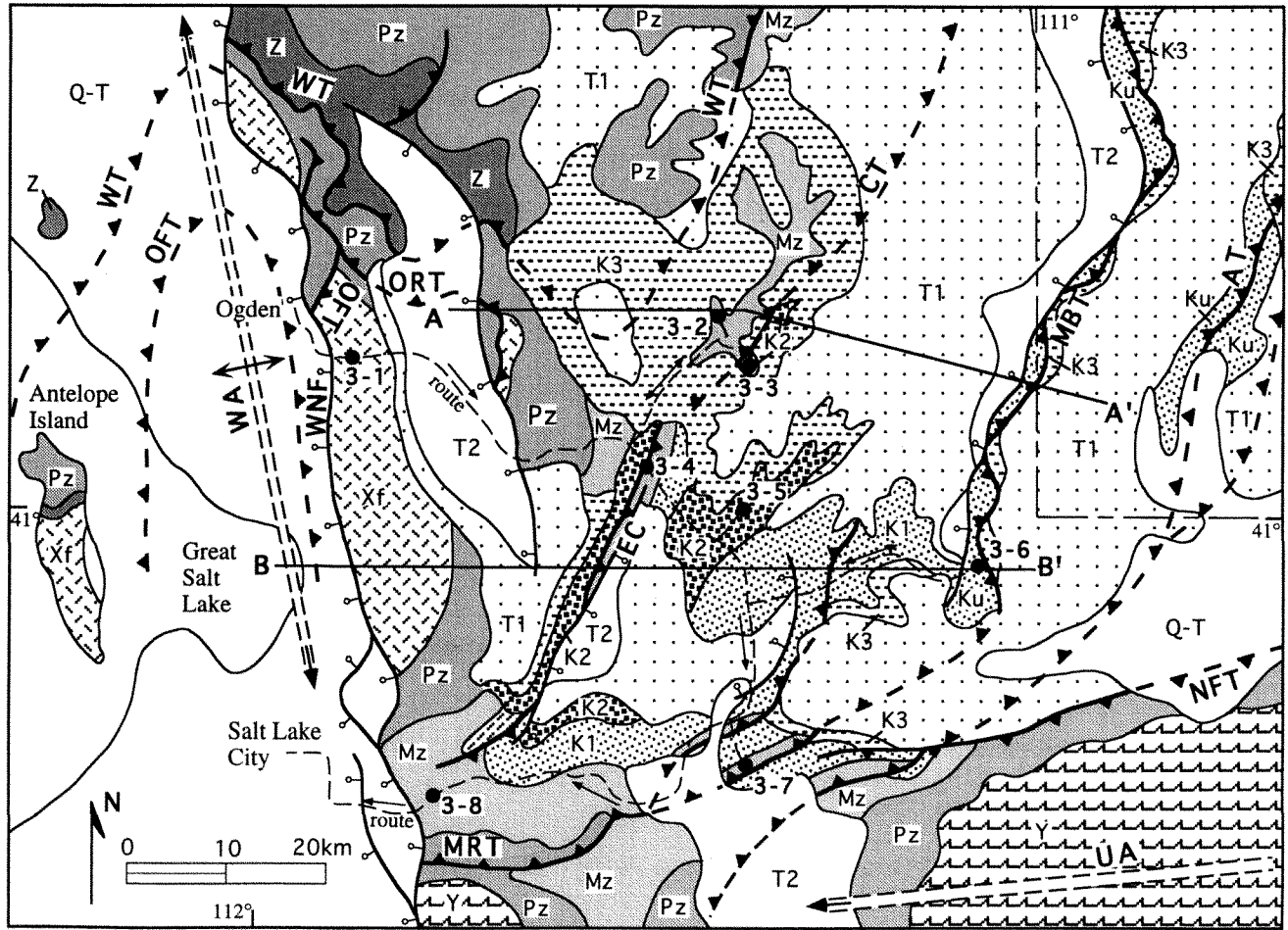


Figure 27. Index map of northeast Utah and adjacent areas. Main structural features are: approximate crests of Wasatch anticlinorium (WA) and Uinta arch (UA), Willard thrust (WT), Ogden floor and roof thrusts (OFT and ORT), Crawford thrust (CT), East Canyon fault zone (EC), Medicine Butte thrust (MBT), Mount Raymond thrust (MRT), Absaroka thrust (AT), Hogsback thrust (HT), and Wasatch normal fault (WNF). Units are: Xf—crystalline basement, Y—Middle Proterozoic sedimentary rocks, Z—Late Proterozoic sedimentary rocks, Pz—Paleozoic strata, Mz—Triassic and Jurassic strata, K1—Cretaceous lower synorogenic deposits of Kelvin and Frontier Formations, K2—Cretaceous middle synorogenic deposits of Echo Canyon and Weber Canyon Conglomerates, K3—upper synorogenic deposits of Hams Fork Member and main body of Evanston Formation, T1—synorogenic deposits of Wasatch Formation, T2—post-thrusting late Eocene-Oligocene Norwood Tuff and Keetley Volcanics, and QT—Miocene to Recent valley-fill deposits. Modified from Hintze (1980), Lamerson (1982), and Bryant (1990). Lines of cross sections in Figure 28 and location of route and stops indicated.

during later slip on an underlying basal thrust. Slip on the Ogden and basal thrust systems, and uplift of anticlinorium occurred over a protracted history, with fission track ages recording pulses at about 90 Ma, 85 to 75 Ma, and 60 to 50 Ma (Naeser et al, 1993), corresponding to phases of slip on the Crawford, Absaroka, and Hogsback thrusts of the eastern thrust system (DeCelles, 1994). Most slip on the Ogden and basal thrust systems was transferred eastward into the developing eastern system (Yonkee, 1992).

Fault rocks along the Ogden thrust system and basement shear zones experienced greenschist-facies alter-

ation during concentrated deformation at mid-crustal levels (Yonkee and Mitra, 1994). A traverse across the Ogden floor thrust illustrates these relations. Gneiss in the wall rock away from the fault shows only limited deformation and minor alteration. Fractured gneiss in a 50- to 200-m-thick transition zone above the fault displays more widespread alteration concentrated along numerous microcracks. A 20- to 50-m-thick fault core consists of highly deformed phyllonite with plastically recrystallized quartz and foliated aggregates of fine-grained mica, and cataclasite with a complex mixture of variably cemented fragments, multiple

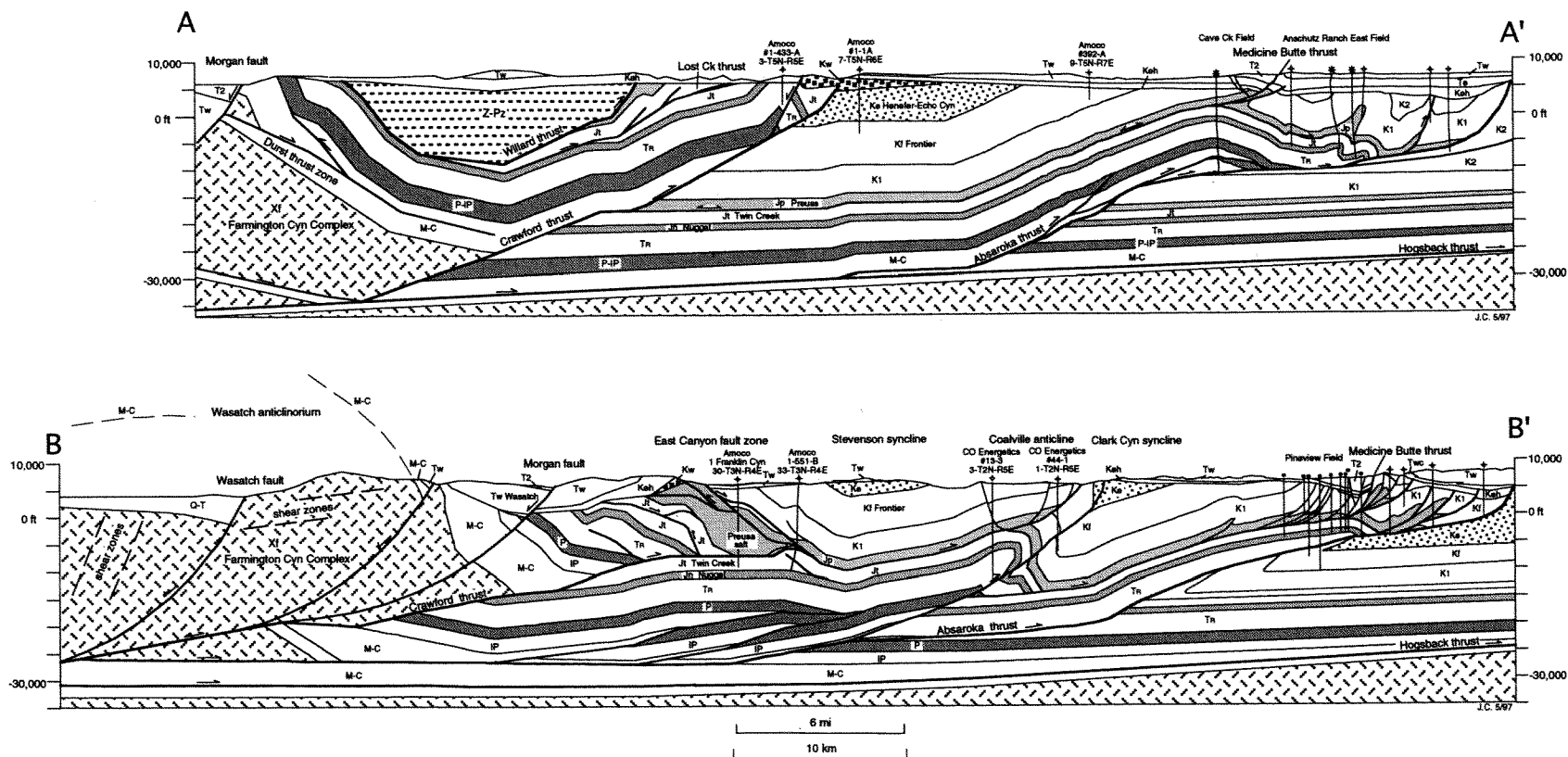


Figure 28. Structural cross sections. See Figure 27 for locations. Units are: Xf—Precambrian basement rocks; M-C—Mississippian to Cambrian strata; P and P—Permian and Pennsylvanian strata; Tr—Triassic strata; Jn—Jurassic Nugget Sandstone; Jt—Jurassic Twin Creek Limestone; Jp—Jurassic Preuss and Stump Formations; Ke—Echo Canyon Conglomerate and Henefer Formation; Kw—Weber Canyon Conglomerate; Keh and Te—Hams Fork Member and main body of Ecanston Formation; Tw—Wasatch Formation; T2—Late Eocene and Oligocene deposits, and QT—Miocene to Recent valley-fill deposits.

A. Section A-A' from Durst Mountain to Anschutz Ranch East field, Utah and Wyoming, illustrating major features near stops 3-2 and 3-3. Absaroka hanging wall interpretation modified from Lamerson (1982).

B. Section B-B' from Great Salt Lake to Pineview field, Utah and Wyoming, illustrating major features near stops 3-4 and 3-6. Modified from Bryant (1990), Royse (1993), and Lamerson (1982).

vein sets, discrete fractures, and fine-grained micaceous matrix (Fig. 29). Gneiss in the wall rock contains about 30 to 40 vol% unrecrystallized quartz, 45 to 60% total feldspar, and only minor amounts of mica, whereas cataclasite and phyllonite from the fault core contain >20% mica, lesser amounts of feldspar, and abundant fine-grained matrix. Overall similar relations are observed across basement shear zones (see stop 3-1).

These textural and mineralogical changes record episodic influx of fluids along fracture and microcrack networks during periods of elevated fluid pressure, periodic sealing, and production of fine-grained matrix by fracturing, plastic recrystallization, and alteration. Mica produced by alteration is weaker than feldspar, plastic deformation of quartz may be related to hydrolytic weakening, and grain size reduction produced increased rates of diffusive mass transfer deformation. Thus basement shear and fault zones experienced significant strain softening and elevated fluid pressures resulting in concentrated slip along relatively weak zones and possible reduction in taper of the orogenic wedge (Yonkee and Mitra, 1994; DeCelles and Mitra, 1995). Note, the heterogeneous basement deformation at mid-crustal levels observed in this area (depths 10 to 15 km, $T \approx 300$ to 400°C) contrasts with the more pervasive basement deformation observed at deep-crustal levels in the Winchell Lake fold-nappe (depths 20 to 30 km, $T \approx 600$ to 750°C)

REGIONAL STRUCTURE OF THE EASTERN THRUST SYSTEM

Four major faults, the Crawford, Medicine Butte, Absaroka, and Hogsback thrusts, are present in the eastern thrust system of the Sevier orogenic wedge in northeastern Utah and southwestern Wyoming (Fig. 27). The thrusts branch upward from a common basal decollement in Cambrian shale, have ramp-flat geometries, and transported Paleozoic to early Mesozoic platform strata and late Mesozoic synorogenic deposits relatively eastward. Aggregate slip on the eastern thrust system decreases from about 100 to 60 km going southward. Because the frontal thrusts continue beneath the Wasatch anticlinorium, basement in the anticlinorium has also been transported long distances (Fig. 28), synchronous with slip on the eastern thrusts (Schirmer, 1988; Coogan, 1992a; Yonkee, 1992; DeCelles, 1994).

The earliest phase of deformation in the frontal part of the wedge is represented by layer-parallel shortening within the Jurassic Twin Creek Limestone in the footwalls of the Willard and Meade thrusts in northern Utah and southeastern Idaho. This shortening produced spaced cleavage and fold trains associated with imbricate thrusts that ramp upward and merge into a regional decollement in salt-

bearing strata of the overlying Preuss Formation. This belt of cleavage and folds accommodated footwall shortening, with displacement transfer eastward into the developing Preuss decollement at shallow levels.

The Crawford thrust, exposed in northeastern Utah and adjacent Wyoming, has a maximum displacement of ~30 km that diminishes southward (Coogan, 1992). North of Weber Canyon the thrust has a western flat in Cambrian strata, a middle ramp, and a hanging wall anticline near its frontal trace (Fig. 28A). South of Weber Canyon the thrust has a major western ramp from Precambrian through Paleozoic strata, an eastern flat in Jurassic salt-bearing rocks, and terminates in a complex frontal anticline and associated backthrust (Fig. 28B). The thrust is inferred to continue toward Salt Lake City based on a consistent southwest-trending belt of folds and spectacular growth structures in the synorogenic Weber Canyon Conglomerate (DeCelles, 1994; Fig. 27). Major slip on the Crawford thrust occurred between about 90 and 80 Ma, with an episode of Early Tertiary minor reactivation (Fig. 30). A final episode of minor normal inversion occurred during the late Eocene to Oligocene, marking partial collapse of the wedge soon after the cessation of thrusting (Constenius, 1996).

The Medicine Butte thrust may be a footwall imbricate of the Crawford thrust and has a large regional flat in salt-bearing rocks of the Preuss Formation (Fig. 28). A complex fold, the Coalville anticline, and associated imbricates are locally developed above the thrust. The Cherry Canyon and Crandall thrusts, exposed to the southwest, also have flats within the Preuss Formation and may link into the Medicine Butte thrust. Although its displacement is probably 10 km or less, this fault was sporadically active from Late Cretaceous to early Tertiary (Lamerson, 1982), and may also have had an initial phase of Early Cretaceous slip associated with detachment folding. The thrust also underwent minor late Eocene to Oligocene normal inversion during collapse of the wedge soon after the cessation of thrusting.

The Absaroka thrust system is the most continuous regional system in the frontal part of the Sevier orogenic wedge (Royse, 1993). The thrust system branches upward from a western flat in Cambrian shale and has eastern flats in Jurassic salt-bearing beds and Cretaceous shales (Lamerson, 1982; Coogan, 1992; Royse, 1993). The hanging wall contains a western anticlinal trend of imbricated Paleozoic strata and an eastern anticlinal trend of folded Mesozoic strata (Fig. 28). Displacement ranges from a maximum of ~40 km in southwestern Wyoming to ~15 km in northeastern Utah (Coogan, 1992; Royse, 1993). Two major frontal imbricates, each with a different displacement history, constitute the Absaroka thrust system in southwestern Wyoming, with phases of slip at about 80 Ma and 65 Ma (Royse et al, 1975; Fig. 30).

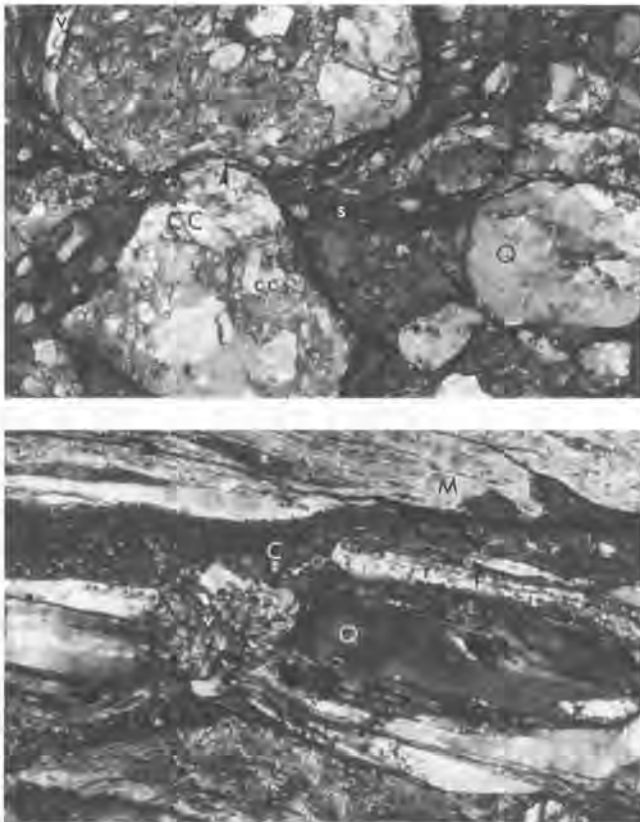


Figure 29. Photomicrographs from Ogden thrust fault zone. Bottoms of photographs represent about 2 mm in length.

A. Cataclasite with widespread alteration. Variably altered and cemented clasts sit within a weakly foliated, chlorite-rich matrix. Some larger clasts of cemented cataclasite (CC) contain smaller fragments of cataclasite that had been previously cemented (cc). Clasts of quartz aggregates (Q) display undulatory extinction. Microveins (v) and dissolution of some clasts contacts (arrow) record diffusive mass transfer deformation.

B. Phyllonite with pervasive alteration. Quartz (Q) forms ribbons that are variably recrystallized (r) and locally fractured with vein material (v) between fragments. Mica (M) forms foliated aggregates that rotate into parallelism with bands of extremely fine-grained, chlorite-rich material (C).

The Hogsback thrust is the easternmost major fault in this part of the Sevier orogenic wedge. The fault trace is relatively straight for about 100 km to the north of the Uinta uplift, where it splits into the Darby and Prospect thrusts. The Hogsback thrust ramps up from a western flat in Cambrian shale, and has ~20 km of total displacement (Dixon, 1982). Southward the thrust appears to ramp laterally downward and connect into the North Flank thrust of the Uinta foreland uplift, recording overlapping of later stages of thrusting in the orogenic wedge with phases of foreland basement uplift (Bradley, 1988).

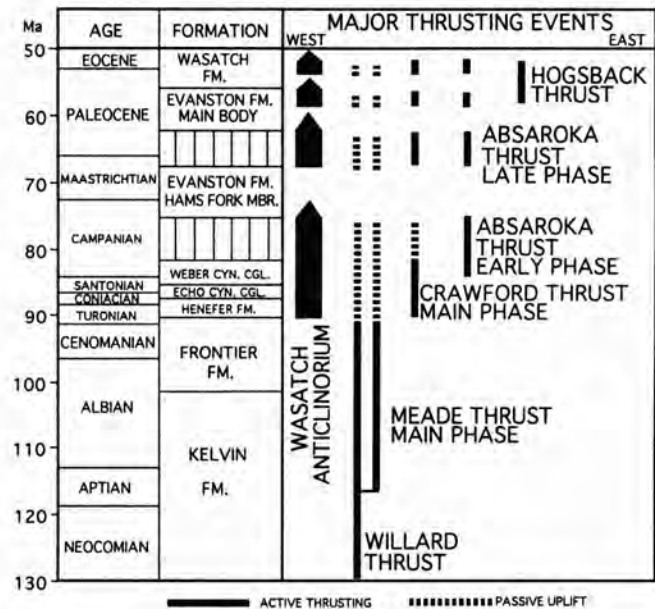


Figure 30. Chart showing Early Cretaceous to early Eocene history of thrust displacements and passive uplift of thrust sheets in frontal part of the Sevier orogenic wedge. Modified from DeCelles (1994).

FORELAND BASIN SYSTEM

As the Sevier orogenic wedge began to develop during Middle to Late Jurassic time, the Cordilleran foreland basin system formed in response to migration of a flexural wave through the lithosphere of western and central Utah. A foreland basin system, as defined by DeCelles and Giles (1996), consists of four depozones that are distinguishable on the basis of regional subsidence patterns, depositional systems, unconformities, and presence or absence of syn-depositional "growth" structures (Fig. 31). The wedge-top depozone is that part of the basin system developed on top of the active orogenic wedge, and is characterized by coarse-grained alluvial and fan delta deposits with well-developed growth structures. The foredeep depozone is developed between the tip of the orogenic wedge and the proximal flank of the forebulge, and is characterized by thick, coarse-grained sediments derived from the orogenic wedge, which thin toward the forebulge. The forebulge depozone is located on top of or on the flanks of the forebulge, and is marked by decreased sediment accommodation and major (>10 Ma duration) unconformities in many foreland basin systems (e.g. Crampton and Allen, 1995). The back-bulge depozone, located cratonward of the forebulge, accumulates sediment derived from both the orogenic wedge and the craton. Back-bulge sediments are characterized by slight thinning toward the crest of the forebulge and craton, generally fine grain size, multi-

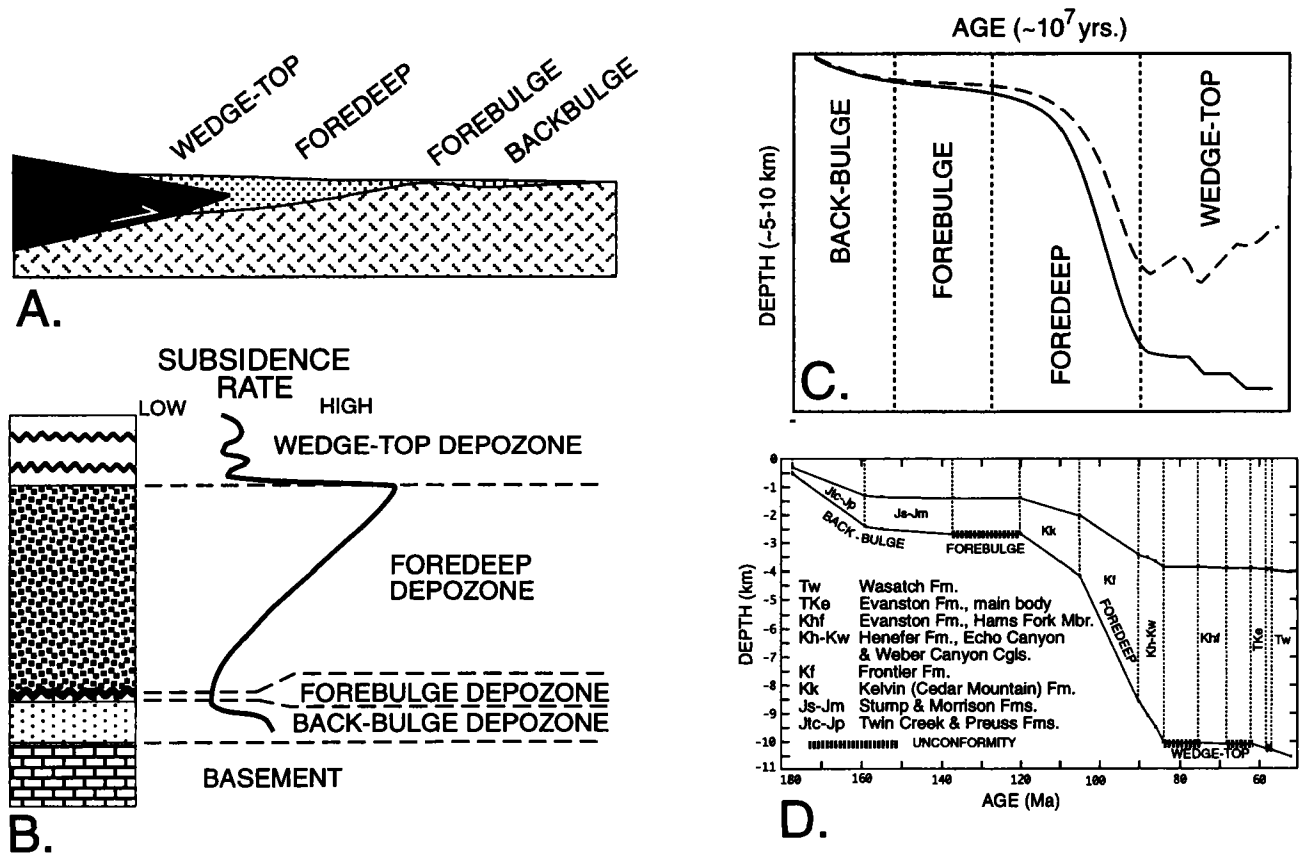


Figure 31. A. Schematic cross section showing distribution of depozones in a foreland basin system relative to an orogenic wedge (black). B. Idealized stratigraphic column resulting from long term, cratonward migration of orogenic wedge and depozones, with subsidence rate curve to right. C. Idealized total sediment accumulation curve (solid line) and tectonic subsidence curve (dashed line) for long term evolution of foreland basin system. D. Long-term sediment accumulation curve for northern Utah, and interpreted depozones. Lower curve is total decompacted sediment thickness and upper curve is total stratigraphic thickness (after DeCelles and Currie, 1996).

ple unconformities, and paleosols in nonmarine settings (DeCelles and Burden, 1992).

Long-term propagation of an orogenic wedge toward the craton over distances approximating the flexural wavelength of the foreland lithosphere will stack deposits of the back-bulge, forebulge, foredeep, and wedge-top depozone vertically, producing a crudely sigmoidal sediment-accumulation history (Figs. 31B, C). This vertical stacking of basin depozone is well illustrated in the Middle Jurassic to Paleocene rocks of the Sevier foreland basin in northeastern Utah (Fig. 31D). The back-bulge depozone is represented by the Middle to Late Jurassic Twin Creek, Preuss, and Morrison Formations. Migration of the forebulge through northeastern Utah is represented by a major Late Jurassic to Early Cretaceous unconformity, and by thick paleosols in the lowermost Kelvin Formation. The onset of rapid sediment accumulation during the Early Cretaceous signals the migration of the foredeep depozone into north-

eastern Utah. Foredeep sedimentation spanned the Neocomian to early Campanian (~130–80 Ma) and included the Kelvin, Frontier, and Henefer Formations, the Echo Canyon and Weber Canyon Conglomerates, and their distal equivalents (Fig. 31D). The wedge-top phase spanned the late Campanian to early Eocene (~80–50 Ma), and included the Hams Fork Member and main body of the Evanston Formation and Wasatch Formation.

KINEMATIC MODEL FOR THE FRONTAL PART OF THE SEVIER OROGENIC WEDGE

The kinematic history of the frontal Sevier orogenic wedge is known from regional cross-cutting structural and stratigraphic relationships (see DeCelles, 1994 for summary), fission track cooling ages (Naeser et al., 1983), and palynological dates from synorogenic sediments that can be tied to individual thrust sheets (Jacobson and Nichols, 1982;

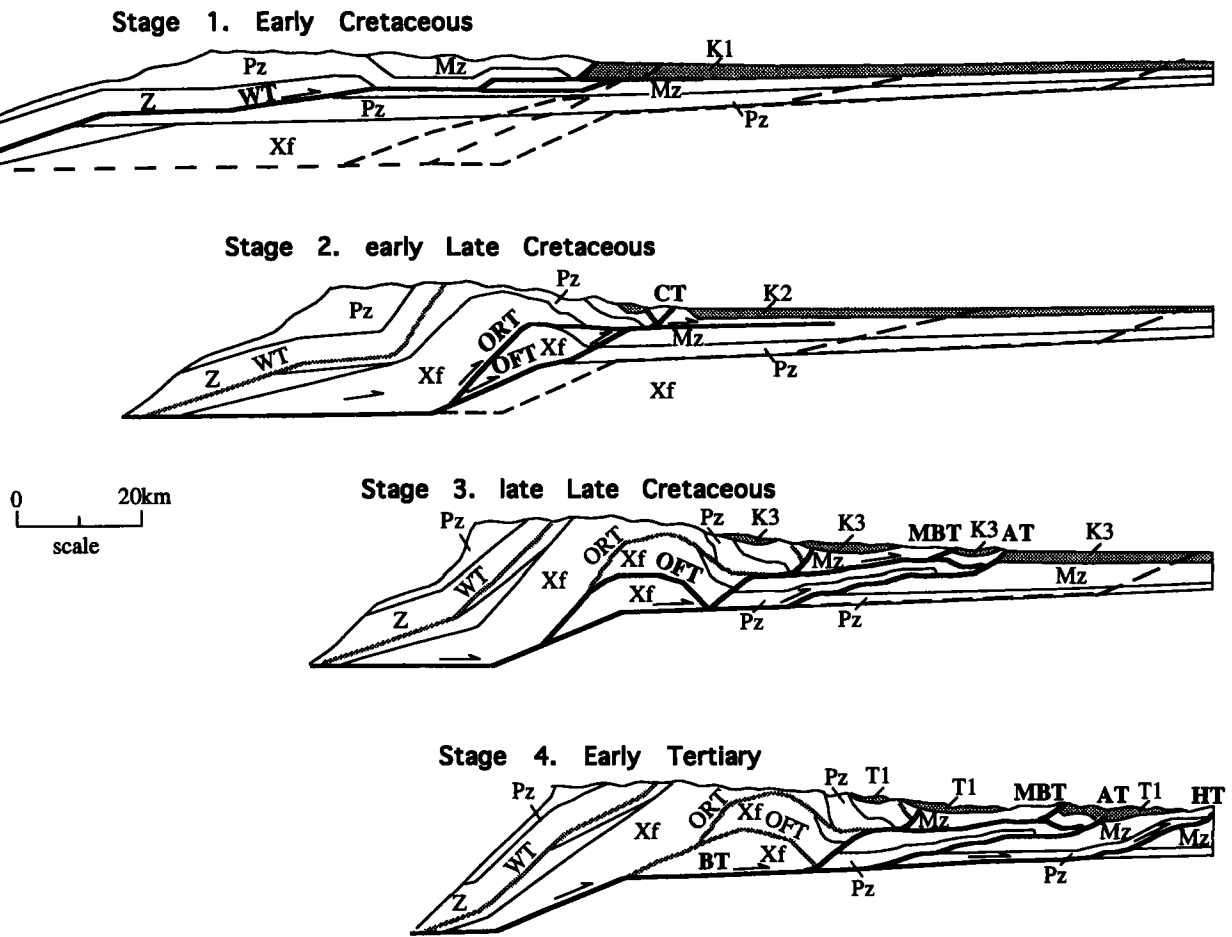


Figure 32. Kinematic model for sequential development of the frontal part of Sevier orogenic wedge in northern Utah. Units and labels for main structural elements are same as in Figure 27; BT—basal thrust. Synorogenic deposits for each stage indicated by stippled pattern (note Mz unit includes synorogenic deposits from previous stages). Modified from Yonkee (1992) and DeCelles (1994).

Lamerson, 1982). An overall eastward sequence of thrust propagation was punctuated by several phases of out-of-sequence and/or synchronous thrusting (Fig. 30). The progressive development of the frontal part of the wedge, in terms of idealized stages, is illustrated in Figure 32.

Prior to thrusting a westward thickening wedge of Late Proterozoic to early Jurassic sedimentary strata had accumulated, with significant relief on top of the basement along a transition from platform to shelf sections. Middle to Late Jurassic back-bulge sediments had also accumulated marking initial development of the Sevier orogenic wedge further west in the hinterland. A Late Jurassic to Early Cretaceous unconformity marked passage of the forebulge as the Sevier wedge began to propagate overall eastward.

Stage 1. The Willard thrust sheet was internally deformed and emplaced between 140 and 90 Ma. Emplacement of the Willard sheet buried the footwall to greater depths

and probably resulted in increased temperatures and fluid influx along developing basement shear zones (Yonkee et al., 1989), and in footwall shortening with development of cleavage, fold trains, and detachments in Jurassic strata (Mitra and Yonkee, 1985). Synorogenic strata of the Kelvin and Frontier Formations were deposited.

Stage 2. Major movement on the Ogden thrust system between about 90 and 80 Ma produced a basement-cored anticlinorium, overlapping with slip on the Crawford thrust. The synorogenic Echo Canyon and Weber Canyon Conglomerates were deposited synchronous with large-scale uplift of the anticlinorium and slip on the Crawford thrust (DeCelles, 1994). The Ogden floor and roof thrusts ramped up through basement to a flat in Cambrian strata that continued farther east as the regional decollement of the eastern thrust system. An estimated 20 km of slip along the Ogden system was largely transferred into slip on the Crawford thrust and early movement on the Medicine Butte

thrust, with about 5 km of slip taken up in flexural slip folding and internal deformation within the anticlinorium.

Stage 3. An estimated 20 km of slip on the basal thrust system was largely transferred eastward into main movement on the Absaroka and Medicine Butte thrusts between 80 and 60 Ma, synchronous with renewed uplift, and an increase in width and amplitude of the basement-cored anticlinorium. The synorogenic Hams Fork Member, which contains basement clasts, was deposited on the wedge top east of the anticlinorium, as well as in a foredeep basin further east in front of the Absaroka thrust. The Ogden thrust system was partly rotated to observed east dips, and shear zones that initiated during early shortening were rotated into a partial fan about the anticlinorium. Large-scale imbrication and folding within the anticlinorium produced thickening that increased taper to help drive slip on the eastern thrust system. The hinterland also began to experience extension and unroofing at this time, concurrent with thrusting in the frontal part of the wedge.

Stage 4. Another estimated 20 km of slip on the basal thrust was largely transferred eastward into movement on the Hogsback thrust between 60 and 50 Ma. The synorogenic Wasatch Formation, which contains basement clasts, was deposited over a wide region on the wedge top east of the anticlinorium, as well as in a foredeep basin east of the Hogsback thrust. Internal thrusts, including the Crawford and Medicine Butte thrusts, had minor reactivation, which helped maintain taper. This stage marked the end of thrusting within the Sevier orogenic wedge.

Following thrusting, the orogenic wedge began to collapse with development of a series of listric normal faults and half grabens that were partly filled with tilted volcanic and clastic debris between about 45 and 30 Ma. These normal faults formed at shallow levels and soled into older thrusts. Later Miocene to Recent extension produced moderate to high-angle normal faults, broadly concurrent with a switch to bimodal volcanism (Best et al, 1980). These younger normal faults, including the Wasatch normal fault, cross cut earlier thrust-related structures.

ACKNOWLEDGMENTS

Many fruitful discussions with Frank Royse, Gautam Mitra, and Tad Schirmer have informed and encouraged us over the years. We thank Tim Lawton, Paul Link, Lon McCarley, and Wanda Taylor for constructive reviews that improved this paper. The research summarized in this paper was supported by National Science Foundation grants EAR-9205382 and EAR-9316700 to DeCelles and EAR-9219809 to Yonkee. Geosec software used to construct some cross sections was obtained through a cooperative grant from Cogniseis Development, Inc. to the University of Arizona.

Road Log for Day 3

0.0	0.0	Depart from entrance to Weber State University at intersection of 3850 South and Harrison Boulevard. Proceed south on Harrison. The Ogden floor thrust is the prominent structure in the Wasatch Range to the east. The thrust places dark-colored Precambrian basement of the Farmington Canyon Complex over light-colored Cambrian Tintic Quartzite and ramps laterally down section to the south. The thrust has about 15 km of top-to-east slip and includes a central core of pervasively altered and intensely deformed phyllonite and cataclasite, which formed by mixed plastic and cataclastic deformation, grain size reduction, and greenschist-facies alteration (Yonkee and Mitra, 1994).
2.3	2.3	View to southeast of the Wasatch Range where basement of the Farmington Canyon Complex is exposed along the east limb of the Wasatch anticlinorium.
0.5	2.8	Junction with U.S. 89. Turn left and proceed southeast along U.S. 89.
2.0	4.8	Junction with I-84. Go under overpass, veer right onto entrance ramp, and proceed east on I-84 toward Morgan, Utah.
0.9	5.7	Cross approximate trace of the Wasatch normal fault at mouth of Weber Canyon.
0.2	5.9	Migmatitic gneiss of the Farmington Canyon Complex forms cliffs along Weber Canyon. The gneiss underwent a complex Archean to Early Proterozoic history of high-grade metamorphism and igneous activity (Hedge et al., 1983).
1.2	7.1	Stop 3-1. Weber Canyon shear zone. Pull over onto dirt road on south side of I-84. Take short hike south to reach a pipeline cut. Be careful of loose rocks.

A 5- to 10-m-thick shear zone, consisting of green phyllonite, cross cuts gray migmatitic gneiss in this area (Hollett, 1979; Yonkee and Mitra, 1994). This shear zone is part of a network of zones that accommodated internal deformation of the basement in the Wasatch anticlinorium between 140 and 110 Ma (Yonkee, 1992). Shear zone sets in the surrounding eastern limb of the anticlinorium define a flattened octahedral pattern, have subhorizontal foliation, and accommodated 10 to 15% bulk layer-parallel shortening prior to large-scale folding. Deformation in the zones occurred at $T \approx 350^\circ\text{C}$, elevated fluid pressures, and depths of 10 to 15 km.

A traverse across the shear zone reveals distinct changes in microtextures, strain, and alteration intensity (Yonkee et al., in review). Quartz and feldspar in the wall rock experienced limited cataclastic and plastic deformation, with minor alteration along some grain boundaries and microcracks (Fig. 33A). Fractured gneiss along the boundary of the shear zone underwent variable plastic deformation and cataclasis, with alteration along connected microcrack networks. Phyllonite in the shear zone formed by pervasive plastic deformation and alteration (Fig. 33B). The wall rock is relatively undeformed but estimated strain ratios are >10:1 in the shear zone, recording highly concentrated deformation that is correlated with an increase in alteration intensity. Gneiss of the wall rock contains about 35 to 40 vol% quartz and 40 to 55% total feldspar, whereas phyllonite in the shear zone contains 40 to 60% recrystallized quartz, 30 to 50% mica, and <10% feldspar (Fig. 34). Whole rock compositions across the shear zone record only minor changes in average contents of SiO₂ and Al₂O₃, but Na₂O and CaO are strongly depleted and MgO and H₂O are significantly enriched in the shear zone, recording pervasive fluid-rock interaction. Changes in mineral abundances and chemical compositions yield volumetric fluid-rock ratios on the order of 10² to 10⁴ and corresponding high fluid fluxes (Yonkee et al., in review). The concentration of deformation in the shear zone reflects strain softening due to fluid-rock interaction during overlapping episodes of fracturing, fluid influx, and alteration. Strain softening mechanisms included reaction softening from alteration of feldspar to mica, hydrolytic weakening of quartz, and grain size reduction.

0.8 7.9 Epidote-filled fractures cross cut gneiss along the roadcut. Minor west-dipping shear zones deform gneiss in cliffs to north.

1.8 9.7 Enter Morgan Valley, a half graben partly filled with east-tilted Eocene to Holocene deposits and bounded to the east by the Morgan normal fault (Sullivan and Nelson, 1992). To the north along the base of the Wasatch Range, steeply east-dipping Cambrian strata are unconformably overlain by the moderately east-dipping Paleocene to Eocene Wasatch Formation.

1.0 10.7 Overview of Morgan Valley. The ridges to the north expose volcanic and volcanoclastic deposits of the late Eocene-Oligocene (39–29 Ma) Norwood Tuff (Bryant, 1990), which overlie the Wasatch Formation. These deposits are up to 3 km thick, have eastward dips that decrease upsection, and accumulated during normal slip

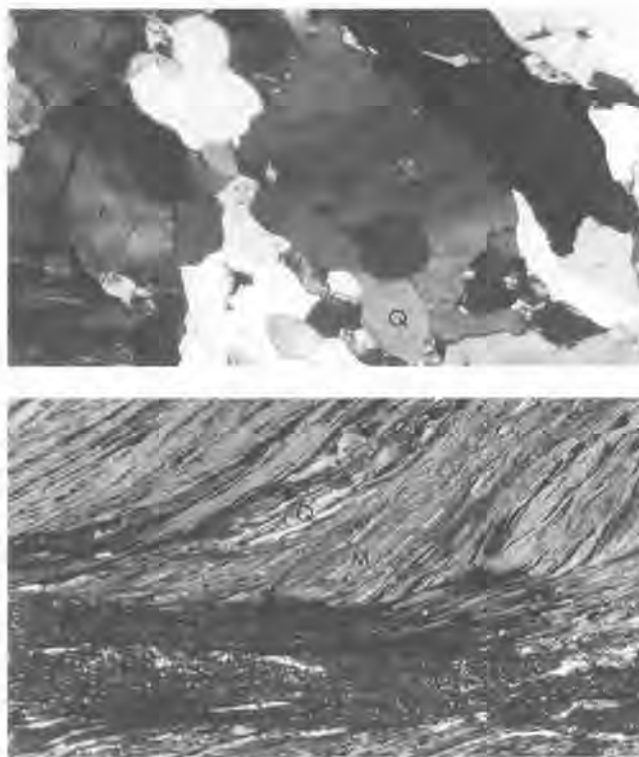


Figure 33. Photomicrographs from Weber Canyon shear zone. Bottoms of photographs represent about 2 mm in length.

A. Granitic gneiss in wall rock away from the shear zone has a granoblastic texture, and is composed mostly of little deformed quartz (Q), K-feldspar (K), and plagioclase (P).

B. Phyllonite from the shear zone consists of strongly foliated, fine-grained mica aggregates (M) and highly recrystallized and ribboned quartz (Q). An extremely fine-grained shear band or C surface (C) rotates foliation.

along the Morgan fault. Initial late Eocene to Oligocene extension along the fault closely followed cessation of thrusting, and probably records initial collapse of the Wasatch anticlinorium (Constenius, 1996). Later slip along the Morgan fault also occurred during Miocene to Recent extension.

0.9 11.6 View to east of Durst Mountain. The Durst thrust, which is the eastward continuation of the Ogden roof thrust, places Precambrian basement over Cambrian shale and limestone along the lower part of the mountain (Mullens and Laraway, 1973). The thrust currently dips east, largely due to rotation of the east limb of the Wasatch anticlinorium. The thrust has about 3 to 4 km of top-to-east

- interbedded cherty limestone and dolostone.
- 0.5 24.2 Hinge zone of second-order syncline exposed to north. Bedding east of the hinge is gently dipping to horizontal, possibly reflecting a subsurface change from a hanging wall ramp to flat along the Durst thrust.
- 1.8 26.0 Drive along hinge zone of a second order anticline, which has a gently dipping western limb and a steeply dipping eastern limb. Steep dips to the east mark a subsurface change to a hanging wall ramp along the Crawford thrust.
- 0.6 26.6 Steeply dipping Weber Formation is overlain by disharmonically folded strata of the Permian Park City Formation.
- 0.3 26.9 Gray siltstone and limestone of the Triassic Dinwoody Formation and red shale of the overlying Triassic Woodside Formation are rotated into disharmonic minor folds to the north and east. 0.8 29.9 The Twin Creek Limestone is well exposed in the cement quarry to the west. Minor faults with top-to-east and top-to-west slip, disharmonic minor folds, and weakly developed spaced cleavage at high angles to bedding produced limited early layer-parallel shortening.
- 0.4 27.3 Hills to the north consist of gray to tan, east-dipping limestone and siltstone of the Triassic Thaynes Formation. An open minor fold and associated back thrust with top-to-west slip are developed along a ridge south of the highway. 0.8 30.7 Veer left (north) onto paved side road where main Lost Creek highway curves to right. The Hams Fork Member of the Evanston Formation dips gently northeast here. The Hams Fork Member is largely a Campanian-Maastrichtian chronostratigraphic unit in northern Utah, and consists of a laterally varied assemblage of conglomerate, sandstone, and carbonaceous mudstone deposited on a broad fluvial megafan.
- 0.5 27.8 Red siltstone and sandstone of the Triassic Ankareh Formation dip east in road cuts.
- 0.3 28.1 Contact with orange to tan sandstone of the Lower Jurassic Nugget Sandstone.
- 0.3 28.4 Contact with red mudstone and evaporites of the Gypsum Spring Member of the Middle Jurassic Twin Creek Limestone. This basal member is overlain by a thick sequence of limestone and minor mudstone deposited during subsidence of a back-bulge basin related to onset of crustal loading to the west (DeCelles and Currie, 1996). 0.5 31.2 Cross synclinal axial trace in the Evanston Formation. This syncline may reflect a subsurface transition in the Crawford thrust sheet from having a basement-cored anticline to the south, to having a flat in Cambrian shale to the north (compare Figs. 28A and 28B).
- 0.1 28.5 Resistant, steeply dipping layers in the middle part of the Twin Creek Limestone form Devils Slide to the south. Gently dipping tectonic stylolites subperpendicular to bedding formed during early layer-parallel shortening and were rotated along with bedding during large-scale folding. 1.2 32.4 Junction with Lost Creek Highway. Turn left onto main highway and proceed north.
- 0.6 29.1 Veer right onto Croyden exit ramp (exit 111), and proceed around ramp. A bed-parallel fault, exposed in the road cut to the southwest, juxtaposes contorted, subvertical limestone and red mudstone of the Watton Canyon and Boundary Ridge Members on the east against silty limestone of the uppermost Giraffe Creek Member of the Twin Creek Limestone on the west. This fault had a complex history, and may have initiated as a gently dipping thrust with top-to-east slip, which was then rotated to subvertical during large-scale folding. This fault has the same stratigraphic throw and structural setting as the Lost Creek thrust exposed to the north. Gently east-dipping beds of the Santonian to Campanian Weber Canyon Conglomerate unconformably overlie the Twin Creek Limestone to the east. Proceed under overpass, cross Weber River, and continue north on Lost Creek Highway.
- 4.1 36.5 Sandstone and conglomeratic sandstone beds of the Evanston Formation are well exposed along the canyon to the west. These beds were previously mapped as Wasatch Formation in adjacent quadrangles (Mullens and Laraway, 1964), but

- new palynological dating and stratigraphic mapping indicate that the base of the overlying Wasatch Formation lies substantially higher.
- 3.4 39.9 Folded and faulted beds of the Leeds Creek Member of the Twin Creek Limestone display pencil fracturing in road cut, and are overlain with angular unconformity by gently dipping beds of the Evanston Formation.
- 0.2 40.1 Junction with Hell Canyon road. Turn left (west) onto dirt road, cross gate, and proceed west up Hell Canyon. This road lies on private land.
- 0.2 40.3 Cross trace of a fault, informally called the Lost Creek thrust, which places highly fractured limestone of the Watton Canyon Member on the west over silty limestone of the Giraffe Creek Member on the east. This fault bounds a series of tight folds in the Twin Creek Limestone that probably formed during Willard footwall shortening. This thrust is intermittently exposed northward along the Lost Creek drainage where it is folded about the frontal anticline of the Crawford thrust.
- 0.2 40.5 **Stop 3-2.** Internal deformation of the Twin Creek Limestone at Hell Canyon (Fig. 27). Park on side of dirt road and return back to Lost Creek Highway when done.
- The earliest thrust-related deformation in this area is an episode of layer-parallel shortening beneath the Willard thrust that produced spaced cleavage, folds, and minor thrusts in the Twin Creek Limestone. Here, the Watton Canyon Member exhibits a complex anticline-syncline pair that probably formed by decollement folding above the Lost Creek thrust. The anticlinal core is internally faulted and thickened by tight, disharmonic minor folds. The west limb of the anticline displays numerous top-to-east contractional faults, and the east limb and adjacent syncline are cut by top-to-east minor thrusts. Limestone beds here also exhibit centimeter-scale spaced cleavage, with more intense cleavage in more clay-rich layers. The cleavage formed at high angles to bedding during early layer-parallel shortening, and was rotated with bedding during minor folding, forming fans around the folds. Cleavage is also locally refracted, recording shear associated with minor faults and flexural-slip folding.
- The folds and cleavage observed here are the southward continuation of a regionally extensive belt of deformation in the footwalls of the Willard thrust in Utah and Meade thrust in southeastern Idaho (Mitra and Yonkee, 1985; Coogan, 1992). Both of these major thrusts have footwall flats in Jurassic strata, and some slip from the thrusts was transferred eastward into footwall deformation. Folds in this belt are generally bounded below by imbricates, such as the Lost Creek thrust, or detachments in evaporites of the Gypsum Spring Member, and above by a regional decollement in salt-bearing strata of the Preuss Formation (Coogan and Yonkee, 1985). The Lost Creek thrust probably branches eastward from the Willard thrust and transfers displacement from deeper levels into shortening at the Twin Creek level, and ultimately merges upward with the Preuss decollement which transfers slip further eastward toward the foreland. A similar displacement transfer system has been documented between the Meade thrust and the Preuss decollement in Idaho (Coogan, 1992; DeCelles et al, 1993). The contribution of such early shortening in the detachment-bounded Twin Creek Limestone and displacement transfer along the Preuss decollement is important for balancing shortening within parts of the Crawford, Medicine Butte, and Absaroka thrust systems (Fig. 28).
- 0.4 40.9 Junction with Lost Creek Highway. Turn right and proceed south.
- 1.9 42.8 Junction with Toone Canyon road. Turn left onto dirt road, cross wooden bridge over Lost Creek, and proceed east toward Toone Canyon. This road lies on private land.
- 0.2 43.0 Silty limestone of the Giraffe Creek Member dips steeply east on the west limb of a tight syncline in the hanging wall of the Lost Creek thrust.
- 0.3 43.3 The Lost Creek thrust, poorly exposed in the hillside north of the road, places light gray limestone of the Leeds Creek Member over red weathering, salt-bearing strata of the Preuss Formation.
- 0.5 43.5 Gate. Cross gently west-dipping silty limestone of the Giraffe Creek Member on the west limb of Toone Canyon anticline. To the east, micritic limestone of the underlying Leeds Creek Member displays close-spaced cleavage at high angles to bedding.
- 0.6 44.1 Cross hinge zone of Toone Canyon anticline, which probably initiated as a fault-propagation fold that was later translated along the Crawford thrust. The anticline has a kink-like hinge at deeper levels to the north, and a box-like geometry here with a gentle backlimb, a broad crest, and an overturned forelimb.

- 0.5 44.6 Steeply dipping to overturned Jurassic Preuss Formation along east limb of Toone Canyon anticline. The gently dipping Evanston Formation unconformably overlies steep Jurassic strata along the north side of canyon.
- 0.5 45.1 Subvertical to overturned conglomerate and sandstone beds of Lower Cretaceous Kelvin Formation are exposed as ribs to the north and east. Laterally discontinuous, pebble to cobble conglomerate beds are dominated by quartzite, chert, and carbonate clasts derived from erosion of Mesozoic to middle Paleozoic strata during emplacement and uplift of the Willard thrust sheet.
- 0.4 45.5 **Stop 3-3.** Stratigraphic bracketing of recurrent Crawford thrust slip episodes in Toone Canyon (Fig. 27).

Cross cutting relationships, distribution, and provenance of synorogenic conglomerates record recurrent episodes of reverse slip along the Crawford thrust, with a final episode of normal inversion. Initial, Coniacian-Santonian slip on the Crawford thrust is recorded by provenance of the Echo Canyon Conglomerate (DeCelles, 1994). Continued Santonian-Campanian slip is recorded by provenance and progressive unconformities in the Weber Canyon Conglomerate observed here where the Crawford thrust places Kelvin Formation in the hanging wall over deformed conglomerate in the footwall (Fig. 35). Conglomerate beds are vertical adjacent to the thrust and offset by minor reverse faults, but bedding flattens eastward and up-section to gentle dips across the hinge of an asymmetric growth syncline. Average modal clast composition of the conglomerate is about 80% quartzite and well-cemented quartz arenite, 10% friable sandstone and siltstone, and 10% carbonate and chert. Identifiable clasts include Cambrian quartzite and Pennsylvanian quartz arenite derived from the east limb of the Wasatch anticlinorium, Jurassic sandstone and siltstone derived from the nearby Toone Canyon anticline, and minor Proterozoic quartzite derived from passive uplift and erosion of the Willard sheet to the northwest. The exposures seen here correspond to the top of an 1,860 m (6,100 ft) thick section of conglomeratic strata drilled within the Crawford footwall by the Amoco 1-1A well to the north (Fig. 28A), indicating that the Crawford sheet overrode its own detritus. Minor reactivation of the Crawford thrust during the early Eocene is documented to the north in Idaho and Wyoming (Hurst and Steidtmann, 1986). The final phase of deformation along the Crawford front is a small increment of normal slip that downdropped the erosional base of the Evanston Formation about 60 m (200 ft) in the Crawford hanging

wall here. Further north the late Eocene-Oligocene Fowkes Formation displays extensional growth geometries along the Crawford thrust front (Constenius, 1996), indicating that initial extensional collapse closely followed the end of thrusting.

The general timing of the Crawford thrust reinforces the regional pattern of a foreland-younging sequence for the initiation of major thrust faults, ie the Crawford initiated after the Willard thrust and before major slip on the Absaroka thrust. However, minor phases of Crawford slip temporally overlapped with emplacement of the Hogsback thrust to the east, as the thrusts were mechanically linked above a common basal decollement. Once established, more internal thrusts accommodated modest amounts of shortening in the wedge, possibly during intervals of stalled thrusting along the front of the wedge. Such pulses of thrust reactivation may be symptomatic of periods of subcritical taper of the wedge, with internal shortening required before critical taper can be reestablished for sliding along the wedge front (DeCelles and Mitra, 1995).

- 2.7 48.2 Return on dirt road back to Lost Creek Highway. Turn left and head south, retracing route back to I-84.
- 7.5 55.7 Turn right onto side road and continue south.
- 1.6 57.3 Pause to note the structural positions of the Weber Canyon, Evanston, and Wasatch synorogenic deposits. In the mountain directly south of us, resistant beds of the Santonian-Campanian Weber Canyon Conglomerate display progressive unconformities that record uplift of the Wasatch anticlinorium, synchronous with slip on the Crawford thrust. The top of the Weber Canyon Conglomerate lies about 360 m (1200 ft) higher than the base of the Campanian-Maastrichtian Hams Fork Member exposed directly to the west, partly reflecting deposition on paleotopographic relief. The Hams Fork Member is over 600 m (2000 ft) thick here, and forms an outcrop band that continues along the east flank of the anticlinorium, recording renewed uplift and wedge-top deposition synchronous with slip on the Absaroka thrust to the east. The Paleocene-early Eocene Wasatch Formation is exposed on the east side of the valley, east of the East Canyon fault zone. This formation lies with angular unconformity over the Hams Fork Member, recording another period of uplift and wedge-top deposition synchronous with



Figure 35. Photomosaic of the Crawford thrust and associated synorogenic deposits along Toone Canyon (view to north). The thrust places poorly exposed Kelvin Formation (Kk) on the west against resistant Weber Canyon Conglomerate (Kwc) on the east, which is deformed into a growth syncline. The overlying Hams Fork Member (Keh) is exposed along the upper ridge.

slip on the Hogsback thrust further east. The current low elevation of the Wasatch Formation is the result of late Eocene-Oligocene normal inversion on the East Canyon fault zone.

- | | | |
|-----|------|--|
| 0.1 | 57.4 | Veer right back onto main Lost Creek Highway and head south. |
| 1.2 | 58.6 | Junction I-84. Take entrance onto east-bound I-84. |
| 0.6 | 59.2 | Roadcuts in Weber Canyon Conglomerate. |
| 0.6 | 59.8 | Stop 3-4. Stratigraphic and structural relations of the Weber Canyon Conglomerate (Fig. 27). Take exit 112 off I-84, pull over for discussion, then proceed east on I-84. |

The cobble- to boulder-conglomerate exposed for a distance of 1.5 km in the road cut along I-84 is referred to as the Weber Canyon Conglomerate (DeCelles, 1994). This conglomerate may be slightly younger or partly correlative with the main body of the Echo Canyon Conglomerate based on limited palynological dates (Coogan, unpublished data), and is overlain by the Evanston Formation. The conglomerate consists of coarse stream-flow and debris-flow facies deposited on the upper parts of laterally intertonguing ancient alluvial fans, visible along the mountain flank to the southwest. The conglomerate is very poorly sorted and packaged in 5- to 25-m-thick units separated by thin siltstone units. Average modal clast composition is 53% sandstone and quartzite, 32% limestone, 9% siltstone, and 6% chert, and identifiable clasts include fragments derived from Mesozoic to Paleozoic strata along the east

limb of the Wasatch anticlinorium. Basement clasts and Proterozoic clasts from the Willard sheet are absent, implying that basement had not been breached by this time and that an ancient drainage divide separated this area from the Willard sheet.

Beds in the lower part of the conglomerate dip east and lie with angular unconformity over subvertical Jurassic strata near the western edge of the road cut, and beds in the lower part of the conglomerate dip steeply west at the eastern edge of the outcrop, defining an asymmetric syncline (Fig. 36). Beds in the upper part of the conglomerate are subhorizontal and progressive unconformities are present within each limb of the syncline. This growth syncline can be traced southwest to near Salt Lake City. East of the syncline, poorly exposed Jurassic and Cretaceous strata form a tip anticline above the Crawford thrust (Fig. 28B), called the Henefer anticline by Schirmer (1985). The anticline is cored here by complexly deformed salt-bearing strata of the Preuss Formation, and may continue to the southwest to near Salt Lake City (Crittenden, 1965b). The east-dipping East Canyon fault zone bounds the west flank of the anticline and east flank of the syncline. This fault zone had a protracted history including: (1) an older phase of top-to-west backthrusting that placed Preuss Formation over the Weber Canyon Conglomerate and overlapped with conglomerate deposition; and (2) a late Eocene-Oligocene phase of east-side-down normal faulting that reactivated backthrusts.

- | | | |
|-----|------|--|
| 1.7 | 61.5 | Red mudstone and sandstone of the Wasatch Formation exposed north of highway have been downdropped on the east side of the East Canyon fault zone. |
|-----|------|--|



Figure 36. Photomosaic of Weber Canyon Conglomerate (*Kwc*) near Henefer, Utah (view to north). The conglomerate displays intraformational unconformities, with dips of bedding decreasing upward within a growth syncline. The lower, eastern part of the conglomerate is deformed by east-dipping backthrusts near a fault contact with the Preuss Formation (*Jp*), and the western part of the conglomerate unconformably overlies the Twin Creek Limestone (*Jt*).

1.1	62.6	Pass Henefer exit. The valley to the southwest is underlain by the Kelvin and Preuss Formations (Mullens and Laraway, 1964). Proceeding east-southeast, progressively younger Cretaceous strata are exposed along the northwest limb of the Stevenson Canyon syncline.	0.5	67.6	Veer right off I-80 onto exit 169 (Echo Canyon exit). Take left at stop sign and proceed north under interstate and railroad overpasses.
1.4	64.0	The Henefer Formation dips east in road cut. This formation consists of four to five upward-coarsening progradational sequences, which were deposited in marine and fluvial environments on the distal parts of a fan-delta. Clasts in coarser conglomeratic layers were derived from erosion of upper Paleozoic to Mesozoic strata, with sources areas from the Willard sheet and from initial uplift of the Wasatch anticlinorium and Crawford sheet. The Henefer Formation grades upward into the Echo Canyon Conglomerate.	0.2	67.8	Turn right and head northeast on old highway. Cliffs to the northeast provide excellent exposures of the upper part of the Echo Canyon Conglomerate. The average modal clast composition in the upper facies is 82% quartzite and quartz arenite, 7% limestone, 5% siltstone, and 6% chert. The dominant clast type is tan to light gray quartz arenite derived from the Pennsylvanian Weber Formation on the east limb of the anticlinorium. Paleocurrents are directed mostly to the east and southeast.
0.7	64.7	Approximate contact with the Echo Canyon Conglomerate. Bedding dips decrease to the east in the trough of the Stevenson Canyon syncline.	2.7	70.5	Approximate contact with the lower part of the Echo Canyon Conglomerate.
1.8	66.5	Conglomerate layers in the cliffs dip gently west on the southeast limb of the Stevenson Canyon syncline (and northwest limb of the Coalville anticline).	2.0	72.5	Stop 3-5. Echo Canyon Conglomerate (Figs. 27 and 37). After stop retrace route southwest back to junction with I-80.
0.6	67.1	Junction with I-80. Veer left and head east onto I-80 toward Evanston, WY.			The lower part of the Echo Canyon Conglomerate is exposed along the lower part of the hillslope to the northwest, and consists of stream-flow conglomerate and minor sandstone. Conglomerates here are not as coarse as units to the west and were probably deposited on the outer reaches of alluvial fans. Clasts in the lower facies have an average modal composition of 50% sandstone and quartz arenite, 20% limestone, 12% siltstone, 6% chert, and 12%



Figure 37. View to northeast of angular unconformity between underlying tilted Echo Canyon Conglomerate (Ke) and overlying Hams Fork Member (Keh) northeast of Echo Junction.

distinctive red to green quartzite and graywacke derived from Proterozoic rocks of the Willard sheet. Paleocurrents indicate flow to the east and southeast. The main body of the Echo Canyon Conglomerate is Coniacian-Santonian (about 85 to 90 Ma; Jacobson and Nichols, 1982), and records early movement on the Crawford thrust and uplift of the Wasatch anticlinorium.

Beds in the Echo Canyon Conglomerate dip gently northwest, and are overlain with angular unconformity by the very gently dipping Campanian-Maestrichtian Hams Fork Member of the Evanston Formation (Fig. 37). The Hams Fork Member contains distinctive clasts of Proterozoic quartzite derived from the Willard thrust sheet and basement clasts that record renewed uplift and erosion of the Wasatch anticlinorium. Wedge-top deposition of the conglomerate east of the anticlinorium was probably synchronous with main movement of the Absaroka thrust (Royse et al., 1975; DeCelles, 1994).

Provenance and structural relations of the different conglomerate facies observed on our transect record the progressive development and denudation of the orogenic wedge. Four idealized temporal stages are recognized. (1) Conglomerate layers in the Kelvin and Frontier Formations record erosion of Mesozoic to upper Paleozoic rocks during emplacement of the Willard thrust sheet. (2) The Echo Canyon Conglomerate records erosion of Mesozoic to middle Paleozoic rocks during early slip on the Crawford thrust and uplift of the Wasatch anticlinorium, and the Weber Canyon Conglomerate, which displays widespread growth structures, records continued uplift of the anticlinorium, slip on the Crawford thrust, and backthrusting on the East Canyon fault zone. (3) The Hams Fork Member records erosion of middle Paleozoic to basement rocks during another phase of uplift of the anticlinorium, concurrent with movement on the Absaroka thrust to the east.

(4) Conglomerate beds of the Wasatch Formation record a final phase of erosion and uplift of the anticlinorium, concurrent with slip on the Hogsback thrust to the east.

4.9 77.4 Return southwest on old highway, turn left and proceed under railroad and interstate overpasses, and continue south along old highway. Progressively older Cretaceous strata will be encountered as we drive across the northwest limb of the Coalville anticline.

1.7 79.1 Approximate contact with the Henefer Formation.

0.6 79.7 Approximate contact with the Cenomanian-Turonian Frontier Formation. Strata exposed in this area are transitional between the conglomerate-dominated lithofacies to the west (Bryant, 1990), and the marine and fluvio-deltaic sandstone and mudstone lithofacies to the east (Ryer, 1976; Schmitt, 1985). Here, the Frontier Formation consists of about 1800 m (6000 ft) of interbedded marine, deltaic, and fluvial sandstone, mudstone, and minor conglomerate deposited along the edge of the western interior seaway.

3.4 83.1 The Oyster Ridge Sandstone Member of the Frontier Formation forms the hogback north of Coalville. Conglomerates in this member have a provenance from upper Paleozoic strata of the Willard thrust sheet (Schmitt, 1985).

0.2 83.3 Junction Chalk Creek Road in Coalville. Turn left and proceed east on Main Street (Chalk Creek Road).

0.5 83.8 Pass cemetery. Fluvial sandstones and floodplain mudstones in the Frontier Formation form alternating ridges and swales to the north.

2.3 86.1 Red mudstone and sandstone of the Wasatch Formation overlie the Frontier Formation with angular unconformity to the north.

0.4 86.5 The Albian Aspen Shale lies within the covered interval to the north.

0.9 87.4 The main part of Aptian-Albian Kelvin Formation dips gently northwest along the northwest limb of the Coalville anticline, and includes numerous channel-fill deposits of fluvial sandstone.

1.2 88.6 Cross hinge zone of the Coalville anticline.

0.1 88.7 The Kelvin Formation dips steeply east on the southeast limb of Coalville anti-

- cline. Seismic profiles and wells indicate that the Coalville anticline is a composite structure (Fig. 28). The tight surface fold seen here is located above a detachment in salt-bearing beds of the Preuss Formation, and is bounded by several imbricate thrusts to the southeast. A sub-surface fold cored by Triassic and Paleozoic rocks lies about 2.5 km (1.5 mi) to the northwest. Both levels display overturned southeast limbs and the composite anticline may have initiated as a fault-propagation fold.
- 0.1 88.8 Cross imbricate thrusts that cut the attenuated southeast limb of Coalville anticline. Depositional thinning of the Hams Fork Member onto the hinge of the anticline may record main-phase folding concurrent with Absaroka thrusting. However, repeated episodes of shortening are recorded by imbricates that cut the Hams Fork Member on the southeast limb, and that locally cut the Wasatch Formation, which overlies the Hams Fork Member with angular unconformity. Late, shallow imbrication above crests of deeper anticlines is a hallmark of alternating break-forward and break-back thrust episodes (Boyer, 1992).
- 0.9 89.7 Pass junction with South Fork road, and continue east on Chalk Creek road.
- 1.1 90.8 Approximate contact with east-dipping Henefer Formation.
- 0.6 91.4 Cross locally faulted hinge zone of Clark Canyon syncline.
- 0.2 91.6 Pass Clark Canyon road. The Henefer Formation dips west on the east limb of the Clark Canyon syncline.
- 1.9 93.5 Pass town of Upton.
- 1.2 94.7 Sandstone beds in the Frontier Formation are overlain by gently dipping Evanston Formation.
- 1.1 95.8 Ledges of gently east-dipping conglomerate of the basal Wasatch Formation overlie the Evanston Formation south of Chalk Creek.
- 2.4 98.2 Cross Chalk Creek, and enter Pineview oil and gas field. Discovery of the Pineview field in 1975 launched an exploration wave that resulted in discovery of 23 other fields in the southern Absaroka thrust sheet during the next seven years. Principal production is from two distinct trends of hangingwall anticlines: the eastern trend, represented by the Pineview and Anschutz Ranch East fields, produces principally from the Jurassic Nugget Sandstone; and the western trend, represented by the Cave Creek field, produces from Paleozoic strata.
- 2.0 100.2 Cross trace of a normal fault that bounds a half graben containing east-tilted Wasatch Formation, Fowkes Formation, and Norwood Tuff. The late Eocene Fowkes Formation was deposited soon after cessation of thrusting and records extension during a period of widespread gravitational collapse along preexisting thrust faults (Constenius, 1996). The normal fault is listric and soles into the Medicine Butte thrust at depth (Fig. 28B), such that extension was accommodated along a shallowly dipping fault segment that formed at shallow depths.
- 0.9 101.1 Cross approximate trace of main Medicine Butte thrust.
- 0.1 101.2 **Stop 3-6.** Medicine Butte thrust system and Hams Fork Member (Fig. 27).
- The Medicine Butte thrust system, like the East Canyon fault zone and shallow structure of Coalville anticline, soles into a regional decollement in salt-bearing strata of the Preuss Formation. The Preuss decollement accommodated slip through multiple phases of thrusting in the region, including an early phase associated with detachment folding, and later phases that are well bracketed by synorogenic sedimentation in this area. South of the road shallowly dipping strata of the Hams Fork Member unconformably overlie steeply dipping Early Cretaceous strata, recording an early, phase of folding and fault slip. Here, however, the main Medicine Butte thrust cuts the Hams Fork Member, which is also thinned and partly rotated above buried imbricates of the thrust system, recording a Campanian-Maastrichtian phase of slip. One of the imbricates also cuts the Wasatch Formation, which locally displays progressive unconformities and has conglomerates that contain distinctive clasts recycled from the Hams Fork Member, recording a phase of late Paleocene slip. This complex displacement history provides another example of break-back thrust slip that may reflect shortening and uplift in the interior of the wedge during periods of sub-critical taper (DeCelles and Mitra, 1995). Some imbricates were reactivated as normal faults during initial late Eocene collapse and development of the half graben to the west.
- The multiple episodes of displacement along the Preuss decollement present challenges to balancing shallow-level shortening with increments of slip on deeper thrusts. The

subsurface geometry of the Absaroka thrust immediately provides a particularly vexing problem (Fig. 28). Deep wells delineate an imbricated zone of Preuss and Cretaceous strata in the hanging wall of the Absaroka thrust, with about 6 km (3.5 mi) of Preuss bed length involved in this shortening. However, no corresponding footwall flat in the Absaroka thrust is observed that would balance this bed length, and thus shortening of Preuss strata here may be unrelated to Absaroka slip. Rather, this shortening may record an early phase of detachment folding and imbrication above a developing Preuss decollement that transferred slip eastward from deeper levels of the Crawford and Willard thrusts. During later deformation, the Absaroka thrust propagated and merged upward to join this preexisting decollement system.

- | | | |
|------|-------|--|
| 17.9 | 119.1 | Return back along Chalk Creek Road to Coalville. Turn left and head south on business route through Coalville. |
| 0.5 | 119.6 | Junction I-80. Take entrance onto I-80 west. |
| 1.3 | 120.9 | Hills to east expose gently dipping beds of the Wasatch Formation. |
| 3.5 | 124.4 | Railroad overpass. Hills to southwest are underlain by the Oligocene (38 to 33 Ma) Keetley Volcanics (Bryant, 1990), which are temporally correlative with the Norwood Tuff. |
| 2.4 | 126.8 | Bear right onto exit 156 toward Wanship, Utah. |
| 0.3 | 127.1 | Junction with U.S. 89. Turn left at stop sign, proceed south on U.S. 89 through Wanship, and cross under I-80 overpass. |
| 0.7 | 127.8 | Northwest-dipping beds of the Kelvin and Preuss Formations are poorly exposed in hillslope to west. |
| 0.4 | 128.2 | Cross approximate trace of Cherry Canyon thrust which places the Preuss Formation on northwest against the Hams Fork Member on southeast (Bradley, 1988). |
| 0.9 | 129.1 | Rockport Reservoir to east. Northwest-dipping beds of Frontier and Kelvin Formations are visible on east side of reservoir. |
| 0.7 | 129.8 | Cross approximate trace of Dry Canyon fault which repeats part of the Kelvin Formation and is overlapped by the Hams Fork Member (Bradley, 1988). |
| 1.1 | 140.5 | Stop 3-7. Relations between frontal thrusts and Uinta uplift (Fig. 38A). Pull into turnout on east side of road for discussion and then return north along U.S. 89. |

A series of northwest-dipping faults imbricate Mesozoic strata within the Rockport Reservoir area (Crittenden, 1974; Bradley, 1988; Bryant, 1990). The Crandall Canyon thrust, visible to the southeast, places red beds of the Preuss Formation over sandstone and black shale of the Frontier Formation. Slickenlines indicate east- to south-east-directed slip, which may have exceeded 15 km based on stratigraphic relations across the thrust (Bradley, 1988). Jurassic strata in the sheet are overlapped by the Hams Fork Member, but the member is also locally cut by the thrust, recording at least two episodes of movement that may correlate with slip on the Medicine Butte or Absaroka thrusts. The Cherry Canyon thrust lies approximately 5 km to the north and places Preuss Formation over the Hams Fork Member, which displays progressive unconformities, recording movement partly concurrently with the Medicine Butte thrust system. This thrust also has an imbricate that offsets the Wasatch Formation and continues northeastward into the Coalville anticline. Additional imbricate faults repeat Jurassic and Cretaceous strata. The Crandall Canyon, Cherry Canyon, and imbricate thrusts share a decollement in the Preuss Formation and may link entirely with the Medicine Butte thrust system to the northeast, or alternatively partly with the Absaroka thrust system (Bradley, 1988). These thrusts probably ramp down section to the southwest and link with the Mount Raymond thrust and a decollement in Permian and Pennsylvanian strata (Fig. 38A; stop 3-8).

The Uinta arch, a major east-trending foreland uplift visible to the southeast, had a protracted uplift history beginning in latest Cretaceous and culminating in the Eocene (Hansen, 1965; Bradley, 1988). The arch is bounded on the north by the North Flank thrust and may continue west into the Cottonwood arch within the Wasatch Range. These arches divide the frontal part of the Sevier orogenic belt into two parts, the Idaho-northern Utah-Wyoming thrust belt on the north and the central Utah thrust belt on the south. Thrusts north of the arch vary systematically in strike and define a salient convex to the east. The salient probably formed by some combination of rotation of thrusts along the north flank of the Uinta arch, variations in thrust transport directions, and decreasing slip along thrusts going south. Slip on the frontal Hogsback thrust overlapped with major uplift of the Uinta arch, and the thrust appears to ramp laterally down to the south and connect with the North Flank thrust (Bradley and Bruhn, 1988). The Uinta arch is part of wider belt of basement-cored foreland uplifts that accommodated crustal shortening east of the thrust belt, and although structural styles are different between the foreland uplifts and thrust belt, later stages of thrusting temporally overlapped and locally interacted with foreland uplifts.

- 3.1 155.3 Pass junction with Utah Highway 224 and continue west on I-80. The trace of the Mount Raymond thrust lies southwest of the highway (Crittenden et al, 1966). The thrust places a hanging wall anticline of Permian to Jurassic strata over the Twin Creek Limestone.
- 2.0 157.3 Pass Jeremy Ranch exit. Heading west the highway cuts obliquely across the north-dipping limb of the Parleys Canyon syncline and a series of smaller-scale, north- to northeast-plunging folds (Crittenden, 1965a, 1965b; Fig. 38A).
- 2.1 159.4 Pass exit to Summit Park. Beds of the Twin Creek Limestone dip north.
- 0.9 160.3 Red beds of Preuss Formation dip northwest in road cuts.
- 2.4 162.7 Pass Lambs Canyon exit. Hillside to the north is composed of the Cretaceous Kelvin Formation, which consists of ≈ 1000 m of interbedded conglomerate, sandstone, and mudstone deposited in fluvial and lacustrine environments. Conglomerate clasts were probably derived from uplift and erosion of the Willard thrust sheet to the northwest. North-dipping beds of the Frontier Formation crop out farther north toward the hinge of the Parleys Canyon syncline. Here the Frontier Formation is over 3000 m thick and includes thick conglomerate intervals deposited during renewed uplift and erosion of the Willard sheet.
- 1.3 164.0 View to west of the Spring Canyon anticline (Crittenden, 1965b), which is cored by faulted Triassic rocks and may connect to the northeast with the Henefer anticline. Conglomerate beds exposed to the north along East Canyon lie with angular unconformity over the Frontier Formation, and display progressive unconformities that may separate parts of the Echo Canyon, Weber Canyon, and Hams Fork conglomerates (Mullens, 1971).
- 2.6 166.6 Pass ranch exit. Micritic beds of the Twin Creek Limestone are cut by multiple minor faults in road cut.
- 1.6 168.2 Complex, disharmonic folds are developed in limestone beds to north. Spaced cleavage is strongly fanned about the folds.
- 0.7 168.9 **Stop 3-8.** Internal deformation of the Twin Creek Formation along Parleys Can-



Figure 39. Well-developed spaced cleavage in micritic limestone of the Twin Creek Formation along Parleys Canyon is defined by spaced seams of residue that are enriched in clays. Rock hammer for scale.

yon (Fig. 38A). Pull over along entrance ramp on north side of highway for discussion, then continue southwest on I-80. Be careful of falling rocks.

Argillaceous to silty, micritic beds of the Twin Creek Limestone exposed along Parleys Canyon display spaced cleavage, minor folds, vein arrays, and minor faults that formed during a complex deformation history (Fig. 39). Two spaced cleavages are present: (1) a more strongly developed cleavage (termed S1) that is generally steeply dipping and strikes north to north-northeast; and (2) a weakly developed cleavage (termed S2) that is generally gently dipping and strikes east to northeast. S2 cleavage seams dissolve some veins that cross cut S1 seams, indicating that S1 formed first. S1 is parallel to hinge lines of smaller-scale, north- to northeast-plunging folds (termed F1 folds) that formed above detachments in Permo-Pennsylvanian strata, but cleavage is fanned around these folds (Fig. 38B). These relations record an early phase of east-southeast directed layer-parallel shortening that produced S1, closely followed by F1 detachment folding. S2 is parallel to the hinge lines of larger-scale, gently east-northeast plunging folds (termed F2 folds), including the Parleys Canyon syncline, Spring Canyon anticline, and Emigration Canyon syncline. S2 is strongly fanned about F2 folds, remaining subperpendicular to bedding in the hinge and limb regions. These relations record a second phase of southeast directed internal shortening that produced S2, closely followed by development of large-scale F2 folds.

Kinematic relations of F1 and F2 folds to regional thrusts are problematical. F1 folds may record an early

phase of shortening that was stratigraphically confined between a lower detachment in Permo-Pennsylvanian strata and an upper decollement in the salt-bearing Preuss Formation. The lower detachment merges with the Mount Raymond thrust to the east, and the combined thrust-detachment system ramps up to the Preuss decollement further east. These relations indicate that slip on the lower detachment was partly transferred into fold-cleavage shortening at the Twin Creek level, and ultimately into an early phase of slip along the Preuss decollement to the east. F2 folds (Parleys Canyon syncline, Spring Canyon anticline, and Emigration syncline) appear to connect along trend with the Stevenson Canyon syncline, Henefer anticline, and Weber Canyon growth syncline, indicating that F2 folds may be related to propagation and slip along the Crawford thrust. The Mount Raymond thrust may have formed later and merged with the earlier decolle-

ment system, with slip on this thrust locally modifying earlier folds. Later uplift on the north flank of the Cottonwood arch then rotated the Mount Raymond thrust and folds to more northerly dips (Bradley, 1988).

0.6	169.5	Locally faulted contact between Nugget Formation and Twin Creek Limestone.
0.4	169.9	Junction with I-215. Continue west on I-80.
1.0	170.9	Cross trace of eastern splay of Wasatch fault zone along base of mountains.
2.9	173.8	Cross trace of western splay of Wasatch fault zone. View to southeast of central part of the Wasatch Range and Cottonwood arch.
2.2	176.0	Junction with I-15. End of road log. Continue to Salt Lake City International Airport.

REFERENCES CITED

(for all 5 parts)

- Allmendinger, R.W., 1992, Fold and thrust tectonics of the western United States exclusive of accreted terranes, in Burchfiel, B.C., Lipman, P.W., and Zoback, M.L., eds., *The Cordilleran orogen: continuous U.S.* Boulder, Colorado, Geological Society of America, *The geology of North America*, v. G-3, p. 583-607.
- Allmendinger, R.W., and Jordan, T.E., 1984, Mesozoic structure of the Newfoundland Mountains, Utah: horizontal shortening and subsequent extension in the hinterland of the Sevier belt. *Geological Society of America Bulletin*, v. 95, p. 1280-1292.
- Allmendinger, R.W., Miller, D.M., and Jordan, T.E., 1984, Known and inferred Mesozoic deformation in the hinterland of the Sevier belt, northwest Utah, in Kerns, G.J., and Kerns, R.L., eds., *Geology of northwest Utah, southern Idaho, and northeast Nevada*. Utah Geological Association Publication 13, p. 21-32.
- Anovitz, L.M., and Essene, E.J., 1987, Phase relations in the system $\text{CaCO}_3\text{-MgCO}_3\text{-FeCO}_3$. *Journal of Petrology*, v. 28, p. 389-414.
- Armstrong, R.L., 1968a, Sevier orogenic belt in Nevada and Utah: *Geological Society of America Bulletin*, v. 79, p. 429-458.
- Armstrong, R.L., 1968b, Mantled gneiss domes in the Albion Range, southern Idaho. *Geological Society of America Bulletin*, v. 79, p. 1295-1314.
- Armstrong, R.L., 1976, The geochronology of Idaho (Part 2). *Isocron/West*, no. 15, p. 1-33.
- Armstrong, R.L., and Hills, F.A., 1967, Rb-Sr and K-Ar geochronologic studies of mantled gneiss domes, Albion Range, southern Idaho, USA. *Earth and Planetary Science Letters*, v. 3, p. 114-124.
- Armstrong, F.C., and Oriol, S.S., 1965, Tectonic development of the Idaho-Wyoming thrust belt. *American Association of Petroleum Geologists Bulletin*, v. 49, p. 1847-1866.
- Best, M.G., McKee, E.H., and Damon, P.E., 1980, Space-time-composition patterns of late Cenozoic mafic volcanism, south-western Utah and adjoining areas: *American Journal of Science*, v. 280, p. 1035-1050.
- Bohlen, S.R., Montanari, A., and Kerrick, D.M., 1991, Precise determination of the equilibrium kyanite-sillimanite and kyanite-andalusite and a revised triple point for Al_2SiO_5 polymorphs. *American Mineralogist*, v. 76, p. 677-680.
- Boyer, S.E., 1992, *Geometric evidence for sequential thrusting in the southern Alberta and northwest Montana thrust belts*, in McClay, K.R., ed., *Thrust Tectonics*. Chapman and Hall, London, p. 377-390.
- Bradley, M.D., 1988, Structural evolution of the Uinta Mountains, Utah, and their interaction with the Utah-Wyoming salient of the Sevier overthrust belt [Ph.D. dissert.]. Salt Lake City, Utah, The University of Utah, 178 p.
- Bradley, M.P., and Bruhn, R.L., 1988, Structural interactions between the Uinta arch and overthrust belt, north-central Utah: implications of strain trajectories and displacement modeling, in Schmidt, C.J., and Perry, W.J., Jr., eds., *Interaction of the Rocky Mountain foreland and the Cordilleran thrust belt*. Geological Society of America Memoir 171, p. 431-445.
- Brooks, W.E., Thorman, C.H., and Snee, L.W., 1995, The $^{40}\text{Ar}/^{39}\text{Ar}$ ages and tectonic setting of the middle Eocene northeast Nevada volcanic field. *Journal of Geophysical Research*, v. 100, p. 10, 403-10, 416.
- Bruhn, R.L., and Beck, S.L., 1981, Mechanics of thrust faulting in crystalline basement, Sevier orogenic belt, Utah. *Geology*, v. 9, p. 200-204.
- Bryant, B., 1984, Reconnaissance geologic map of the Precambrian Farmington Canyon Complex and the surrounding rocks in the Wasatch Mountains between Ogden and Bountiful, Utah: U.S. Geological Survey Miscellaneous Geologic Investigations Map I-1447.
- Bryant, B., 1990, Geologic map of the Salt Lake City 30' X 60' quadrangle, north-central Utah, and Uinta County, Wyoming: U.S. Geological Survey Miscellaneous Investigations Series Map I-1944, scale 1:100,000.
- Bryant, B., and Nichols, D.J., 1988, Late Mesozoic and early Tertiary reactivation of an ancient crustal boundary along the Uinta trend and its interaction with the Sevier orogenic belt, in Schmidt, C.J., and Perry, W.J., Jr., eds., *Interaction of the Rocky Mountain foreland and the Cordilleran thrust belt*. Geological Society of America Memoir 171, p. 411-430.
- Camilleri, P.A., 1994a, On the rheological, structural, and metamorphic evolution of footwalls to thick thrust sheets. *Geological Society of America Abstracts with Programs*, v. 26, no. 7, p. A525.
- Camilleri, P.A., 1994b, Mesozoic and Cenozoic tectonic and metamorphic evolution of the Wood Hills and Pequoop Mountains, Elko County, Nevada [Ph.D. dissert.]. Laramie, Wyoming, University of Wyoming, 196 p.
- Camilleri, P.A., and Chamberlain, K.R., 1997, Mesozoic tectonics and metamorphism in the Pequoop Mountains and Wood Hills region, northeast Nevada: Implications for the architecture and evolution of the Sevier orogen. *Geological Society of America Bulletin*, v. 109, p. 74-94.
- Camilleri, P.A., Miller, D.M., Snoko, A.W., and Wells, M.E., 1992, Structure and fabric of metamorphic terrains in the northeastern Great Basin: Implications for Mesozoic crustal shortening and extension, in Wilson, J.R., ed., *Field guide to geologic excursions in Utah and adjacent areas of Nevada, Idaho, and Wyoming*: Utah Geological Survey Miscellaneous Publication 92-3, p. 19-58.
- Coats, R.R., 1987, *Geology of Elko County, Nevada*. Nevada Bureau of Mines and Geology Bulletin 101, 112 p.
- Coats, R.R., and Riva, J.F., 1983, Overlapping thrust belts of Late Paleozoic and Mesozoic ages, northern Elko County, Nevada, in Miller, D.M., Todd, V.R., and Howard, K.A., eds., *Structural and stratigraphic studies in the eastern Great Basin*. Geological Society of America Memoir 157, p. 305-327.
- Compton, R.R., 1972, Geologic map of Yost quadrangle, Box Elder County, Utah, and Cassia County, Idaho. U.S. Geological Survey, Miscellaneous Geologic Investigations Map I-672.
- Compton, R.R., 1975, Geologic map of Park Valley quadrangle, Box Elder County, Utah, and Cassia County, Idaho: U.S. Geological Survey, Miscellaneous Geologic Investigations Map I-873.
- Compton, R.R., 1980, Fabrics and strains in quartzites of a metamorphic core complex, Raft River Mountains, Utah, in Crittenden, M.D., Jr., Coney, P.J., and Davis, G.H., eds., *Cordilleran metamorphic core complexes*: Geological Society of America Memoir 153, p. 385-398.
- Compton, R.R., 1983, Displaced Miocene rocks on the west flank of the Raft River-Grouse Creek core complex, Utah, in Miller, D.M., Todd, V.R., and Howard, K.A., eds., *Tectonic and stratigraphic studies in the eastern Great Basin*. Geological Society of America Memoir 157, p. 271-279.
- Compton, R.R., and Todd, V.R., 1979, Oligocene and Miocene metamorphism, folding, and low-angle faulting in northwestern Utah. *Reply Geological Society of America Bulletin*, v. 90, p. 307-309.
- Compton, R.R., Todd, V.R., Zartman, R.E., and Naeser, C.W., 1977, Oligocene and Miocene metamorphism, folding, and low-angle faulting in northwestern Utah. *Geological Society of America Bulletin*, v. 88, p. 1237-1250.
- Constenius, K.N., 1996, Late Paleogene extensional collapse of the Cordilleran fold and thrust belt. *Geological Society of America Bulletin*, v. 108, p. 20-39.
- Coogan, J.C., 1992, Structural evolution of piggyback basins in the Wyoming-Idaho-Utah thrust belt, in Link, P.K., Kuntz, M.A., and Platt, L.B., eds., *Regional geology of eastern Idaho and western Wyoming*. Geological Society of America Memoir 179, p. 55-81.
- Coogan, J.C., and Royle, F., Jr., 1990, Overview of recent developments in thrust belt interpretation, in Roberts, S., ed., *Geologic field tours*

- of western Wyoming and adjacent Idaho, Montana, and Utah: Geological Survey of Wyoming Public Information Circular, 29, p. 89–124.
- Coogan, J.C., and Yonkee, W.A., 1985, Salt detachments within the Meade and Crawford thrust systems, Idaho and Wyoming, in Kerns, G.J., and Kerns, R.L., eds., *Orogenic patterns and stratigraphy of north-central Utah and southeastern Idaho*: Utah Geological Association Publication 14, p. 75–82.
- Covington, H.R., 1983, Structural evolution of the Raft River Basin, Idaho, in Miller, D.M., Todd, V.R., and Howard, K.A., eds., *Tectonic and stratigraphic studies in the Eastern Great Basin*. Geological Society of America Memoir 157, p. 229–237.
- Crampton, S.L., and Allen, P.A., 1995, Recognition of forebulge unconformities associated with early stage foreland basin development. Example from the North Alpine foreland basin. *American Association of Petroleum Geologists Bulletin*, v. 79, p. 1495–1514.
- Crittenden, M.D., Jr., 1965a, Geologic map of the Mount Aire quadrangle, Salt Lake County, Utah: U.S. Geological Survey Map GQ-379, scale 1:24,000.
- Crittenden, M.D., Jr., 1965b, Geologic map of the Sugar House quadrangle, Salt Lake County, Utah: U.S. Geological Survey Map GQ-380, scale 1:24,000.
- Crittenden, M.D., Jr., 1972, Willard thrust and Cache allochthon, Utah: *Geological Society of America Bulletin*, v. 83, p. 2871–2880.
- Crittenden, M.D., Jr., 1974, Regional extent and age of thrusts near Rockport Reservoir and relation to possible exploration targets in northern Utah: *American Association of Petroleum Geologists Bulletin*, v. 58, p. 2428–2435.
- Crittenden, M.D., Jr., 1979, Oligocene and Miocene metamorphism, folding, and low-angle faulting in northwestern Utah. *Geological Society of America Bulletin*, v. 90, p. 305–306.
- Crittenden, M.D., Jr., 1985a, Geologic map of the Mantua quadrangle and part of the Willard quadrangle, Box Elder, Weber, and Cache Counties, Utah: U.S. Geological Survey Map I-1605, scale 1:24,000.
- Crittenden, M.D., Jr., 1985b, Geologic map of the North Ogden quadrangle and part of the Ogden and Plain City quadrangles, Box Elder and Weber Counties, Utah. U.S. Geological Survey Map I-1606, scale 1:24,000.
- Crittenden, M.D., Jr., 1988, Bedrock geologic map of the Promontory Mountains, Box Elder County, Utah: U.S. Geological Survey Open-file Report 88-646, scale 1:50,000.
- Crittenden, M.D., Jr., and Sorensen, M.L., 1979, The Facer Formation, a new early Proterozoic unit in northern Utah. *U.S. Geological Survey Bulletin* 1482-F, 28 p.
- Crittenden, M.D., Jr., Calkins, F.C., and Sharp, B.J., 1966, Geologic map of the Park City West quadrangle, Utah: U.S. Geological Survey Map GQ-535, scale 1:24,000.
- Dahlen, F.A., and Suppe, J., 1988, Mechanics, growth, and erosion of mountain belts, in Clark, S.P., Jr., Burchfiel, B.C., and Suppe, J., eds., *Processes in continental lithospheric deformation*. Boulder, Colorado, Geological Society of America, Special Paper 218, p. 161–178.
- Davis, F.D., 1985, Geologic map of the northern Wasatch front, Utah: Utah Geological and Mineral Survey Map 53A.
- DeCelles, P.G., 1994, Late Cretaceous-Paleocene synorogenic sedimentation and kinematic history of the Sevier thrust belt, northeast Utah and southwest Wyoming. *Geological Society of America Bulletin*, v. 106, p. 32–56.
- DeCelles, P.G., and Burden, E.T., 1992, Non-marine sedimentation in the overfilled part of the Jurassic-Cretaceous Cordilleran foreland basin. Morrison and Cloverly Formations, central Wyoming, USA. *Basin Research*, v. 4, p. 291–314.
- DeCelles, P.G., and Currie, B.S., 1996, Long-term sediment accumulation in the middle Jurassic-early Eocene Cordilleran retroarc foreland-basin system: *Geology*, v. 24, p. 591–594.
- DeCelles, P.G., and Giles, K.A., 1996, Foreland basin systems: *Basin Research*, v. 8, p. 105–123.
- DeCelles, P.G., and Mitra, G., 1995, History of the Sevier orogenic wedge in terms of critical taper models, northeast Utah and southwest Wyoming. *Geological Society of America Bulletin*, v. 107, p. 454–462.
- DeCelles, P.G., Pile, H.T., and Coogan, J.C., 1993, Kinematic history of the Meade thrust based on provenance of the Bechler Conglomerate at Red Mountain, Idaho, Sevier thrust belt. *Tectonics*, v. 12, p. 1436–1450.
- Dixon, J.S., 1982, Regional structural synthesis, Wyoming salient of the western overthrust belt: *American Association of Petroleum Geologists Bulletin*, v. 66, p. 1560–1580.
- Doelling, H., 1980, Geology and Mineral resources of Box Elder County, Utah: Utah Geologic and Mineral Survey Bulletin 115, 251 p.
- Ellis, M., and Watkinson, A.J., 1987, Orogen-parallel extension and oblique tectonics. The relation between stretching lineations and relative plate motions. *Geology*, v. 15, p. 1022–1026.
- Epstein, A.G., Epstein, J.B., and Harris, L.C., 1977, Conodont color alteration—An index to organic metamorphism: *U.S. Geological Survey Professional Paper* 995, 27 p.
- Evans, J.P., and Neves, D.S., 1993, Footwall deformation along the Willard thrust, Sevier Orogenic Belt. Implications for mechanisms, timing, and kinematics. *Geological Society of America Bulletin*, v. 104, p. 516–527.
- Gilbert, G.K., 1928, Studies of Basin-Range structure. U.S. Geological Survey Professional Paper 153, 89 p.
- Glick, L.L., 1987, Structural geology of the northern Toano Range, Elko County, Nevada [M.S. thesis]: San Jose, California, San Jose State University, 141 p.
- Grambling, J.A., 1990, Internally-consistent geothermometry and H₂O barometry in metamorphic rocks—The example garnet-chlorite-quartz. *Contributions to Mineralogy and Petrology*, v. 105, p. 617–628.
- Hansen, W.R., 1965, Geology of the Flaming Gorge area, Utah-Colorado-Wyoming. U.S. Geological Survey Professional Paper 490, 196 p.
- Hansen, R.L., 1980, Structural analysis of the Willard thrust fault near Ogden Canyon, Utah [M.S. thesis] Salt Lake City, Utah, The University of Utah, 82 p.
- Hedge, C.E., Stacey, J.S., and Bryant, B., 1983, Geochronology of the Farmington Canyon Complex, Wasatch Mountains, Utah, in Miller, D.M., Todd, V.R., and Howard, K.A., eds., *Tectonic and stratigraphic studies in the eastern Great Basin*. Geological Society of America Memoir 157, p. 37–44.
- Hefner, M.L., Loptien, G.D., and Ohlin, H.N., 1990, Geology and mineralization of the Black Pine Gold Deposit, Cassia County, Idaho, in Shaddrick, D.R., Kizis, J.A., and Hunsaker, E.L., eds., *Geology and ore deposits of the northeastern Great Basin*: Geological Society of Nevada, p. 167–173.
- Heller, P.L., Bowdler, S.S., Chambers, H.P., Coogan, J.C., Hagen, E.S., Shuster, M.W., Winslow, N.S., and Lawton, T.F., 1986, Timing of initial thrusting in the Sevier orogenic belt, Idaho-Wyoming and Utah. *Geology*, v. 14, p. 388–391.
- Hintze, L.F., 1980, Geologic map of Utah. Utah Geological and Mineral Survey Map, scale 1:500,000.
- Hodges, K.V., and Spear, F.S., 1982, Geothermometry, geobarometry, and the Al₂SiO₅ triple point at Mt. Moosilauke, New Hampshire. *American Mineralogist*, v. 67, p. 1118–1134.
- Hodges, K.V., and Walker, J.D., 1992, Extension in the Cretaceous Sevier orogen, North American Cordillera: *Geological Society of America Bulletin*, v. 104, p. 560–569.
- Hodges, K.V., Snoke, A.W., and Hurlow, H.A., 1992, Thermal evolution of a portion of the Sevier hinterland: the northern Ruby Mountains-

- East Humboldt Range and Wood Hills, northeastern Nevada. *Tectonics*, v. 11, p. 154–164.
- Hoisch, T.D., 1991, Equilibria within the mineral assemblage quartz + muscovite + biotite + garnet + plagioclase: Contributions to Mineralogy and Petrology, v. 108, p. 43–54
- Hope, R.A., 1972, Geologic map of the Spruce Mountain quadrangle Elko County, Nevada: U.S. Geological Survey Map GQ-942, scale 1:62,500.
- Hollett, D.W., 1979, Petrological and physicochemical aspects of thrust faulting in the Precambrian Farmington Canyon Complex, Utah [M.S. thesis]: Salt Lake City, Utah, The University of Utah, 99 p
- Hose, R.K., and Danes, Z.F., 1973, Development of the late Mesozoic to early Cenozoic structures of the eastern Great Basin, in de Jong, K.A., and Scholten, R., eds., *Gravity and Tectonics*: New York, J. Wiley and Sons, p. 429–441
- Hurst, D.J., and Steidtmann, J.R., 1986, Stratigraphy and tectonic significance of the Tump conglomerate in the Fossil Basin, southwest Wyoming: *Mountain Geologist*, v. 23, p. 6–13.
- Jacobson, S.R., and Nichols, D.J., 1982, Palynological dating of syntectonic units in the Utah-Wyoming thrust belt: the Evanston Formation, Echo Canyon Conglomerate, and Little Muddy Creek Conglomerate, in Powers, R.G., ed., *Geologic studies of the Cordilleran thrust belt*. Rocky Mountain Association of Geologists, Denver, Colorado, p. 735–750
- Jordan, T.E., 1981, Thrust loads and foreland basin evolution, Cretaceous, western United States. *American Association of Petroleum Geologists Bulletin*, v. 65, n. 12, p. 2506–2520.
- Jordan, T.E., 1983, Structural geometry and sequence, Bovine Mountain, northwestern Utah, in Miller, D.M., Todd, V.R., and Howard, K.A., eds., *Tectonic and stratigraphic studies in the Eastern Great Basin*. Geological Society of America Memoir 157, p. 215–288.
- Kleemann, U., and Reinhardt, J., 1994, Garnet-biotite thermometry revisited, the effect of AlVI and Ti in biotite. *European Journal of Mineralogy*, v. 6, n. 6, p. 925–941.
- Lamerson, P.R., 1982, The Fossil Basin and its relationship to the Absaroka thrust system, Wyoming and Utah, in Powers, R.B., ed., *Geologic studies of the Cordilleran thrust belt*: Denver, Colorado, Rocky Mountain Association of Geologists, p. 279–337.
- Lush, A.P., McGrew, A.J., Snoke, A.W., and Wright, J.E., 1988, Allochthonous Archean basement in the northern East Humboldt Range, Nevada. *Geology*, v. 16, p. 349–353.
- Malavieille, J., 1987, Kinematics of compressional and extensional ductile shearing deformation in a metamorphic core complex of the northeastern Basin and Range. *Journal of Structural Geology*, v. 9, p. 541–554
- Manning, A.H., and Bartley, J.M., 1994, Postmylonitic deformation in the Raft River metamorphic core complex, northwestern Utah: Evidence of a rolling hinge. *Tectonics*, v. 13, p. 596–612
- McGrew, A.J., 1992, Tectonic evolution of the northern East Humboldt Range, Elko County, Nevada [Ph.D. dissert.]: Laramie, Wyoming, University of Wyoming, 191 p.
- McGrew, A.J., and Snee, L.W., 1994, $^{40}\text{Ar}/^{39}\text{Ar}$ thermochronologic constraints on the tectonothermal evolution of the northern East Humboldt Range metamorphic core complex. *Tectonophysics*, v. 238, p. 425–450.
- Miller, D.M., 1980, Structural geology of the Albion Mountains, south-central Idaho, in Crittenden, M.D., Coney, P.J., and Davis, G.H., *Cordilleran metamorphic core complexes*: Geological Society of America Memoir 153, p. 399–423
- Miller, D.M., 1983, Allochthonous quartzite sequence in the Albion Mountains, Idaho, and proposed Proterozoic Z and lower Cambrian correlations in the Pilot Range, Utah and Nevada, in Miller, D.M., Todd, V.R., and Howard, K.A., eds., *Tectonic and stratigraphic studies in the eastern Great Basin*. Geological Society of America Memoir 157, p. 191–213.
- Miller, D.M., and Allmendinger, R.W., 1991, Jurassic normal and strike-slip faults at Crater Island, northwestern Utah. *Geological Society of America Bulletin*, v. 103, p. 1239–1251.
- Miller, D.M., and Hoisch, T.D., 1992, Mesozoic structure, metamorphism, and magmatism in the Pilot and Toano Ranges, in Wilson, J.R., ed., *Field guide to geologic excursions in Utah and adjacent areas of Nevada, Idaho, and Wyoming*: Utah Geological Survey Miscellaneous Publication 92-3, p. 79–92.
- Miller, D.M., and Hoisch, T.D., 1995, Jurassic tectonics of northeastern Nevada and northwestern Utah from the perspective of barometric studies, in Miller, D.M., and Busby, C., eds., *Jurassic magmatism and tectonics of the North American Cordillera*. Geological Society of America Special Paper 299, p. 267–294.
- Miller, D.M., Armstrong, R.L., Compton, R.R., and Todd, V.R., 1983, Geology of the Albion-Raft River-Grouse Creek Mountains area, northwestern Utah and southern Idaho. *Utah Geological and Mineral Survey Special Studies*, 59, p. 1–59.
- Miller, D.M., Hillhouse, W.C., Zartman, R.E., and Lanphere, M.A., 1987, Geochronology of intrusive and metamorphic rocks in the Pilot Range, Utah and Nevada, and comparison with regional patterns: *Geological Society of America Bulletin*, v. 99, p. 866–879.
- Miller, D.M., Repetski, J.E., and Harris, A.G., 1991, East-trending Paleozoic continental margin near Wendover, Utah, in Cooper, J.D., and Stevens, C.H., eds., *Paleozoic paleogeography of the western United States—II*. Society of Economic Paleontologists and Mineralogists, Pacific Section, v. 67, p. 439–461.
- Miller, E.L., and Gans, P.B., 1989, Cretaceous crustal structure and metamorphism in the hinterland of the Sevier thrust belt, western U.S. Cordillera. *Geology*, v. 17, p. 59–62
- Mitra, S., 1990, Fault-propagation folds: Geometry, kinematic evolution, and hydrocarbon traps. *American Association of Petroleum Geologists Bulletin*, v. 74, p. 921–945.
- Mitra, G., and Yonkee, W.A., 1985, Relationship of spaced cleavage to folds and thrusts in the Idaho-Utah-Wyoming thrust belt. *Journal of Structural Geology*, v. 7, p. 361–373.
- Mueller, K.J., 1992, Tertiary basin development and exhumation of the northern East Humboldt-Wood Hills metamorphic complex, Elko County, Nevada [Ph.D. dissert.]. Laramie, University of Wyoming, 205 p
- Mueller, K.J., and Snoke, A.W., 1993a, Progressive overprinting of normal fault systems and their role in Tertiary exhumation of the East Humboldt-Wood Hills metamorphic complex, northeast Nevada. *Tectonics*, v. 12, p. 361–371
- Mueller, K.J., and Snoke, A.W., 1993b, Cenozoic basin development and normal fault systems associated with the exhumation of metamorphic complexes in northeast Nevada, in Lahren, M.M., Trexler, J.H., and Spinosa, C., eds., *Crustal evolution of the Great Basin and Sierra Nevada*. Geological Society of America field trip guidebook, Geology Department, University of Nevada, Reno, p. 1–34
- Mullens, T.E., 1971, Reconnaissance study of the Wasatch, Evanston, and Echo Canyon Formations in part of northern Utah. *U.S. Geological Survey Bulletin* 1311-D, p. 1–31
- Mullens, T.E., and Laraway, W.H., 1964, Geology of the Devils Slide quadrangle, Morgan and Summit Counties, Utah. *U.S. Geological Survey Map MF-290*, scale 1:24,000.
- Mullens, T.E., and Laraway, W.H., 1973, Geologic map of the Morgan 7 1/2-minute quadrangle, Morgan County, Utah: *U.S. Geological Survey Map MF-318*, scale 1:24,000.
- Naeser, C.W., Bryant, B., Crittenden, M.D., Jr., and Sorensen, M.L., 1983, Fission-track ages of apatite in the Wasatch Mountains, Utah: an uplift study, in Miller, D.M., Todd, V.R., and Howard, K.A., eds.,

- Tectonic and stratigraphic studies in the eastern Great Basin: Geological Society of America Memoir 157, p. 29–36
- Oldow, J.S., 1984, Evolution of a late Mesozoic back-arc fold and thrust belt, northwestern Great Basin, U.S.A.. *Tectonophysics*, v. 102, p. 245–274.
- Pavlis, T.L., and Bruhn, R.L., 1988, Stress history during propagation of a lateral fold-tip and implications for the mechanics of fold thrust belts. *Tectonophysics*, v. 145, p. 113–127.
- Pease, F.S., 1956, History of exploration for oil and gas in Box Elder County, Utah, and vicinity. Utah Geological Society Guidebook to the Geology of Utah, no. 11, Geology of parts of northwestern Utah, p. 17–31.
- Personius, S.F., 1988, Preliminary surficial geologic map of the Brigham City segment and adjacent parts of the Weber and Colliston segments, Wasatch fault zone, Box Elder and Weber Counties, Utah. U.S. Geological Survey Map MF-2042.
- Peters, M.T., and McGrew, A.J., 1994, Timing of extension and metamorphism in the East Humboldt Range metamorphic core complex: Geological Society of America Abstracts with Programs, v. 26, no. 2, p. 81
- Peters, M.T., and Wickham, S.M., 1994, Petrology of upper amphibolite facies marbles from the East Humboldt Range, Nevada, USA: evidence for high temperature, retrograde, hydrous volatile fluxes at mid-crustal levels. *Journal of Petrology*, v. 35, p. 205–238.
- Platt, J.P., 1996, Dynamics of orogenic wedges and uplift of high-pressure metamorphic rocks. *Geological Society of America Bulletin*, v. 97, p. 1037–1053.
- Rejebian, V.A., Harris, A.G., and Huebner, J.S., Conodont color and textural alteration: An index to regional metamorphism, contact metamorphism, and hydrothermal alteration: *Geological Society of America Bulletin*, v. 99, p. 471–479.
- Royse, F., Jr., 1993, An overview of the geologic structure of the thrust belt in Wyoming, northern Utah, and eastern Idaho, in Snoke, A.W., Steidtmann, J.R., and Roberts, S.M., eds., *Geology of Wyoming: Geological Survey of Wyoming Memoir 5*, p. 272–311.
- Royse, F., Jr., Warner, M.A., and Reese, D.L., 1975, Thrust belt structural geometry and related stratigraphic problems, Wyoming-Idaho-northern Utah, in Bolyard D.W., ed., *Deep drilling frontiers of the central Rocky Mountains. Rocky Mountain Association of Geologists Symposium*, p. 41–54.
- Saltzer, S.D., and Hodges, K.V., 1988, The Middle Mountain shear zone, southern Idaho. Kinematic analysis of an early Tertiary high-temperature detachment: *Geological Society of America Bulletin*, v. 100, p. 96–103.
- Sanderson, D., 1973, Models of strain variation in nappes and thrust sheets, a review. *Tectonophysics*, v. 137, p. 289–302
- Schirmer, T.W., 1985, Basement thrusting in north-central Utah: A model for the development of the northern Utah highland, in Kerns, G.J., and Kerns, R.L., eds., *Orogenic patterns and stratigraphy of north-central Utah and southeastern Idaho: Utah Geological Association Publication 14*, p. 129–143.
- Schirmer, T.W., 1988, Structural analysis using thrust-fault hanging-wall sequence diagrams. Ogden duplex, Wasatch Range, Utah: *American Association of Petroleum Geologists Bulletin*, v. 72, p. 573–585.
- Schmid, S.M., and Casey, M., 1986, Complete fabric analysis of some commonly observed quartz c-axis patterns: in Hobbs, B.C., and Heard, H.C., eds., *Mineral and Rock Deformation: Laboratory Studies, American Geophysical Union Geophysical Monograph 36*, p. 263–296
- Schmitt, J.G., 1985, Synorogenic sedimentation of Upper Cretaceous Frontier Formation conglomerates and associated strata, Wyoming-Idaho-Utah thrust belt. *The Mountain Geologist*, v. 22, p. 5–16.
- Smith, J.F., 1982, Geologic Map of the Strevell 15 minute quadrangle, Cassia County, Idaho. U.S. Geological Survey, Map 1-1403.
- Smith, J.F., 1983, Paleozoic rocks in the Black Pine Mountains, Cassia County, Idaho. U.S. Geological Survey Bulletin 1536, 36 p.
- Smith, R.B., and Sbar, M.L., 1974, Contemporary tectonics and seismicity of the western United States with emphasis on the intermountain seismic belt: *Geological Society of America Bulletin*, v. 85., p. 1205–1218.
- Snoko, A.W., 1980, The transition from infrastructure to suprastructure in the northern Ruby Mountains, Nevada, in Crittenden, M.D., Jr., Coney, P.J., and Davis, G.H., eds., *Cordilleran metamorphic core complexes. Geological Society of America Memoir 153*, p. 287–333.
- Snoko, A.W., 1992, Clover Hill, Nevada: structural link between the Wood Hills and East Humboldt Range, in Wilson, J.R., ed., *Field guide to geologic excursions in Utah and adjacent areas of Nevada, Idaho, and Wyoming. Utah Geological Survey Miscellaneous Publication 92-3*, p. 107–122.
- Snoko, A.W., and Lush, A.P., 1984, Polyphase Mesozoic-Cenozoic deformational history of the Ruby Mountains-East Humboldt Range, Nevada, in Lintz, J., Jr., ed., *Western geological excursions: Geological Society of America annual meeting field trip guidebook, Mackay School of Mines, Reno, Nevada*, v. 4, p. 232–260
- Snoko, A.W., and Miller, D.M., 1988, Metamorphic and tectonic history of the northeastern Great Basin, in Ernst, W.G., ed., *Metamorphism and crustal evolution of the western United States: Englewood Cliffs, New Jersey, Prentice Hall, Rubey Volume VII*, p. 606–648.
- Snoko, A.W., McGrew, A.J., Valasek, P.A., and Smithson, S.B., 1990, A crustal cross section for a terrain of superimposed shortening and extension. Ruby Mountains-East Humboldt Range Nevada, in Salisbury, M.H., and Fountain, D.M., eds., *Exposed cross sections of the continental crust. NATO ASI Series, Kluwer Academic Publishers, Boston, Massachusetts*, p. 103–135.
- Sorensen, M.L., and Crittenden, M.D., Jr., 1979, Geologic map of the Huntsville quadrangle, Weber and Cache Counties, Utah: U.S. Geological Survey Map GQ-1503, scale 1:24,000.
- Spear, F.S., 1993, Metamorphic phase equilibria and pressure-temperature paths: *Mineralogical Society of America Monograph*, Washington, D.C., 799 p.
- Spear, F.S., and Cheney, J.T., 1989, A petrogenetic grid for pelitic schists in the system $\text{SiO}_2\text{-Al}_2\text{O}_3\text{-FeO-MgO-K}_2\text{O-H}_2\text{O}$: *Contributions to Mineralogy and Petrology*, v. 101, p. 149–164.
- Speed, P., Elison, M.W., and Heck, F.R., 1988, Phanerozoic tectonic evolution of the Great Basin, in Ernst, W.G., ed., *Metamorphism and crustal evolution of the western United States (Rubey Volume VII). Englewood Cliffs, New Jersey, Prentice Hall*, p. 572–605.
- Sullivan, J.T., and Nelson, A.R., 1992, Late Quaternary displacement on the Morgan fault, a back valley fault in the Wasatch range of north-eastern Utah: U.S. Geological Survey Professional Paper 1500-I, 19 p.
- Suppe, J., and Medwedeff, D.A., 1990, Geometry and kinematics of fault-propagation folding: *Eclogae Geologicae Helveticae*, v. 83, p. 409–454
- Taylor, W.J., Bartley, J.M., Fryxell, J.E., Schmitt, J.G., Vandervoort, D.S., 1993, Tectonic style and regional relations of the Central Nevada thrust belt, in Lahren, M.M., Trexler, J.H., and Spinoso, C., eds., *Crustal evolution of the Great Basin and the Sierra Nevada: Geological Society of America field trip guidebook, Geology Department, University of Nevada, Reno*, p. 57–96.
- Thorman, C.H., 1970, Metamorphosed and nonmetamorphosed Paleozoic rocks in the Wood Hills and Pequoop Mountains, northeast Nevada. *Geological Society of America Bulletin*, v. 81, p. 2417–2448
- Thorman, C.H., and Snee, L.W., 1988, Thermochronology of metamorphic rocks in the Wood Hills and Pequoop Mountains, northeastern Nevada: *Geological Society of America Abstracts with Programs*, v. 20, no. 7, p. A18.
- Thorman, C.H., Ketter, K.B., Snoko, A.W., Brooks, W.E., and Mueller, K.J., 1990, Evidence for involvement of the Roberts Mountains allochthon in Mesozoic tectonics and its effect on mineral deposits and petroleum

- accumulation models in northeast Nevada, *in* Buffa, R.H., and Coyner, A.R., eds., *Geology and ore deposits of the Great Basin, field trip guidebook and compendium: Geological Society of Nevada*, p. 869–905.
- Todd, V.R., 1980, Structure and petrology of a Tertiary gneiss complex in northwestern Utah, *in* Crittenden, M.D., Jr., Coney, P.J., and Davis, G.H., eds., *Cordilleran metamorphic core complexes: Geological Society of America Memoir 153*, p. 349–383.
- Todd, V.R., 1983, Late Miocene displacement of pre-Tertiary and Tertiary rocks in the Matlin Mountains, northwestern Utah, *in* Miller, D.M., Todd, V.R., and Howard, K.A., eds., *Tectonic and stratigraphic studies in the eastern Great Basin: Geological Society of America Memoir 157*, p. 239–270.
- Wells, M.L., 1992, Kinematics and timing of sequential deformations in the eastern Raft River Mountains: *in* Wilson, J.R., ed., *Field Guide to geologic excursions in Utah and adjacent areas of Nevada, Idaho, and Wyoming: Utah Geological Survey Miscellaneous Publication 92-3*, p. 59–78.
- Wells, M.L., 1996, Interim geologic map of the Kelton Pass 7.5' quadrangle, Box Elder Country, Utah and Cassia County, Idaho. Utah Geological Survey, Open File Report 96-342, 70 p. and 2 plates, scale 1:12,000 and 1:24,000.
- Wells, M.L., 1997, Alternating contraction and extension in the hinterlands of orogenic belts. an example from the Raft River Mountains, Utah: *Geological Society of America Bulletin*, v. 109, p. 107–126
- Wells, M.L., and Allmendinger, R.W., 1990, An early history of pure shear in the upper plate of the Raft River metamorphic core complex, Black Pine Mountains, southern Idaho. *Journal of Structural Geology*, v. 12, p. 851–868
- Wells, M.L., and Snee, L.W., 1993, Geologic and thermochronologic constraints on the initial orientation of the Raft River detachment and footwall shear zone: *Geological Society of America Abstracts with Programs*, v. 25, p. 161–162.
- Wells, M.L., and Struthers, J.R., 1995, Influence of rheological constraints on mid-crustal extensional shear zone geometry: *Geological Society of America Abstracts with Programs*, v. 27, p. A-283.
- Wells, M.L., Dallmeyer, R.D., and Allmendinger, R.W., 1990, Late Cretaceous extension in the hinterland of the Sevier thrust belt, northwestern Utah and southern Idaho: *Geology*, v. 18., p. 929–933.
- Wells, M.L., Snee, L.W., and Blythe, A.E., 1994, Mesozoic and Cenozoic extensional history of the northeastern Great Basin. insights from the Raft River and Grouse Creek Mountains. *Geological Society of America Abstracts with Programs*, v. 26, p. 103
- Wells, M.L., Peters, M.T., and Miller, D.M., 1996, Neoproterozoic age for the lower part of the Raft River Sequence, Implications for Mesozoic evolution of the Sevier belt hinterland: *Geological Society of America Abstracts with Programs*, v. 28, p. 122.
- West, J., and Lewis, H., 1982, Structure and palinspastic reconstruction of the Absaroka thrust, Anschutz Ranch area, Utah and Wyoming, *in* Powers, R.B., ed., *Geologic studies of the Cordilleran thrust belt. Rocky Mountain Association of Geologists*, p. 633–639
- Williams, P.L., Covington, H.R., and Pierce, K.L., 1982, Cenozoic stratigraphy and tectonic evolution of the Raft River basin, Idaho, *in* Bonnicksen, B., and Breckinridge, R.M., eds., *Cenozoic geology of Idaho. Idaho Bureau of Mines and Geology Bulletin 26*, p. 491–504
- Wiltshcko, D.V., and Dorr, J.A., Jr., 1983, Timing of deformation in overthrust belt and foreland of Idaho, Wyoming, and Utah. *American Association of Petroleum Geologists Bulletin*, v. 67, p. 1304–1322
- Wright, J.E., and Snoke, A.W., 1993, Tertiary magmatism and mylonitization in the Ruby-East Humboldt metamorphic core complex, north-eastern Nevada. U-Pb geochronology and Sr, Nd, Pb, isotope geochemistry: *Geological Society of America Bulletin*, v. 105, p. 935–952.
- Yonkee, W.A., 1990, Geometry and mechanics of basement and cover deformation, Farmington Canyon complex, Sevier orogenic belt, Utah [Ph.D. dissert.]. Salt Lake City, Utah, University of Utah, 255 p.
- Yonkee, W.A., 1992, Basement-cover relations, Sevier orogenic belt, northern Utah. *Geological Society of America Bulletin*, v. 104, p. 280–302.
- Yonkee, W.A., 1994, Variations in finite strain and deformation styles within the Willard thrust sheet, Sevier orogenic belt, Utah. *Geological Society of America Abstracts with Programs*, v. 26, p. A256.
- Yonkee, W.A., 1996, Mechanics of an exhumed fault zone, Willard thrust, Utah: *Geological Society of America Abstracts with Programs*, v. 28, p. A188–189.
- Yonkee, W.A., and Mitra, G., 1994, Comparison of basement deformation styles in parts of the Rocky Mountain foreland, Wyoming, and Sevier orogenic belt, northern Utah, *in* Schmidt, C.J., Chase, R.B., and Erslev, E.A., eds., *Laramide basement deformation in the Rocky Mountain foreland of the western United States. Geological Society of America Special Paper 280*, p. 197–228.
- Yonkee, W.A., Parry, W.T., Bruhn, R.L., and Cashman, P.C., 1989, Thermal models of thrust faulting constraints from fluid inclusion observations, Willard thrust sheet, Idaho-Utah-Wyoming thrust belt. *Geological Society of America Bulletin*, v. 101, p. 304–313.